République Algérienne Démocratique et Populaire

Ministère de l'Enseignement Supérieur et de la Recherche Scientifique

Université Echahid Hamma Lakhdar - El Oued

Faculté de Sciences Exactes

Département de Chimie

Thèse

Présentée en vue de l'obtention du diplôme de Doctorat LMD

Domaine : Sciences de la Matière

Filière : Chimie

Spécialité : Chimie Organique

Intitulé

Biosynthèse et caractérisation de nanoparticules d'oxyde de nickel à partir de différents extraits de plantes et étude de leurs activités biologiques

Présentée par

Okba LOUAFI

Date de Graduation : 07/05/2023

Devant le jury

Mohammed DEHAMCHIA	**Professeur**	**Université d'El-Oued**	**Président**
Abdelhamid KHELEF	**Professeur**	**Université d'El-Oued**	**Encadreur**
Adel SAKRI	**Professeur**	**Université de Biskra**	**Examinateur**
Mahmoud OMARI	**Professeur**	**Université de Biskra**	**Examinateur**
Djamel BARKAT	**Professeur**	**Université de Biskra**	**Examinateur**
Mohammed ZIDANE	**MCA**	**Université d'El-Oued**	**Examinateur**
Salah Eddine LAOUINI	**Professeur**	**Université d'El-Oued**	**Invité**

2022-2023

PEOPLE'S DEMOCRATIC REPUBLIC OF ALGERIA

MINISTRY OF HIGHER EDUCATION

AND SCIENTIFIC RESEARCH

University of Echahid Hamma Lakhdar - El Oued

Faculty of exact science

Department of chemistry

Thesis Submitted in Partial Fulfilment of the Requirement for the Degree of

LMD Doctorate

Field: Material Sciences

Branch: Chemistry

Specialty: Organic Chemistry

Entitled

Biosynthesis and characterization of nickel oxide nanoparticles using different plant extracts and study of their biological activities

Presented by

Okba LOUAFI

Graduation date: 07/05/2023

In front of the jury

Mohammed DEHAMCHIA	**Professor**	**University of El-Oued**	**President**
Abdelhamid KHELEF	**Professor**	**University of El-Oued**	**supervisor**
Adel SAKRI	**Professor**	**University of Biskra**	**Examiner**
Mahmoud OMARI	**Professor**	**University of Biskra**	**Examiner**
Djamel BARKAT	**Professor**	**University of Biskra**	**Examiner**
Mohammed ZIDANE	**MCA**	**University of El-Oued**	**Examiner**
Salah Eddine LAOUINI	**Professor**	**University of El-Oued**	**Invited**

2022-2023

Dedication

To the two who gave me life

To the two who gave me another life

To my beloved mother (رحمها الله)

To my beloved father

To my brothers and sisters

To all my family and friends

Acknowledgments

Firstly, I thank the Almighty God for giving me the strength and patience to accomplish this modest work.

I'd like to thank my supervisor, Pr. Abdelhamid Khelef, for his assistance in completing my thesis. This thesis has been significantly enhanced by his scientific guidance and understanding, as well as several insightful discussions and suggestions.

My sincere thanks also extend to the jury members: Pr. Mohammed DEHAMCHIA, Pr. Adel SAKRI, Pr. Mahmoud OMARI, Pr. Djamel BARKAT, Dr. Mohammed ZIDANE for accepting to discuss my thesis.

I'd like to thank Professor Salah Eddine LAOUINI for accepting to attend the thesis discussion.

Finally, a special thanks to my friend Mohammed laid Tedjani for his aid and support in the laboratory.

Abstract

ملخص

Résumé

Abstract

In recent years, nanoparticles synthesized by the green method have attracted the attention of many researchers due to their improved properties that are desirable in many fields. This study aims to biosynthesize nickel oxide nanoparticles and evaluate their antioxidant activities. Two plant extracts (*Artemisia herba alba* leaves and *Punica granatum L* peel) were utilized as reducing and stabilizing-agents for the green synthesis process. To control and improve the crystal size and antioxidant activity of NONPs, we focused on studying two parameters: plant extract and nickel nitrate concentration. Several characterization techniques such as UV/Vis, X-ray diffraction, FT-IR, SEM, and EDX were used to validate the formation of NONPs and study their structural and morphological properties.

Results verified the successful biosynthesis of nickel oxide nanoparticles. UV/Vis absorption spectrum showed a maximal absorption at 300 nm which is related to NiO. The FTIR spectrum exhibited common peaks between 400 and 1000 cm^{-1}, which corresponds to the Ni-O stretching vibration mode. In addition, the XRD patterns confirmed that NONPs are of high purity and crystallinity, with a nanoscale-size ranging from 7.49 to 14.51 nm. The images obtained by a scanning electron microscope (SEM) indicated that some of the obtained nanoparticles have a spherical shape, while others have an irregular shape. Additionally, the antioxidant activity of NONPs samples was evaluated using three different techniques, which showed significant antioxidant activity in all the performed tests.

Keywords: Green synthesis, *Punica Granatum L*, *Artemisia herba alba*, Antioxidant activity, Nickel oxide nanoparticles.

Résumé

Ces dernières années, les nanoparticules synthétisées par la méthode verte ont attiré l'attention de nombreux chercheurs en raison de leurs propriétés améliorées qui sont souhaitables dans de nombreux domaines. Cette étude vise à biosynthétiser des nanoparticules d'oxyde de nickel et à évaluer leurs activités antioxydantes. Deux extraits de plantes (feuilles d'*Artemisia herba alba* et écorce de *Punica granatum L*) ont été utilisés comme agents réducteurs et stabilisants pour le processus de synthèse verte. Pour contrôler et améliorer la taille des cristaux et l'activité antioxydante des NONPs, nous nous sommes concentrés sur l'étude de deux paramètres : l'extrait végétal et la concentration en nitrate de nickel. Plusieurs techniques de caractérisation telles que UV/Vis, diffraction des rayons X, FT-IR, MEB et EDX ont été utilisées pour valider la formation des NONPs et étudier leurs propriétés structurelles et morphologiques.

Les résultats ont confirmé la réussite de la biosynthèse des nanoparticules d'oxyde de nickel. Le spectre d'absorption UV/Vis a montré une absorption maximale à 300 nm qui est liée à NiO. Le spectre FTIR présentait des pics communs entre 400 et 1000 cm-1, ce qui correspond au mode de vibration d'étirement Ni-O. De plus, les modèles XRD ont confirmé que les NONPs sont de haute pureté et cristallinité, avec une taille nanométrique allant de 7,49 à 14,51 nm. Les images obtenues par un microscope électronique à balayage (SEM) ont indiqué que certaines des nanoparticules obtenues ont une forme sphérique, tandis que d'autres ont une forme irrégulière. De plus, l'activité antioxydante des échantillons de NONPs a été évaluée à l'aide de trois techniques différentes, qui ont montré une activité antioxydante significative dans tous les tests effectués.

Mots clés : Synthèse verte, *Punica Granatum L*, *Artemisia herba alba*, Activité antioxydante, nanoparticules d'oxyde de nickel.

ملخص

في السنوات الأخيرة، جذبت الجسيمات النانوية المُصنّعة بالطريقة الخضراء انتباه العديد من الباحثين نظرًا لخصائصها المحسّنة المرغوبة في العديد من المجالات. يهدف هذا العمل إلى التخليق الحيوي لجسيمات أكسيد النيكل النانوية ودراسة أنشطتها المضادة للأكسدة. تم استخدام مستخلصين نباتيين (أوراق الشيح الأبيض وقشور فاكهة الرمان) كعوامل اختزال وتثبيت لعملية التوليف الأخضر. للتحكم في حجم البلورات والنشاط المضاد للأكسدة وتحسينهما، ركزنا على دراسة متغيرين: المستخلص النباتي وتركيز نترات النيكل. تم استخدام العديد من تقنيات التوصيف مثل الأشعة فوق البنفسجية (UV-Vis)، الاشعة تحت الحمراء (FTIR)، انعراج الاشعة السينية (XRD)، المجهر الالكتروني الماسح (SEM) والاشعة السينية المشتتة للطاقة (EDX) للتحقق من صحة تكوين الجسيمات النانوية ودراسة خصائصها الهيكلية والمورفولوجية.

أثبتت النتائج نجاح التخليق الحيوي لجسيمات أكسيد النيكل النانوية. أظهر طيف امتصاص UV / Vis أقصى امتصاص عند 300 نانومتر وهو مرتبط بـ اكسيد النيكل. أظهر طيف FTIR قممًا مشتركة بين 400 و1000 سم $^{-1}$، وهو ما يتوافق مع وضع اهتزاز تمدد أكسيد النيكل. بالإضافة إلى ذلك، أكدت أنماط XRD أن جسيمات أكسيد النيكل النانوية عالية النقاء والتبلور، بحجم نانوي يتراوح من 7.49 إلى 14.51 نانومتر. أشارت الصور التي تم الحصول عليها بواسطة المجهر الإلكتروني الماسح (SEM) إلى أن بعض الجسيمات النانوية التي تم الحصول عليها لها شكل كروي، في حين أن البعض الآخر لها شكل غير منتظم. بالإضافة إلى ذلك، تم تقييم النشاط المضاد للأكسدة لعينات أكسيد النيكل النانوية باستخدام ثلاث تقنيات مختلفة، والتي أظهرت نشاطًا كبيرًا مضادًا للأكسدة في جميع الاختبارات التي تم إجراؤها.

الكلمات المفتاحية: التوليف الاخضر، الشيح، الرمان، النشاط المضاد للأكسدة، جسيمات أكسيد النيكل النانوية.

List of abbreviations

p. granatum L	*Punica granatum L*
A. herba alba	*Artemisia herba alba*
NONPs	Nickel oxide nanoparticles
NiO	Nickel oxide
NPs	Nanoparticles
AAE	Ascorbic acid equivalent
EFeSO4	Iron sulfate equivalent
DPPH	2,2-diphenyl-1-picrylhydrazil
FRAP	Ferric reducing antioxidant power
TAC	Total antioxidant capacity
TPTZ	2,4,6-Tri(2-pyridyl)-1,3,5-triazine
IC50	Inhibitory Concentration
ARP	Anti radical power
UV-Vis	Ultraviolet–visible spectroscopy
FTIR	Transform Infrared spectroscopy
XRD	X-Ray Diffraction
SEM	Scanning Electron Microscopy
EDX	Energy Dispersive X-ray analysis
nm	Nanometer
%**inhibition**	Percentage inhibition
g	Gram
mg	Milligram
mM	Millimolar

List of figures

Chapter I: Generalities on *Artemisia herba alba* and *Punica granatum L*

Figure I.1 Photograph of *Artemisia herba alba*: **(a)** at the at the beginning of the flowering season; and **(b)** at the ending of the flowering season…… **(10)**

Figure I.2 geographic distribution of *Artemisia herba alba*…… **(12)**

Figure I.3 The main Flavonoids identified in *Artemisia herba alba*…… **(15)**

Figure I.4 Some Sesquiterpene lactones identified in *A. herba alba*…… **(17)**

Figure I.5 Photograph of *Punica granatum L*: **(a)** tree; **(b)** leaves; **(c)** flowers; and **(d)** fruits…… **(19)**

Figure I.6 The main anthocyanoside, flavonoids and alkaloids compounds identified in *Punica granatum L*…… **(23)**

Chapter II : Overview on nanoparticles

Figure II.1 Photograph of the famous Lycurgus Cup…… **(39)**

Figure II.2 The range of nanoparticle sizes compared to major chemical and biological structures…… **(41)**

Figure II.3 Approaches for the Synthesis of nanoparticles…… **(43)**

Figure II.4 laser ablation method diagram…… **(44)**

Figure II.5 Sputtering method diagram…… **(45)**

Figure II.6 Organic NPs: **(a)** Dendrimers; **(b)** Liposomes and Micelles**;** and **(c)** Ferritin…. **(47)**

Figure II.7 carbon based NPs: **(a)** fullerenes; **(b)** graphene; **(c)** carbon nanotubes; **(d)** nanofibers; and **(e)** carbon black…… **(48)**

Figure II.8 crystal structure of nickel oxide (NiO)…… **(50)**

Figure II.9 Mechanism of green synthesis of metal oxide nanoparticles…… **(51)**

Figure II.10 Probable biomolecules involved in the synthesis of nanoparticles …… **(52)**

Chapter III : Materials and Methods

Figure III.1 Steps for the green synthesis of NONPs…… **(64)**

Figure III.2 Schematic representation of Bragg's law principle…… **(65)**

Figure III.3 Schematic representation of scanning electron microscope (SEM)…… **(67)**

Figure III.4 The different modes of vibration of the most particles…… **(68)**

Figure III.5 Schematic diagram of the reaction between DPPH• and antioxidants…… **(70)**

Figure III. 6 Calibration curve of ascorbic acid for evaluation of total antioxidant capacity…… **(71)**

Figure III. 7 Schematic diagram of the reaction of FRAP test…… **(72)**

Figure III. 8 Calibration curve of iron sulfate ……..…… **(73)**

Chapter IV : Results and Discussion

Figure IV. 1 UV/Vis absorption spectra of $NONP_S$ prepared from *A. herba alba* leaves extract at different molarities**: (a)** 0.01M; **(b)** 0.025M; **(c)** 0.05M; and **(d)** 0.075 M…….…. **(79)**

Figure IV. 2 UV/Vis absorption spectra of $NONP_S$ prepared from *P. granatum L* peel extract at different molarities**: (a)** 0.01M; **(b)** 0.025M; **(c)** 0.05M; and **(d)** 0.075 M…… **(80)**

Figure IV.3 Optical properties of $NONP_S$ prepared from *A. herba alba* leaves extract at different molarities: **(a)** 0.01M; **(b)** 0.025M; **(c)** 0.05M; and **(d)** 0.075 M……..…… **(81)**

Figure IV.4 Optical properties of $NONP_S$ prepared from *P. granatum L* peel extract at different molarities: **(a)** 0.01M; **(b)** 0.025M; **(c)** 0.05M; and **(d)** 0.075 M……. **(82)**

Figure IV.5: (a) FTIR spectrum of *Artemisia herba alba* leaves extract; **(b)** FTIR spectrums of NONPs samples; **(c)** and **(d)** FTIR spectrums illustrative for the extract, and NONPs samples……..……..……. **(84)**

Figure IV.6: (a) FTIR spectrum of *Punica granatum L* peel extract; **(b)** FTIR spectrums of NONPs samples; **(c)** and **(d)** FTIR spectrums illustrative for the extract, and NONPs samples……..…... **(85)**

Figure IV.7 XRD analysis of $NONP_S$ prepared from *Artemesia herba alba* leaves extract at different molarities: **(a)** 0.01M; **(b)** 0.025M; **(c)** 0.05M; and **(d)** 0.075 M…….... **(86)**

Figure IV.8 XRD analysis of $NONP_S$ prepared from *Punica granatum L* peel extract at different molarities: **(a)** 0.01M; **(b)** 0.025M; **(c)** 0.05M; and **(d)** 0.075 M……. **(87)**

Figure IV.9 SEM images of $NONP_S$ biosynthesized using *Artemesia herba alba* leaves extract at different molarities: **(a)** 0.01M; **(b)** 0.025M; **(c)** 0.05M; and **(d)** 0.075 M…… **(89)**

Figure IV.10 SEM images of $NONP_S$ biosynthesized using *Punica granatum L* peel extract at different molarities: **(a)** 0.01M; **(b)** 0.025M; **(c)** 0.05M; and **(d)** 0.075 M……. **(90)**

Figure IV.11 EDX analysis of NONPs prepared using *Artemesia herba alba* leaves extract……..……... **(91)**

Figure IV.12 EDX analysis of NONPs prepared using *Punica granatum L* peel leaves extract…….…. **(91)**

Figure IV.13 The total antioxidant capacity of NONPs samples biosynthesized at different molarities: **(a)** using *Artemisia herba alba* leaves extract, and **(b)** using *Punica granatum L* peel extract…….…. **(93)**

Figure IV.14: Ferric reducing antioxidant power of NONPs samples biosynthesized at different molarities: **(a)** using *Artemisia herba alba* leaves extract, and **(b)** using *Punica granatum L* peel extract**…….....……. (94)**

Figure IV.15 Percent inhibition of DPPH• for samples prepared using *Artemisia herba alba* leaves extract at different molarities: **(a)** 0.01M; **(b)** 0.025M; **(c)** 0.05M; and **(d)** 0.075M**…… (95)**

Figure IV.16 $IC_{50\%}$ values of for samples biosynthesized by *Artemisia herba alba* leaves extract**……..……..……..(96)**

Figure IV.17 Percent inhibition of DPPH• for samples prepared using *Punica granatum L* peel extract at different molarities: **(a)** 0.01M; **(b)** 0.025M; **(c)** 0.05M; and **(d)** 0.075M**…… (97)**

Figure IV.18 $IC_{50\%}$ values of for samples biosynthesized *Punica granatum L* peel extract**…….…..... (98)**

List of tables

Chapter I: Generalities on Artemisia herba alba and Punica granatum L

Table I.1 Botanical classification of *Artemisia herba alba*……..……..…. **(11)**

Table I.2 some Vernacular names of *Punica granatum L*……...……. **(20)**

Table I.3 Botanical classification of *Punica granatum L*…….**(20)**

Chapter II : Overview on nanoparticles

Table II.1 History of Nanotechnology……..…….....**(40)**

Table II.2 Some example calculations for volume and surface-area of nanoparticles…….… **(42)**

Chapter IV : Results and Discussion

Table IV. 1 The band gap values of NONPs synthesized using two plant extracts (*Artemisia herba alba* leaves, and *Punica granatum L* peel) at different molarities……..……...…….... **(83)**

Table IV. 2 The average crystallite size of NONPs biosynthesized using two plant extracts (*Artemisia herba alba* leaves, and *Punica granatum L* peel) at different molarities……...……...……. **(88)**

Table IV.3 $IC_{50\%}$ and ARP values of DPPH• for different samples biosynthesized by *Artemisia herba alba* leaves extract…… **(96)**

Table IV.4 $IC_{50\%}$ and ARP values of DPPH• for different samples biosynthesized by *Punica granatum L* peel extract…….…….....**(98)**

Table of contents

Dedication.....(I)
Acknowledgments.....(II)
Abstract ..... (IV)
Résumé .....(V)
ملخص..... (VI)
List of abbreviations.....(VII)
List of figures .....(VIII)
List of tables .....(XI)
General introduction.....(2)
References…….…. (5)

Chapter I: Generalities on Artemisia herba alba and Punica granatum L

I.1 The species *Artemisia herba alba*.....(10)
I.1.1 Morphology and ecology.....(10)
I.1.2 Nomenclature.....(11)
I.1.2.1 Scientific name.....(11)
I.1.2.2 Vernacular name.....(11)
I.1.3 Taxonomy.....(11)
I.1.4 Geographic distribution.....(11)
I.1.5 Traditional Uses of *Artemisia herba alba*.....(12)
I.1.6 Chemical composition of *Artemisia herba alba*.....(12)
I.1.6.1 Essential oils.....(13)
I.1.6.2 Flavonoids of *Artemisia herba alba*.....(14)
I.1.6.3 Sesquiterpene lactones.....(16)
I.1.7 Biological activities of *Artemisia herba alba*.....(18)
I.1.8 Toxicological properties.....(18)
I.2 The species *Punica granatum L*.....(18)
I.2.1 Morphology and ecology.....(18)
I.2.2 Nomenclature.....(19)
I.2.2.1 Scientific name.....(19)
I.2.2.2 Vernacular name.....(19)
I.2.3 Taxonomy.....(20)
I.2.4. Origin and Geographical Distribution of *Punica granatum L*.....(20)

I.2.5 Traditional Uses of *Punica granatum L*.....(21)
I.2.6 Some chemical composition of *Punica granatum L*.....(21)
I.2.6.1 Organic Acids and Phenolic Acids.....(21)
I.2.6.2 hydrolyzable tannins and their derivatives.....(21)
I.2.6.3 Other compositions..... (21)
I.2.7 The biological activities of *Punica granatum L* peel.....(24)
I.2.7.1 Antioxidant activity.....(24)
I.2.7.2 Antibacterial activity.....(24)
I.2.7.3 Antidiabetic activity.....(24)
I.2.7.4 Antifungal activity.....(25)
I.2.7.5 Anti-cancer activity.....(25)
I.2.7.6 Antiulcer activity.....(25)
I.2.8 Toxicity Studies.....(25)
References.....(27)

Chapter II : Overview on nanoparticles

II.1 The history of nanotechnology.....(38)
II.2 Definitions.....(40)
II.2.1 Nanotechnology.....(40)
II.2.2 Nanomaterials.....(40)
II.2.3 Nanoparticles.....(41)
II.3 General properties of nanoparticles.....(41)
II.3.1 Optical properties.....(41)
II.3.2 Surface properties.....(42)
II.3.3 Mechanical properties.....(42)
II.3.4 Electrical properties.....(43)
II.3.5 Catalytic Properties.....(43)
II.4 Strategies for the Synthesis of nanoparticles.....(43)
II.4.1 Top-down approach.....(43)
II.4.2 The bottom-up approach.....(44)
II.4.1.1 Laser ablation.....(44)
II.4.1.2 Thermal decomposition.....(44)
II.4.1.3 Sputtering.....(45)
II.4.2.1 Sol-gel.....(45)
II.4.2.2 Biosynthesis.....(45)

II.5 Classifications of nanoparticles.....(46)
II.5.1 The classification of nanoparticles based on their dimensions.....(46)
II.5.1.1 Zero-dimensional nanoparticles.....(46)
II.5.1.2 One-dimensional nanoparticles.....(46)
II.5.1.3 Two-dimensional nanoparticles.....(46)
II.5.1.4 Three-dimensional nanoparticles.....(46)
II.5.2 Classifications of nanoparticles based on their origin.....(46)
II.5.2.1 Natural or Anthropogenic Nanoparticles.....(46)
II.5.3 Classifications of nanoparticles based on their chemical compositions.....(47)
II.5.3.1 Organic nanoparticles.....(47)
II.5.3.2 Inorganic nanoparticles.....(47)
II.5.3.2.1 Metals nanoparticles.....(48)
II.5.3.2.2 Metal oxides nanoparticles.....(48)
II.5.3.3 Carbon-based nanoparticles.....(48)
II.5.3.3.1 Graphene.....(49)
II.5.3.3.2 carbon nano tubes (CNT) .....(49)
II.5.3.3.3 carbon black.....(49)
II.5.3.3.4 carbon nanofibers.....(49)
II.6 General properties and applications of nickel oxide (NiO) .....(49)
II.7 Green synthesis of nanoparticles using plants extracts……..……(50)
II.7.1 Mechanism of green synthesis of nanoparticles by plant extracts……...…….(51)
II.7.2 The importance of plant secondary metabolites in the formation of nanoparticles..(52)
II.8 Study of antioxidant activity……..(52)
II.8.1 Oxidative stress……(53)
II.8.1.1 Definition of oxidative stress……(53)
II.8.1.2 Free radicals……...…...(53)
II.8.1.3 Source of free radicals…….……..……...(53)
II.8.1.4 Role of antioxidant……(53)
References.....(55)

Chapter III : Materials and Methods

III.1 Materials and methods.....(63)
III.1.1 The Collection and preparation of plant extracts.....(63)
III.1.2 The biosynthesis of NONPs.....(64)
III.1.3 Characterization techniques.....(65)

III.1.3.1 X Ray Diffractions (XRD) .....(65)
III.1.3.2 Scanning Electron Microscopy (SEM).....(66)
III.1.3.3 UV-visible absorption spectroscopy.....(67)
III.1.3.4 Fourier Transform Infrared (FTIR) spectroscopy.....(68)
III.1.2 Evaluation of antioxidant activity.....(69)
III.1.2.1 Chemicals.....(69)
III.1.2.2 DPPH• scavenging assay.....(69)
III.1.2.3 Total antioxidant activity (TAC) .....(70)
III.1.2.4 Ferric reducing antioxidant power (FRAP) assay.....(71)
References.....(75)

Chapter IV : Results and Discussion

IV.1 Visual observations.....(78)
IV.2 Characterization of NONPs.....(78)
IV.2.1 UV/visible spectroscopy analysis.....(78)
IV.2.2 FTIR spectroscopy analysis.....(83)
IV.2.3 X-ray diffraction (XRD) .....(85)
IV.2.4 Scanning Electron Microscopy (SEM) .....(89)
IV.2.5 The Energy Dispersive X-ray analysis (EDX) .....(90)
IV.3 The results of the antioxidant activity test of NONPs.....(92)
IV.3.1 Total Antioxidant Capacity (TAC) .....(92)
IV.3.2 Ferric Reducing Antioxidant Power.....(93)
IV.3.3 DPPH radical scavenging.....(94)
Conclusion.....(98)
References.....(101)
General conclusion.....(107)
APPENDIXES.....(110)

GENERAL INTRODUCTION

General introduction

In the last two decades, researchers have focused significantly on nanosized materials due to their new and improved characteristics over bulk materials. These properties have made nanomaterials desirable and suitable for several sectors [1]. Inorganic nanomaterials, in particular nickel oxide nanoparticles, are of great interest to chemists, physicists, and biologists due to their exceptional characteristics suitable for diverse applications such as high stability, superconductivity, adsorption of harmful pollutants and dyes, electro-catalysis, antioxidants, anticancer, antifungal, antibacterial properties [2-7].

Several physical and chemical methods, including sol-gel, co-precipitation, hydrothermal, solvothermal, and thermal decomposition, have been utilized to synthesize nickel oxide nanoparticles [4,8]. However, these approaches are expensive, toxic and hazardous to both humans and the environment which restricts their biological applicability [9]. These problems have been overcome by developing an alternative method for nanoparticle production (green synthesis method) which uses natural compounds found in different plant parts. In addition, this method eliminates the use of hazardous products and produces non-toxic and biodegradable nanoparticles, making it a suitable alternative to other synthesis methods in many fields.

Nanoparticles have gained importance in the biomedical field due to their widespread usage in various applications like drug delivery, molecular imaging, gene therapy, and diagnostic assays [10]. These advanced materials are being investigated as potential sources of improved antioxidants. Consequently, their antioxidant activity is commonly studied and tested [11-14]. Additionally, researchers have studied the antioxidant activity of metal oxide nanoparticles, synthesized using chemical, physical, or biological methods, in single or bi-metallic phases. These nanoparticles offer several advantages compared to conventional antioxidants, including their ability to act as targeted delivery agents and to provide controlled release at the site of action. [15].

The effectiveness of nanoparticles as antioxidants is often determined by their size and shape[16- 19]. As a result, it's essential to have control over these properties to utilize their potential fully. Usually, this is achieved by adjusting the synthesis parameters like reaction pH, annealing temperature, reaction duration, and precursor concentration [20]. These parameters impact the rate of nucleation and nanoparticle growth, leading to variations in size and shape and size [21-23].

This work aims to biosynthesize nickel oxide nanoparticles and study of their antioxidant activity. For the first time, *Artemisia herba alba* leaves extract and *Punica granatum L* peel extract were used to biosynthesize nickel oxide nanoparticles at four different molarities of nickel nitrate (0.01, 0.025, 0.05 and 0.075 M).

This work is divided into four chapters:

- The first chapter represents a bibliographic study on *Artemisia herba alba* and *Punica granatum L.*
- The second chapter provides an overview on nanoparticles, including their classification, properties, and fabrication methods.
- The third chapter explains the steps for the green synthesis of nickel oxide nanoparticles, the principal characterization techniques, and the methods used to evaluate the antioxidant activity of the different samples.
- The fourth chapter presents the results of characterization and antioxidant activity of the different samples, followed by discussions and interpretations.
- Finally, a general conclusion summarizes the main results obtained during this thesis and suggestions for further study.

References

[1] D. Barani, M. L. Tedjani, Z. Younes, S. Meneceur, S. E. Laouini, and H. Hammami, "Biomass-mediated synthesis of ZnO and Mg@ZnO nanoparticles for enhancing the degradation of m-toluidine and p-toluidine," *Biomass Convers. Biorefinery*, no. October, 2022, doi: 10.1007/s13399-022-03411-2.

[2] K. Lingaraju, H. Raja Naika, H. Nagabhushana, K. Jayanna, S. Devaraja, and G. Nagaraju, "Biosynthesis of Nickel oxide Nanoparticles from Euphorbia heterophylla (L.) and their biological application," *Arab. J. Chem.*, vol. 13, no. 3, pp. 4712–4719, 2020, doi: 10.1016/j.arabjc.2019.11.003.

[3] M. S. S. Kumar *et al.*, "Multifunctional applications of Nickel oxide (NiO) nanoparticles synthesized by facile green combustion method using Limonia acidissima natural fruit juice," *Inorganica Chim. Acta*, vol. 515, p. 120059, Jan. 2021, doi: 10.1016/j.ica.2020.120059.

[4] B. A. Abbasi, J. Iqbal, T. Mahmood, R. Ahmad, S. Kanwal, and S. Afridi, "Plant-mediated synthesis of nickel oxide nanoparticles (NiO) via Geranium wallichianum: Characterization and different biological applications," *Mater. Res. Express*, vol. 6, no. 8, 2019, doi: 10.1088/2053-1591/ab23e1.

[5] J. Iqbal, B. A. Abbasi, T. Mahmood, S. Hameed, A. Munir, and S. Kanwal, "Green synthesis and characterizations of Nickel oxide nanoparticles using leaf extract of Rhamnus virgata and their potential biological applications," *Appl. Organomet. Chem.*, vol. 33, no. 8, pp. 0–2, 2019, doi: 10.1002/aoc.4950.

[6] A. K. H. Bashir *et al.*, "Biosynthesis of NiO nanoparticles for photodegradation of free cyanide solutions under ultraviolet light," *J. Phys. Chem. Solids*, vol. 134, no. June, pp. 133–140, 2019, doi: 10.1016/j.jpcs.2019.05.048.

[7] A. A. Ezhilarasi, J. J. Vijaya, K. Kaviyarasu, M. Maaza, A. Ayeshamariam, and L. J. Kennedy, "Green synthesis of NiO nanoparticles using Moringa oleifera extract and their biomedical applications: Cytotoxicity effect of nanoparticles against HT-29 cancer cells," *J. Photochem. Photobiol. B Biol.*, vol. 164, no. November, pp. 352–360, 2016, doi: 10.1016/j.jphotobiol.2016.10.003.

[8] K. Motevalli, Z. Zarghami, and M. Panahi-Kalamuei, "Simple, novel and low-temperature synthesis of rod-like NiO nanostructure via thermal decomposition route using a new starting reagent and its photocatalytic activity assessment," *J. Mater. Sci. Mater. Electron.*, vol. 27, no. 5, pp. 4794–4799, 2016, doi: 10.1007/s10854-016-4360-5.

[9] F. T. Thema, E. Manikandan, A. Gurib-Fakim, and M. Maaza, “Single phase Bunsenite NiO nanoparticles green synthesis by Agathosma betulina natural extract,” *J. Alloys Compd.*, vol. 657, pp. 655–661, Feb. 2016, doi: 10.1016/j.jallcom.2015.09.227.

[10] E. Boisselier and D. Astruc, “Gold nanoparticles in nanomedicine: preparations, imaging, diagnostics, therapies and toxicity,” *Chem. Soc. Rev.*, vol. 38, no. 6, pp. 1759–1782, 2009, doi: 10.1039/b806051g.

[11] A. Watanabe *et al.*, “In vitro free radical scavenging activity of platinum nanoparticles,” *Nanotechnology*, vol. 20, no. 45, pp. 1–9, 2009, doi: 10.1088/0957-4484/20/45/455105.

[12] Y. Liu *et al.*, “Comprehensive insights into the multi-antioxidative mechanisms of melanin nanoparticles and their application to protect brain from injury in ischemic stroke,” *J. Am. Chem. Soc.*, vol. 139, no. 2, pp. 856–862, 2017, doi: 10.1021/Jacs.6b11013.

[13] J. P. Saikia, S. Paul, B. K. Konwar, and S. K. Samdarshi, “Nickel oxide nanoparticles: A novel antioxidant,” *Colloids Surfaces B Biointerfaces*, vol. 78, no. 1, pp. 146–148, 2010, doi: 10.1016/j.colsurfb.2010.02.016.

[14] A. Bouafia, S. E. Laouini, A. Khelef, M. L. Tedjani, and F. Guemari, “Effect of Ferric Chloride Concentration on the Type of Magnetite (Fe3O4) Nanoparticles Biosynthesized by Aqueous Leaves Extract of Artemisia and Assessment of Their Antioxidant Activities,” *J. Clust. Sci.*, pp. 1–9, Aug. 2020, doi: 10.1007/s10876-020-01868-7.

[15] M. Kajita, K. Hikosaka, M. Iitsuka, A. Kanayama, N. Toshima, and Y. Miyamoto, “Platinum nanoparticle is a useful scavenger of superoxide anion and hydrogen peroxide,” *Free Radic. Res.*, vol. 41, no. 6, pp. 615–626, 2007, doi: 10.1080/10715760601169679.

[16] M. Misawa and J. Takahashi, “Generation of reactive oxygen species induced by gold nanoparticles under x-ray and UV Irradiations,” *Nanomedicine Nanotechnology, Biol. Med.*, vol. 7, no. 5, pp. 604–614, 2011, doi: 10.1016/j.nano.2011.01.014.

[17] A. Avalos, A. I. Haza, D. Mateo, and P. Morales, “Cytotoxicity and ROS production of manufactured silver nanoparticles of different sizes in hepatoma and leukemia cells,” *J. Appl. Toxicol.*, vol. 34, no. 4, pp. 413–423, 2014, doi: 10.1002/jat.2957.

[18] L. Z. Flores-López, H. Espinoza-Gómez, and R. Somanathan, “Silver nanoparticles: Electron transfer, reactive oxygen species, oxidative stress, beneficial and toxicological effects.,” *J. Appl. Toxicol.*, vol. 39, no. 1, pp. 16–26, 2019, doi: 10.1002/jat.3654.

[19] B. D. Chithrani, A. A. Ghazani, and W. C. W. Chan, “Determining the size and shape dependence of gold nanoparticle uptake into mammalian cells,” *Nano Lett.*, vol. 6, no. 4, pp. 662–668, 2006, doi: 10.1021/nl052396o.

[20] T. M. Laid, K. Abdelhamid, L. S. Eddine, and B. Abderrhmane, “Optimizing the biosynthesis parameters of iron oxide nanoparticles using central composite design,” *J. Mol. Struct.*, vol. 1229, p. 129497, 2021, doi: 10.1016/j.molstruc.2020.129497.

[21] P. Jayaprakash, M. P. Mohamed, and M. L. Caroline, “Growth, spectral and optical characterization of a novel nonlinear optical organic material: D-Alanine DL-Mandelic acid single crystal,” *J. Mol. Struct.*, vol. 1134, pp. 67–77, 2017, doi: 10.1016/j.molstruc.2016.12.026.

[22] H. Liu, H. Zhang, J. Wang, and J. Wei, “Effect of temperature on the size of biosynthesized silver nanoparticle: Deep insight into microscopic kinetics analysis,” *Arab. J. Chem.*, vol. 13, no. 1, pp. 1011–1019, 2020, doi: 10.1016/j.arabjc.2017.09.004.

[23] C. Chetan, R. F. Bhajantri, B. Soumya, C. Shivaprasad, A. Maliakarjun, and K. Satyappa, “‘effect of calcination temperature on synthesized ZnO nanoparticles,’” *AIP Conf. Proc.*, vol. 2244, no. July 2021, pp. 1–4, 2020, doi: 10.1063/5.0009107.

Chap I: Generalities on Artemisia herba alba and Punica granatum L

Chapter I: Generalities on Artemisia herba alba and Punica granatum L

Medicinal plants have been employed to prevent or treat human diseases since ancient times. All of these therapeutic properties are due to the presence of bioactive compounds (secondary metabolites) which are found in various organs of plants. Algeria has diverse medicinal plants rich in bioactive compounds. Among the most common medicinal plants in Algeria are *Artemisia herba alba* and *Punica granatum L (pomegranate).*

Artemisia is one of the major medicinal plants in the family Asteraceae includes approximately 200 to more than 500 species **[1]**. Many *Artemisia* species have a significant economic impact in a variety of fields, including cosmetics , pharmaceutical industry, and medicine **[2]**.

Artemisia herba alba is known for decades as desert wormwood (known in Arabic as *Shih*, *Armoise Blanche* (Fr)). Is typically found in semi-arid and arid climatic, and is used in folk medicine for the treatment of several diseases such as colds, coughing, as an antidiabetic agent, for bronchitis, diarrhea, neuralgias, and hypertension **[3]**.

Several investigations have been conducted to examine the biological activities of *Artemisia herba-alba* as an antimicrobial (bacteria and fungi) **[4,5]**, antioxidant **[6]**, antileshmanial, anthelmintic, and antispasmodic agent **[1]**. Moreover, various Phytochemical studies have shown that this genus is rich in Sesquiterpene lactones, monoterpenes, flavonoids, and coumarins **[7]**.

Punica granatum L., commonly known as pomegranate, has garnered much attention due to its richness in active compounds and its therapeutic properties. Many cultures have traditionally used all components of the pomegranate tree in folk medicine to treat diverse ailments including parasitic infections, ulcers, dysentery, diarrhea, hemorrhages, respiratory ailments, and bacterial infections **[8]**.

Punica granatum L. is a species of the Punicaceae family **[9]**; its fruit is composed of three parts: seeds, peel, and arils. *Punica granatum L* fruit peel is considered an agro-industrial waste and is also employed for cattle feed and for the extraction of natural dyes and formulation of many food products such as ice cream, and yogurts to improve their functional characteristics **[10]**. Moreover, it includes a variety of bioactive constituents such as flavonoid, tannin, anthocyanin, catechin, and proanthocyanidins which are responsible for a wide range of biological effects including anticancer, anti-atherosclerotic, anti-inflammatory**,** antimicrobial, antidiarrheal, and

antioxidant activities [11], furthermore, it contains a diversity of minerals like calcium, magnesium, phosphorus, potassium, and sodium [12].

The edible part of the *Punica granatum L* fruit are a very important part due to their high free radical scavenging capacity and richness in polyunsaturated fatty acids, sugars, vitamins, polyphenols, polysaccharides and minerals [13,14]. Many studies have proven that edible part of *Punica granatum L* has various of biological activities such as anti-inflammatory, anti-cancer, antimicrobial and antioxidant activities [12,15].

I.1 The species *Artemisia herba alba*

I.1.1 Morphology and ecology

A. herba alba is a greenish-silver perennial plant that grows to a height of 20-40 cm. with rigid and erect stems. The grey leaves of sterile shoots are petiolate, ovate to orbicular in outline whereas leaves of flowering stems are much smaller. The flowering heads are sessile, oblong, and tapering at the base, its vegetative growth occurs in the autumn, and its flowering begins in September and lasts until December [7]. *Artemisia herba alba* occurs mainly in a variety of bioclimates, from semi-arid to arid climatic. is well adapted in both warm and cold regions during the winter, and grows in salt soils and poorly drained areas, It has a seasonal dimorphism, losing its wide winter leaves at the beginning of the dry season and replacing them with smaller summer leaves whose anatomical structure is different [16].

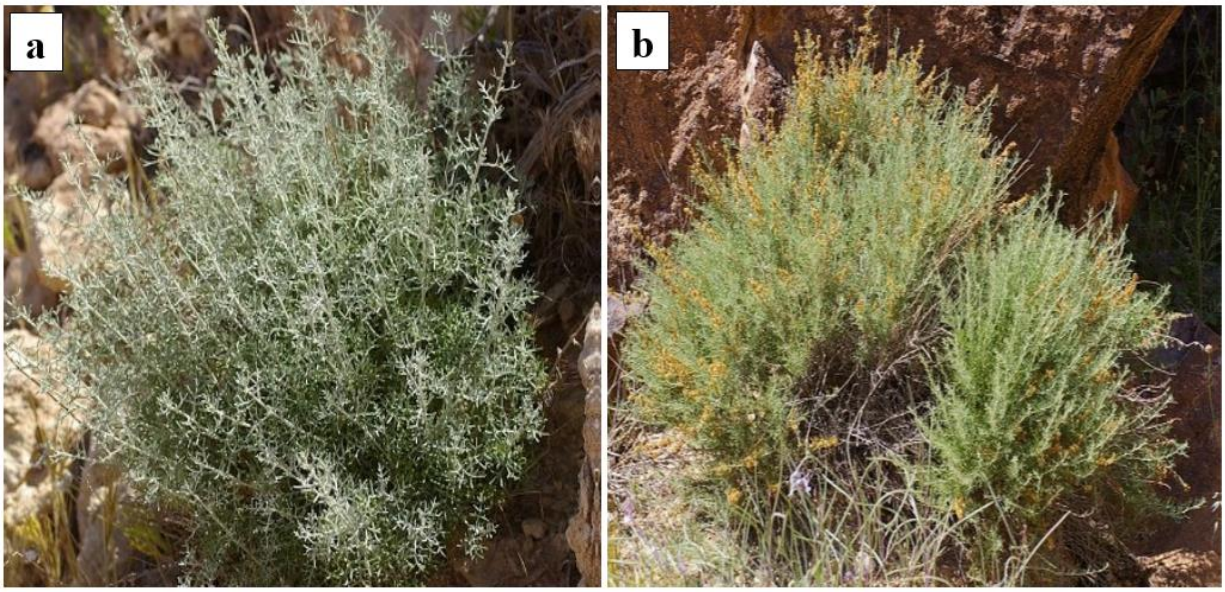

Figure I.1 Photograph of *Artemisia herba alba*: **(a)** at the at the beginning of the flowering season; and **(b)** at the ending of the flowering season [17].

I.1.2 Nomenclature

I.1.2.1 Scientific name: *Artemisia herba alba* is known by several scientific names: *Artemisia herba-alba Asso, Artemisia inculta Del, Seriphidium herba-alba (Asso) Soják* [17,18].

I.1.2.2 Vernacular name: Arabic (الشيحor الشيح الخرساني), French (Armoise blanche), English (Wormwood) [18].

I.1.3 Taxonomy

The botanical classification of *Artemisia herba alba* is shown below, according to [7].

Table I.1 Botanical classification of *Artemisia herba alba*.

Kingdom	**Plantae**
Subkingdom	Tracheobionta
Superdivision	Spermatophyta
Division	Magnoliophyta
Class	Magnoliopsida
Subclass	Asteridae
Order	Asterales
Family	Asteraceae
Subfamily	Asteroideae
Tribe	Anthemideae
Subtribe	Artemisiinae
subgenus	Seriphidium
species	*Artemisia herba alba*

I.1.4 Geographic distribution

Artemisia herba alba is a type of medicinal and aromatic plant that is small in size and is usually found in dry and arid environments. It is prevalent in various regions, including Egypt in the Middle East, Tunisia, Algeria, and Morocco in North Africa, and Spain and Italy in Southern Europe. The plant's distribution extends to the Northwestern Himalayan region as well [2,7].

Figure I.2 geographic distribution of *Artemisia herba alba* **[7]**.

I.1.5 Traditional Uses of Artemisia herba alba

Artemisia herba alba, commonly known as "wormwood," is a plant that is native to the steppes of the Middle East and North Africa. Local populations extensively use it to add flavor to tea and coffee and to treat various ailments like coughs, colds, intestinal issues, bronchitis, neuralgias, hypertension, and as an antidiabetic agent. **[3,4,19]**.

Artemisia herba alba is widely employed in Algerian folk medicine to treat gastric disorders such as (diarrhea, abdominal cramps). and it is used in cases of healing external wounds, eye infection, colds, obesity, and it is also considered helminthiasis. In south-eastern Morocco, *Artemisia herba alba* is employed in the treatment of hypertension and diabetes **[20]**. In addition, is extensively employed by the Bedouins of the Negev (Palestine) to treat gastrointestinal disorders **[21]**. and In Tunisia is used as an antidiabetic **[22]**.

I.1.6 Chemical composition of *Artemisia herba alba*

In Maghreb *Artemisia herba alba* plants are an important source of forage. In reality, the plant has significantly lower cellulose even though its external appearance indicates the opposite (17 to 33%). The amount of raw protein in the dry substance varies from 6 to 11%, of which 72% are amino acids. The rate of β-carotene varies between 1.3 and 7 mg/kg depending on the season **[23]**. The energy value of *Artemisia herba alba*, relatively low in winter (0.2 to 0.4 FU/kg DS),

increases rapidly in spring (0.92 FU/kg DS) to decrease again in summer (0. 6 FU/kg DS), in autumn, the rains of September cause a new period of growth and the energy value increases again (0.8 FU/kg DS) [24].

Artemisia herba alba is a plant rich in secondary metabolites that have therapeutic potential. Several secondary metabolites have been extracted and identified from *Artemisia herba alba*, the most significant of which are include volatile constituents (essential oil), and non-volatile constituents such as flavonoids and Sesquiterpene lactones.

I.1.6.1 Essential oils

Extensive research has been conducted on the phytochemical constituents of *A. herba alba*, particularly its essential oils. These oils exhibit variations in composition depending on the geographical location of the plant's growth, including differences between localities within the same country. As a result, various chemotypes of the plant have been identified.

In an Algerian oil, a camphor chemotype was predominant in Boussaâda (49. 3 %) [25], in Souk Ahrass (34 .34%) [26], and in Msila (19. 4%) [27]. Another study from Djelfa showed that oil A. *herba alba* chemotype is davanon which consists mainly of davanon (62.2%) [28], another Chemotype containing chrysanthenone (16.2%) was found in Oum el bouaghi [29].

In various regions of Tunisia, the major components of *A. herba alba* oil were found to be α and β-thujones. For instance, in Tabarka, the dominant component was β-thujones (23.29%) [30], In Gafsa, α- thujones accounted for 8.73% [31], while in Mednine, both β-thujones (58%) and α-thujones (49.3%) were present [32]. In Matmata, α-thujones made up 43.85% [33]. Additionally, in another study of Tunisian *Artemisia herba alba* oil, the primary constituents were found to be thujones, cineole, camphor, chrysanthenone, borneol, sabinyl acetate, chrysanthenyl acetate, davanone, and davana ethers. Some samples also contained significant amounts of monoterpenes and sesquiterpenes as major components [34].

In Morocco, various Chemotypes were identified in several regions, in Taroudant the major component was α- thujones (59.07 %) [35], Verbenol was predominant in Er-Rachidia (21.83 %) [36]. In another study, the plant was collected from Guercif during two different periods and a chrysanthenone Chemotype was isolated and identified; the first was identified in April with a rate (47.71%), and the second Chemotype was identified in June with a rate (48.45%) [37], Moreover, experimental evidence showed the presence of a camphor and chrysanthenone chemotypes with a rate (31.9%),(52.5%) respectively in Machraa, in Laayoun chrysanthenone (35.3%), camphre (43.3%), in Tafouralt chrysanthenone (42.5%), camphre (46.2%), in Sidi Chefi chrysanthenone

(30.6%), camphre (43%), in Bentayet camphre (43 and 39.6%), in Midar camphre (45.6 and 42.8%), in Boudnib α- thujones (73.8 and 44.2%) and in Guelmina α- thujones (54.4 and 65.3%) [38].

In Jordan *A. herba alba* essential oil was characterized, α /β-thujones, 1,8-cineole were found to be the major Chemotypes with a rate equal to (22.9%), (25.1%), (20.1%) respectively [2]. Another α –thujones was found in Amman to be the major component with value (16.2%) [39].

Studies from Jaén located in Spain showed that 1,8-cineole, p-cymene, davanone, and chrysanthenone were found to be the major constituents with rates (41.8%), (20.6%), (18.1%), (36.4%) [40], in Aranjuez a camphor chemotype (15%) was predominant [41].

I.1.6.2 Flavonoids of *Artemisia herba alba*

The flavonoids found in *A. herba alba* show a wide variety of chemical compounds. An analysis of aerial parts collected from northern Iraq reported the existence of Quercetin chemotype [42].

An examination of aerial parts collected from Tunisia showed the existence of Catechin, Epicatechin, Naringenin, Quercetin, Kaempferol, and Apigenin [43].

In the Algerian region of Djelfa, a comprehensive analysis of the aerial parts of *A. herba alba* led to the successful identification of twelve previously uncharacterized flavonoids. These newly discovered flavonoids include 5,3′-dihydroxy-7,4′-dimethoxyflavanone, Tomentin, Vitexin, Tectorigenin, Iristectorigenin A, Chrysoeriol, Iristectorigenin B, Irigenin, Cirsiliol, Skullcapflavon II, Skullcapflavon I, and cirsilineol. This investigation marks the first-time characterization of these specific flavonoids from *A. herba alba* in Djelfa, Algeria. [44].

Studies from Sinai is located in Egypt showed that aerial parts of *A. herba alba* contain eight flavonoids O- and C-glycoside [7]. Moreover, experimental evidence from Lebanon detected the presence of two flavonoids hispidulin and cirsilineol [45].

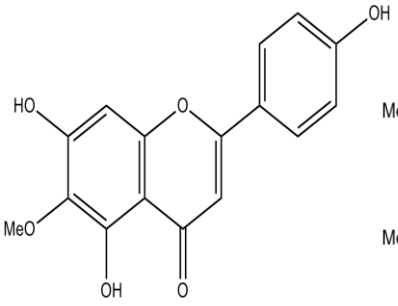

Hispidulin

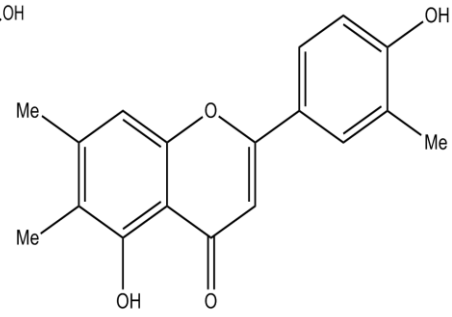

Cirsilineol

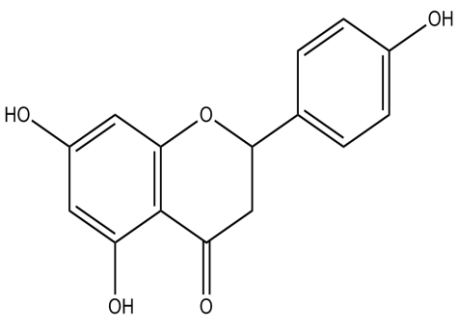

Naringenin

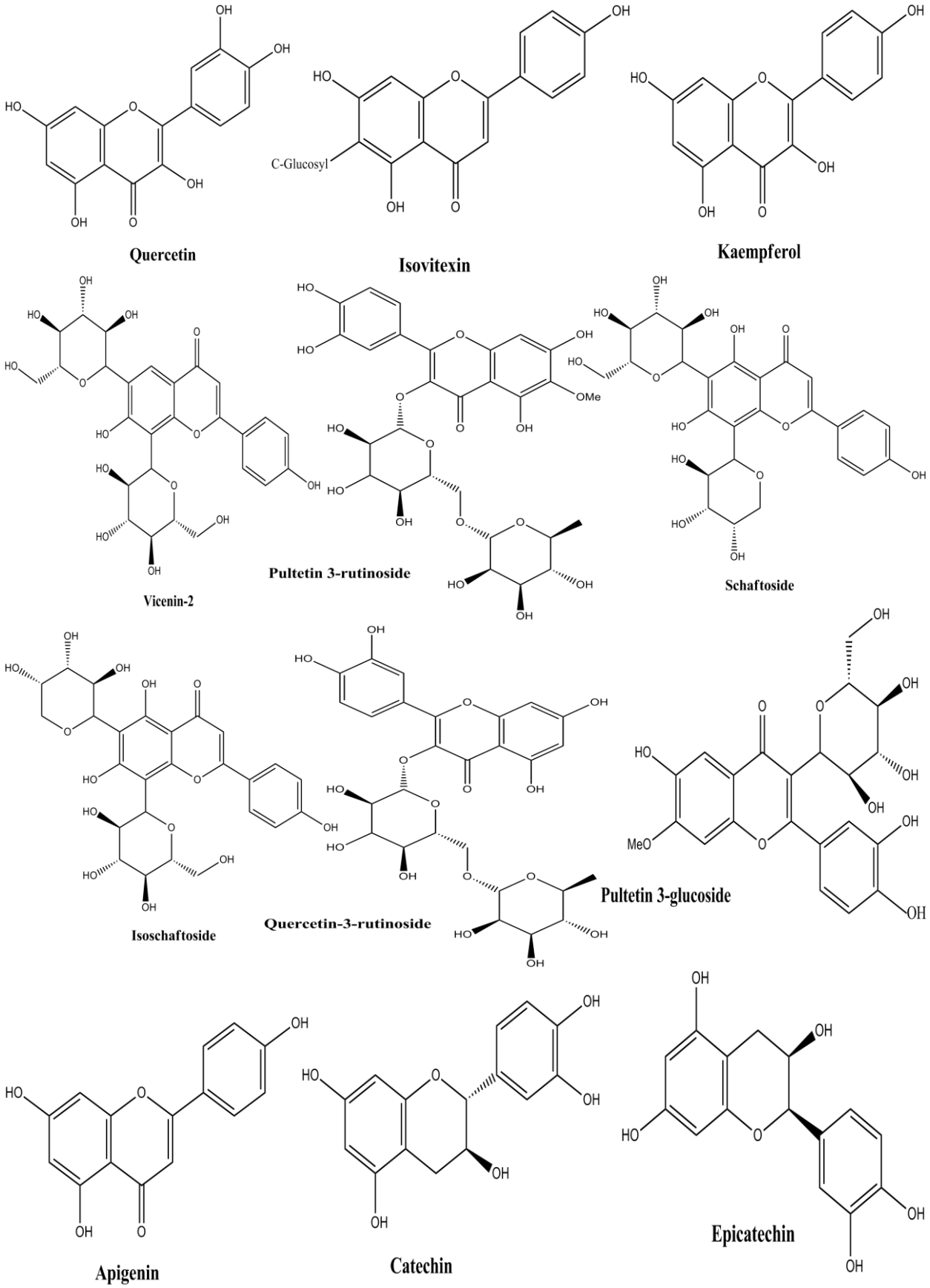

Figure I.3 The main Flavonoids identified in *Artemisia herba alba* **[7,43]**.

I.1.6.3 Sesquiterpene lactones

Sesquiterpene lactones are among the most important natural constituents identified in *Artemisia herba alba*, and they are mainly responsible for the importance of these plants in medicine and pharmacy.

Several chemotypes of Sesquiterpene lactones have been found in the aerial parts of *Artemisia herba alba*, the Eudesmanolides followed by germacranolides seem the most abundant chemotypes in this species.

Various experimental evidence has studied the chemical components of the Moroccan, Algerian, and Egyptian species of *A. herba alba*, and demonstrated that this genus is rich in Sesquiterpene lactones **[1,7,46]**.

In Palestine, several phytochemical studies have identified five different chemotypes from aerial parts of *A. herba alba* in addition several Sesquiterpene lactones have been successfully identified in *A. herba-alba* collected from several locations in Spain **[7]**.

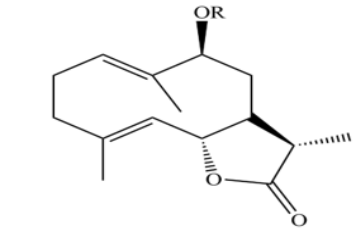

R=COMe, Herbolide A **(1)**
R= H, Deacetylherbolide A **(2)**

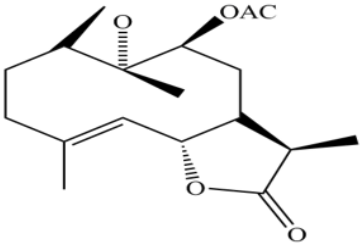

Herbolide B **(3)**

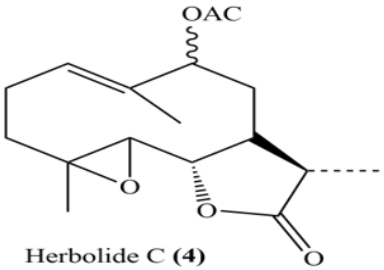

Herbolide C **(4)**

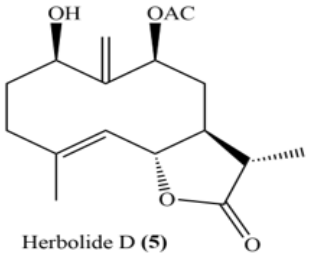

Herbolide D **(5)**

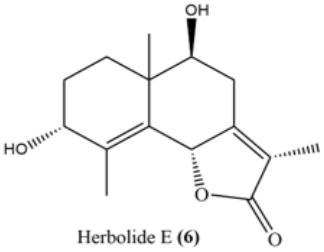

Herbolide E **(6)**

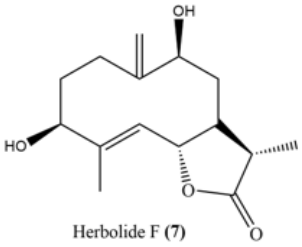

Herbolide F **(7)**

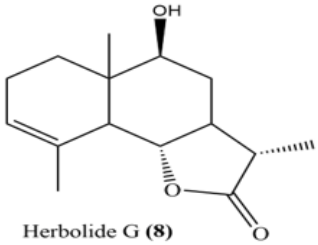

Herbolide G **(8)**

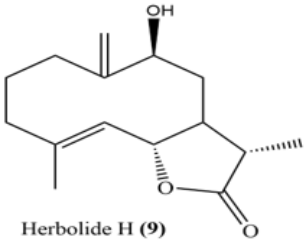

Herbolide H **(9)**

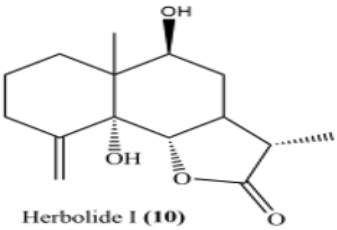

Herbolide I **(10)**

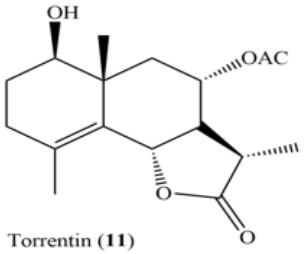

Torrentin **(11)**

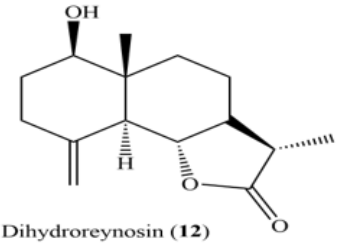

Dihydroreynosin **(12)**

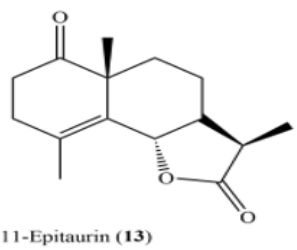

11-Epitaurin **(13)**

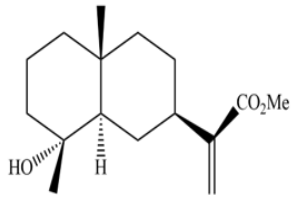

Vachanic acid (**14**)

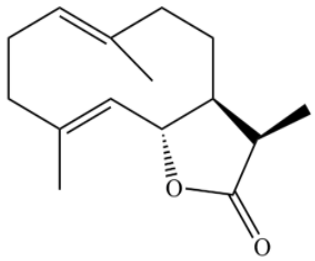

α,13–Dihydrocostunolide (**15**) 11

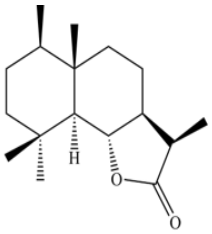

R1=H,R2=Me,R3=OH, 11-Epicolartin (**16**)
R1=OH,R2=Me,R3=OH, 1β–Hydroxy-11-epicolartin (**17**)
R1=OH,R2=Me,R3=Me, 1β–Hydroxy-4,11-diepicolartin (**18**)

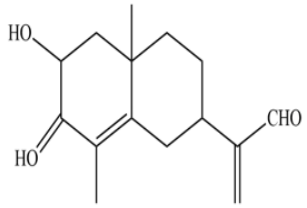

2β-Hydroxy-13-oxo-α-cyperene (**19**)

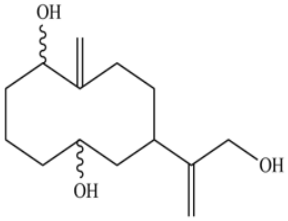

1β,5,12–Trihydroxygermacra-1(10),4(15),11(13)-triene (**20**)

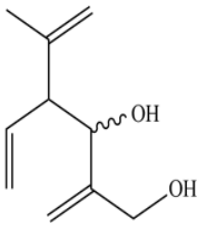

7-Hydroxy-5,6-dehydro-4,5-dihydrolyratrol (**21**)

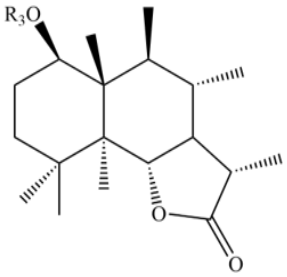

R1=H,R2=OH,R3=Ac,R4=H,R5=H,5a-Hydroxy-11,
13-Dihydroreynosin acetate (**22**)
R1=R2=R3=R4=H,R5=OH,9b-Hydroxy-11,13-dihydroreynosin (23)

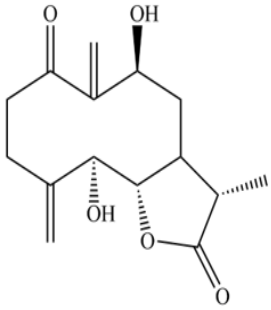

5β,9β–Dihydroxy-1-oxo-germacra-1(10),4(15)-dien-12,6-olide (**24**)

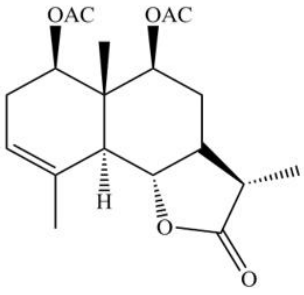

1ß,9ß-Diacetoxyeudesm-3-en-6ß,11ßH-12,6-olide (**25**)

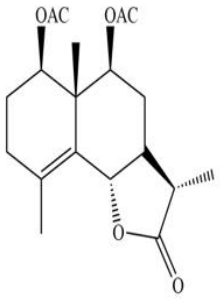

1ß,9ß-Diacetoxyeudesm-4-en-6ß,11bH-12,6-olide (**26**)

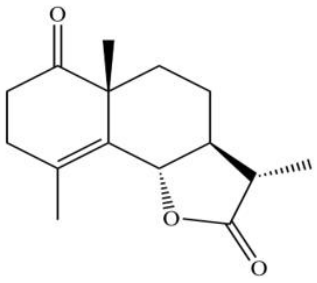

Taurin (**27**)

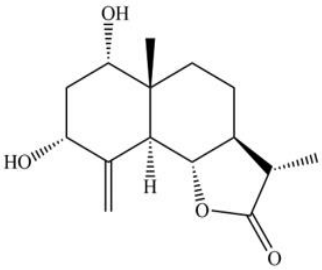

Erivanin (**28**)

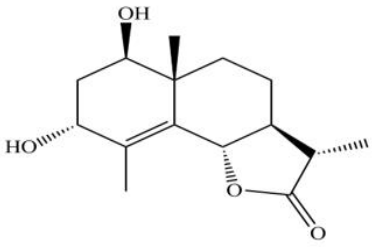

Isoerivanin (**29**)

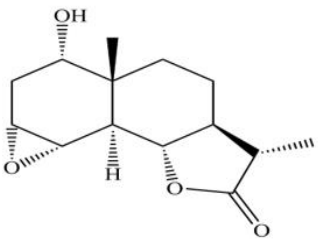

Herbalbin (**30**)

Figure I.4 Sesquiterpene lactones from *A. herba alba* growing in Egypt, Morocco, Spain, Algeria and palastine **[1,7,46]**.

I.1.7 Biological activities of *Artemisia herba alba*

In addition to their traditional uses, various experimental evidence has proven that *Artemisia herba Alba* has various biological features as an antioxidant **[6,47-49]**, antibacterial **[4,32,50]**, anti-venom **[51]**, Antileshmanial **[7]**, antifungal and anti-inflammatory **[2,5]**, antidiabetic **[52]**, anti-malarial, antispasmodic, antihypertensive **[16]**.

I.1.8 Toxicological properties

Little studies have proven that aqueous *Artemisia herba alba* extract has a toxic effect on fertility and the reproductive system after injecting it into female rats in two different periods **[53]**, Treatment at a dose of 375 and 500 µg.ml−1 of the extract induced a reduction in bone marrow cells division with induction of chromatid exchanges and micronucleus formation **[54]**. According to another recent study, *Artemisia herba alba* causes acute renal failure **[55]**.

I.2 The species *Punica granatum L*

I.2.1 Morphology and ecology

Pomegranate develops as a shrub or small tree, with many trunks that have a bushy appearance. It typically grows to a height of 5 to10m and is evergreen in the tropics but deciduous in subtropical and temperate areas **[56]**. The trunk is coated by a red-brown bark that eventually turns gray, the branches are rigid, angular, and frequently spiny **[57]**. The bark color shifts from the initial pink, purple, or light green with pink-purple spots or stripes to dark gray with maturation, Young leaves are reddish in color, and as they mature, they turn green **[58]**. Leaves are opposite or sub-opposite, often crowded on short lateral shoots, short-petioled, simple, entire, exstipulate, 2–8 cm long, oblong or obovate, glossy, bright green, glabrous, and glandular **[56,59]**. The flowers appear in clusters of 1 to 5 one of them terminal and the rest marginal, short, or without peduncle, their color is red and rarely yellow or white, odorless **[60]**. *Pomegranate* fruits are globose or slightly flattened, 5 to 12cm in diameter, and have a weight of 200-650 g **[57,59]**. The color of the fruit peel varies from green, pink, reddish, and dark red, with some cultivars, it appears black in color, with a thickness ranging from 1.5 to 4.24 mm depending on the variety **[57]**. The edible part (arils) of *pomegranate* fruit is separated by white pericarp, and is about 55%-60% of the total fruit weight and contains 80% juice and 20% seeds, the color of arils can change from white to deep red depending on the variety **[57,58]**.

Punica granatum L can occur in desert margins and is well adapted to hot dry summer, and cold winter having saline water and soil, it also can grow in various types of soils, Deep sandy

clay soils are ideal for *pomegranate* cultivation, and places with hot and long summers provide the optimum growth, performance, and product quality, *Pomegranate* is harmed at temperatures below 12 °C, so sweet pomegranates are more susceptible than sour pomegranates **[60]**. Flowering occurs from May to August, with fruits occurring at the end of September **[61]**.

Figure I.5 Photograph of *Punica granatum L*: (**a)** tree; **(b)** leaves; **(c)** flowers; and **(d)** fruits.

I.2.2. Nomenclature

I.2.2.1 Scientific name: *Punica granatum L*.

I.2.2.2 Vernacular name: According to the languages spoken in each country, the vernacular name of *Punica granatum L* varies.

Table I.2 Displays some Vernacular names of *Punica granatum L* **[62]**.

India	Dadima, Dalima, Dalim, Anar
Brazilian	Roma, Romeira, Romazeira
German	Granatapfel
French	Grenade
Spanish	Granada (the fruit), granado (the plant)
Italian	Melograna to, Melogranograna to, Pomograna to
Arabic	roman
English	*pomegranate*

I.2.3 Taxonomy

The botanical classification of *Punica granatum L* is shown below, according to **[63]**.

Table I.3 Botanical classification of *Punica granatum L*.

Kingdom	Plantae
Division	Tracheophyta
Class	Magnoliopsida
Order	Myrtales
Family	Lythraceae
Genus	Punica
Species	*Punica granatum L*

I.2.4. Origin and Geographical Distribution of *Punica granatum L*

Punica granatum L is the most common and widely cultivated species. it is mainly native to Persia (modern-day Iran) and adjacent countries **[64]**. Today, *pomegranate* is cultivated in most regions of the world, is distributed in Mediterranean nations (Algeria, Tunisia, Turkey, Egypt,

Spain, and Morocco) as well as the United States of America, Russia, this plant is thought to have spread primarily from Iran to other parts of the world, such as the Mediterranean area, Turkish European borders, the American southwest, California, and Mexico [62].

I.2.5 Traditional Uses of *Punica granatum L*

Punica granatum L is widely utilized in folk medicine by many cultures to treat several diseases. the different plant parts of plant including the seed extract, fruit, flower, and leaves were used in folk medicine to treat ulcers, snakebite, hepatic damage, dysentery, diarrhea, helminthiasis, hemorrhage, and respiratory problems [64]. The peel and the juice of the fruit are used as an oral drug in the treatment of colic, colitis, leucorrhea, and gastric disorders, diabetes, cancer, and blood pressure control [65,66].

I.2.6 Some chemical composition of *Punica granatum L*

I.2.6.1 Organic Acids and Phenolic Acids

The predominant organic acids in *Punica granatum L* juice are malic acid and critic acid [67]. In addition, different organic acids were investigated in *Punica granatum L* juice such as fumaric acid, oxalic acid, quinic acid, succinic acid, tartaric acid, and ascorbic acid, most of which have been found in leaves, fruit rind, seeds [67-71]. Typically, *pomegranate* fruit peel, juice, and flowers contain phenolic acids, especially benzoic acid, and cinnamic acid derivatives [71].

I.2.6.2 hydrolyzable tannins and their derivatives

Among the phytochemical constituents of *Punica granatum L*, hydrolyzable tannins have been intensively examined. A study showed that ellagitannins extracted from fruit peel are the predominant [72]. Moreover, an experimental evidence showed the presence of ellagitannins C-glycosides, punicacorteins A–D (ellagitannins with a gallagic Acid), and punigluconin (an ellagitannins with a gluconic acid core) in stem barks [73]. Granatins A and B are the most abundant hydrolyzable tannins in leaves, with punicalagins and punicalins found in trace amounts, moreover ellagitannins with galloyl and/ hexahydroxydiphenoyl substitutions have been found in leaves [71].

I.2.6.3 Other compositions

Anthocyanoside, another main component found in the flower and fruit, is responsible for the red color of arils. delfinidin-3,5-diglucoside, Cyanidin-3-glucoside, delfinidin-3-glucoside, cyanidin-3,5-diglucoside, cyanidinrutinoside, cyanidinpentoside, pelargonidin-3,5-diglucoside, and pelargonidin-3-glucoside are the predominant anthocyanins identified in the different parts of *Punica granatum L* [74-76].

Punica granatum L leaves and peel contains a diversity of flavonoids such as catechin, Quercetin, gallocatechin, Epicatechin, Kaempferol, and Apigenin [76,77]. Other bioactive compounds were found in different parts of *Punica granatum L* including alkaloids (e.g. Pseudopelletierine, Pelletierine, Isopelletierine, Methylpelletierine,1-pelletierine, dl-pelletierine, and Methylisopelletierines) [76].

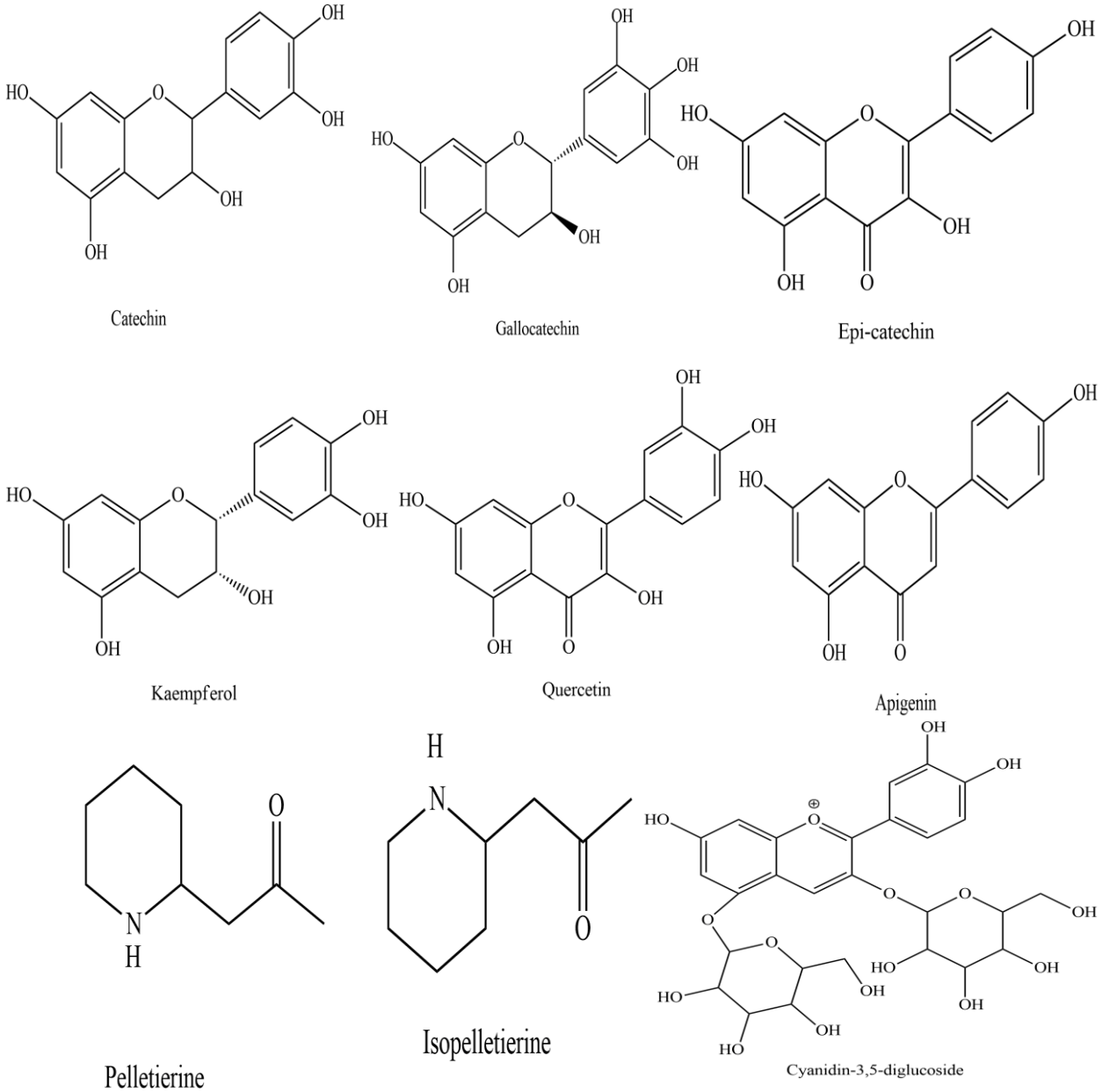

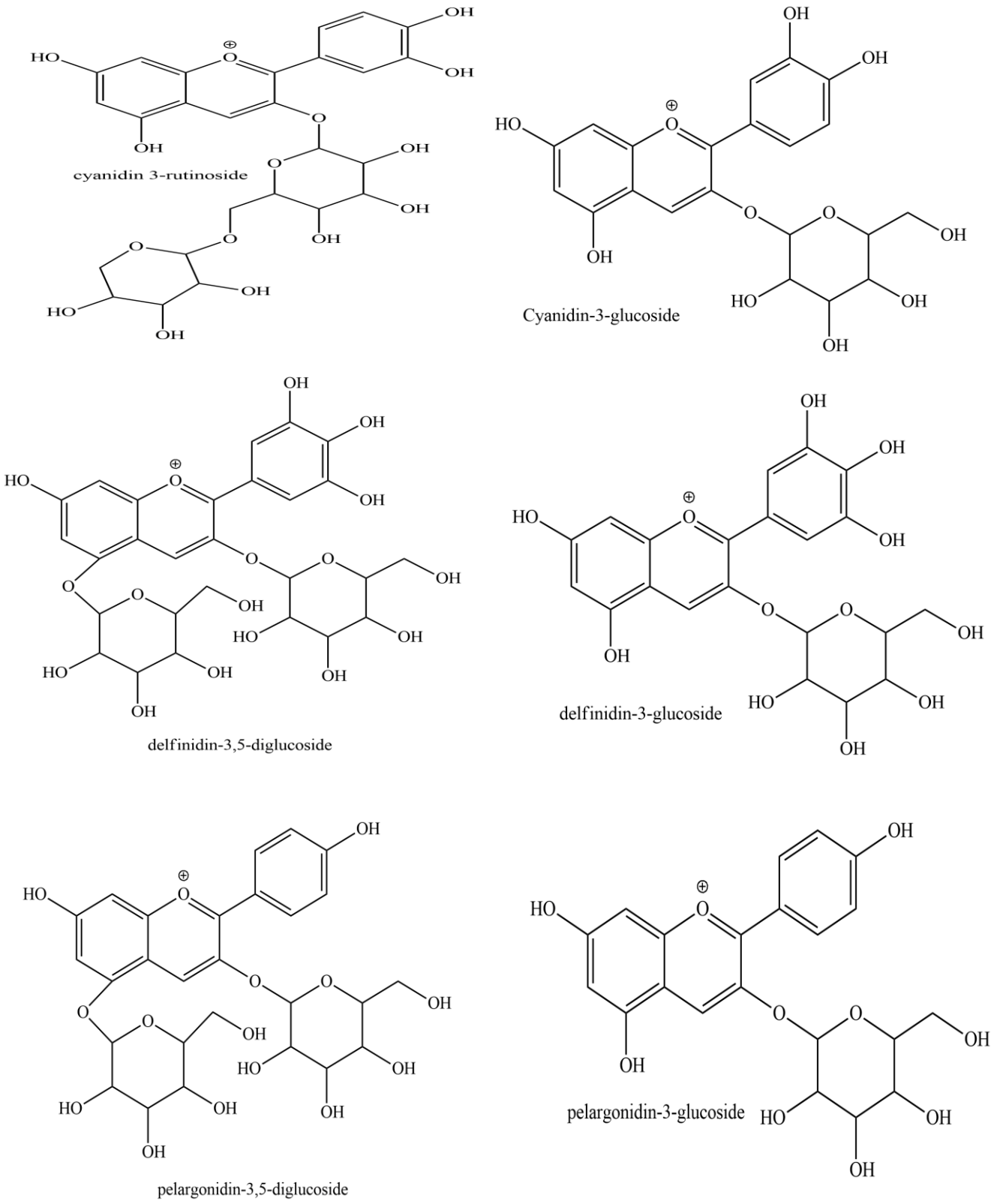

Figure I.6 The main anthocyanoside, flavonoids and alkaloids compounds identified in *Punica granatum L* **[76]**.

I.2.7 The biological activities of *Punica granatum L* peel

I.2.7.1 Antioxidant activity

In prior research, the antioxidant activity of 28 different fruits (peel, pulp, and seed) was evaluated using the ferric reducing power (FRAP) assay. In comparison to other fruit parts, *Punica granatum L* peel extract showed the highest reducing power **[78]**.

In another investigation, DPPH and ABTS assays were used to assess the antioxidant activity of the peel of eight different fruits. Results indicated that the *Punica granatum L* peel extract had the highest antioxidant activity in both assays **[79]**.

Punica granatum L is known for its antioxidant properties. All parts of the plant, including the juice, seeds, and peel, contain bioactive compounds that are responsible for these properties. The fruit peel is one of the most important parts of this plant because of its significant antioxidant activity compared to other plant parts **[80-82]**.

I.2.7.2 Antibacterial activity

The antibacterial activity of *Punica granatum L* peel extract was tested against bacteria isolated from poultry meat (Pseudomonas stutzeri), results demonstrated a high sensitivity of Pseudomonas stutzeri to *Punica granatum L* peels extract as compared to standard antibiotic discs employed **[83]**.

A test against some food-borne pathogens including Listeria mono-cytogenes, S. aureus, Escherichia coli and Yersinia enterocolitica confirmed that methanolic extract of peel has a significant inhibition against the different strains as compared to the other extracts **[84]**. Another study showed that the different extracts including, fruit peels, and edible parts of *Punica granatum L* have an important antibacterial activity against all strains tested **[85]**.

The effect of *pomegranate* peel extract concentration (0.1, 0.2, 0.3, 0.4, and 0.5 mg/ml) on the growth of pathogenic bacteria (Staphylococcus aureus, Escherichia coli, Proteus Vulgaris, Candida tropical, Candida albicans) was studied in a previous study. In which all strains showed significant sensitivity at 0.3 mg/ml, except Escherichia coli, which showed considerable sensitivity at 0.2 mg/ml **[86]**.

I.2.7.3 Antidiabetic activity

The anti-diabetic activity was performed on a group of diabetic and normal rats. The treatment with *Punica granatum L* peel extract resulted in a significant decrease in blood glucose

and an increase in insulin levels in both groups of rats, as well as an improvement in body weight. The pancreas of both groups of rats showed an increase in the number of beta cells **[87]**.

I.2.7.4 Antifungal activity

an assessment demonstrated that ethanolic extract of *Punica granatum L* peels has an inhibitory effect against two phytopathogenic strains **[88]**.

Punica granatum L peel aqueous extracts were tested in vitro for antifungal activity against six rot fungi that cause fruit and vegetable degradation during storage, findings revealed no effect on the growth rate of P. digitatum, On the other hand, an increase in the growth rate of both P. expansum and B. cinerea, while the growth rates of both A. alternata, S. botryosum, and Fusarium spp were effectively inhibited by peel aqueous extract **[89]**.

I.2.7.5 Anti-cancer activity

Previous studies showed that *pomegranate* peel prevents the invasion of cancer cells. It has been shown to possess anti-cancer properties in cases of breast cancer, lung cancer, and prostate cancer **[90]**.

The cytotoxic effects of pomegranate peel extract on HTB140, HTB177, MCF7, and HCT116 human cancer cell lines, as well as MRC-5 regular fibroblasts, were assessed using MTT assay. The findings revealed that *pomegranate* peel extract displayed selective cytotoxicity for cancer cells **[91]**.

I.2.7.6 Antiulcer activity

Punica granatum L peel extract has an activity inhibitor of stomach ulcers induced by aspirin and ethanol due to its antioxidant properties. For doses of 250 and 500 mg/kg of hydro alcoholic peels extract (70% methanol v/v), the percentage inhibition is respectively 22.37% and 74.21% for ulcers induced by aspirin and 21.95% and 63.41% for those induced by ethanol **[92]**.

I.2.8 Toxicity Studies

There are relatively none in vivo or in vitro studies that describe the toxic or detrimental effect of *Punica granatum L* peel on any mammalian system **[10]**.

References

References

[1] M. Talbi, T. Ainane, D. Boriky, L. Bennani, M. Blaghen, and M. Elkouali, "Antibacterial activity of eudesmanolide compounds isolated from medicinal plant Artemisia herba-alba," *J.Mater. Environ. Sci.*, vol. 6, no. 8, pp. 2125–2128, 2015.

[2] M. S. Abu-Darwish *et al.*, "Artemisia herba-alba essential oil from Buseirah (South Jordan): Chemical characterization and assessment of safe antifungal and anti-inflammatory doses," *J. Ethnopharmacol.*, vol. 174, pp. 153–160, Nov. 2015, doi: 10.1016/j.jep.2015.08.005.

[3] N. Bouzidi, K. Mederbal, and B. R. G, "Antioxidant Activity of Essential Oil of Artemisia herba alba," vol. 6, no. 5, pp. 59–65, 2016.

[4] S. Lakehal, C. Chaouia, and F. Z. Benrebiha, "chemical composition and antibacterial activity of the essential oil of Artemisia herba alba asso. from Djelfa," *Rev. Agrobiol.*, vol. 7, no. 2, pp. 491–501, 2017.

[5] M. Mehani *et al.*, "Antifungal activity of Artemisia herba-alba on various Fusarium," *Phytotherapie*, vol. 16, no. 2, pp. 87–90, 2018, doi: 10.1007/s10298-016-1071-2.

[6] S. E. Laouini, A. Kelef, and M. R. Ouahrani, "Free radicals scavenging activity and phytochemical composition of *astermisia* (*Herba-Alba*) extract growth in Algeria," *J. Fundam. Appl. Sci.*, vol. 10, no. 1, p. 268, 2018, doi: 10.4314/jfas.v10i1.20.

[7] A. E. H. H. Mohamed, M. A. El-Sayed, M. E. Hegazy, S. E. Helaly, A. M. Esmail, and N. S. Mohamed, "Chemical constituents and biological activities of Artemisia herba-alba," *Rec. Nat. Prod.*, vol. 4, no. 1, pp. 1–25, 2010, doi: 10.13140/RG.2.1.2544.8806.

[8] M. N. Al-Muammar and F. Khan, "Obesity: The preventive role of the pomegranate (Punica granatum)," *Nutrition*, vol. 28, no. 6, pp. 595–604, 2012, doi: 10.1016/j.nut.2011.11.013.

[9] N. Kumar and S. Kumar, "Functional Properties of Pomegranate (Punica granatum L.)," *Pharma Innov. J.*, vol. 7, no. 10, pp. 71–81, 2018.

[10] S. K. Middha, T. Usha, and V. Pande, "A Review on antihyperglycemic and antihepatoprotective activity of eco-friendly punica granatum peel waste," *Evidence-based Complement. Altern. Med.*, vol. 2013, pp. 1–10, 2013, doi: 10.1155/2013/656172.

[11] N. M. Abdel-Hady, “Quantitative Diversity of Phenolic Content in Peels of Some Selected Egyptian Pomegranate Cultivars Correlated to Antioxidant and Anticancer Effects,” vol. 9, no. 8, pp. 4823–4830, 2013.

[12] A. H. Rahmani, M. A. Alsahli, and S. A. Almatroodi, “Active constituents of pomegranates (Punica granatum) as potential candidates in the management of health through modulation of biological activities,” *Pharmacogn. J.*, vol. 9, no. 5, pp. 689–695, 2017, doi: 10.5530/pj.2017.5.109.

[13] V. Akbarpour, K. Hemmati, and M. Sharifani, “Physical and Chemical Properties of Pomegranate (Punica granatum L.) Fruit in Maturation Stage,” *Environ. Sci*, vol. 6, no. 4, pp. 411–416, 2009.

[14] I. L. Pereira De Melo, E. Bonifácio, T. De Carvalho, and J. Mancini-Filho, “Journal of Human Nutrition & Food Science Pomegranate Seed Oil (Punica Granatum L.): A Source of Punicic Acid (Conjugated α-Linolenic Acid),” *J Hum Nutr Food Sci*, vol. 2, no. 1, pp. 1–11, 2014.

[15] M. Fourati *et al.*, “Bioactive Compounds and Pharmacological Potential of Pomegranate (Punica granatum) Seeds - A Review,” *Plant Foods Hum. Nutr.*, vol. 75, no. 4, pp. 477–486, 2020, doi: 10.1007/s11130-020-00863-7.

[16] A. Moufid and M. Eddouks, “Artemisia herba alba: A Popular Plant with Potential Medicinal Properties,” *Pakistan J. Biol. Sci.*, vol. 15, no. 24, pp. 1152–1159, 2012, doi: 10.3923/pjbs.2012.1152.1159.

[17] M. L, D, Belkacemi, “etude pyhtochimique d’une plante medicinal de l’est algerien (Artemisia herba alba),” 2011.

[18] R. Belhattab, L. Amor, J. G. Barroso, L. G. Pedro, and A. Cristina Figueiredo, “Essential oil from Artemisia herba-alba Asso grown wild in Algeria: Variability assessment and comparison with an updated literature survey,” *Arab. J. Chem.*, vol. 7, no. 2, pp. 243–251, 2014, doi: 10.1016/j.arabjc.2012.04.042.

[19] M. B. Goudjil *et al.*, “Bioactivity of Artemisia Herba alba essential oil against plant pathogenic fungi,” *Der Pharma Chem.*, vol. 8, no. 3, pp. 46–52, 2016.

[20] A. Tahraoui, J. El-Hilaly, Z. H. Israili, and B. Lyoussi, “Ethnopharmacological survey of plants used in the traditional treatment of hypertension and diabetes in south-eastern Morocco (Errachidia province),” *J. Ethnopharmacol.*, vol. 110, no. 1, pp. 105–117, 2007, doi: 10.1016/j.jep.2006.09.011.

[21] I. Jaouadi, A. T. Koparal, R. B. Bostancioğlu, M. T. Yakoubi, and M. El Gazzah, “The anti-angiogenic activity of Artemisia herba-alba’s essential oil and its relation with the harvest period,” *Aust. J. Crop Sci.*, vol. 8, no. 10, pp. 1395–1401, 2014.

[22] S. Bourgou, S. Tammar, N. Salem, K. Mkadmini, and K. Msaada, “Phenolic Composition, Essential Oil, and Antioxidant Activity in the Aerial Part of Artemisia Herba-Alba from Several Provenances: A Comparative Study,” *Int. J. Food Prop.*, vol. 19, no. 3, pp. 549–563, 2016, doi: 10.1080/10942912.2015.1040495.

[23] F. Fenardji, M. Klur, C. Fourlon, and R. Ferrando, “Contribution à l’étude de l’armoise blanche (Artemisia herba alba L.),” *Rev. d’élevage médecine vétérinaire des pays Trop.*, vol. 27, no. 2, p. 203, 1974, doi: 10.19182/remvt.7966.

[24] A. Ferchichi, C. C. E. Ferjani, and R. Arides, “Caractérisation de la variabilité du comportement phytologique de certaines populations d ’ Artemisia herba-alba du sud tunisien,” no. June 2014, pp. 211–216, 1989.

[25] N. Dahmani-Hamzaoui and A. Baaliouamer, “Chemical composition of algerian artemisia herba-alba essential oils isolated by microwave and hydrodistillation,” *J. Essent. Oil Res.*, vol. 22, no. 6, pp. 514–517, 2010, doi: 10.1080/10412905.2010.9700386.

[26] D. Amel, T. Faiza, B. Sabrina, B. Mahieddine, H.-S. Nacera, and C. Azzedine, “Chemical composition and insecticidal activity of essential oil of Artemisia herba alba (Asteraceae) against Ephestia kuehniella (Lepidoptera: Pyralidae),” *Int. J. Biosci.*, vol. 10, no. 2, pp. 130–137, 2017, doi: 10.12692/ijb/10.2.130-137.

[27] T. Dob and T. Benabdelkader, “Chemical Composition of the Essential Oil of Artemisia herba-alba Asso Grown in Algeria,” *J. Essent. Oil Res.*, vol. 18, no. 6, pp. 685–690, 2006, doi: 10.1080/10412905.2006.9699206.

[28] Z. TOUIL, Souhila, B,F, “composition chimique et activité antimicrobienne des huiles essentielles d’Artemisia herba alba asso et artemisia campestris L. de la region aride de djelfa,” *agrobiologia*, pp. 1–138, 2012.

[29] S. Rekkab, I. Abaza, S. Chibani, A. Kabouche, and Z. Kabouche, "Chemical composition of the essential oil of aerial parts of Artemisia herba-alba Asso. from Oum El-Bouaghi (Algeria) and chemotaxonomic survey," *J. Mater. Environ. Sci.*, vol. 7, no. 12, pp. 4383–4390, 2016.

[30] S. Selmi *et al.*, "Antioxidant properties of Artemisia herba-alba and Eucalyptus camaldulensis essentials oils on malathion-induced reproductive damage in rat," *RSC Adv.*, vol. 6, no. 112, pp. 110661–110673, 2016, doi: 10.1039/c6ra18268b.

[31] S. Zouari, N. Zouari, N. Fakhfakh, A. Bougatef, M. A. Ayadi, and M. Neffati, "Chemical composition and biological activities of a new essential oil chemotype of Tunisian Artemisia herba alba Asso," *J. Med. Plants Res.*, vol. 4, no. 10, pp. 871–880, 2010, doi: 10.5897/JMPR09.506.

[32] H. Mighri, H. Hajlaoui, A. Akrout, H. Najjaa, and M. Neffati, "Antimicrobial and antioxidant activities of Artemisia herba-alba essential oil cultivated in Tunisian arid zone," *Comptes Rendus Chim.*, vol. 13, no. 3, pp. 380–386, 2010, doi: 10.1016/j.crci.2009.09.008.

[33] A. Akrout, "Etude des huiles essentielles de quelques plantes pastorales de la région de Matmata (Tunisie)," *Oprion Méditerranéennes*, vol. 292, pp. 289–292, 1983.

[34] H. Mohsen and F. Ali, "Essential oil composition of artemisia herba-alba from Southern Tunisia," *Molecules*, vol. 14, no. 4, pp. 1585–1594, 2009, doi: 10.3390/molecules14041585.

[35] H. Boukhebti *et al.*, "Chemical composition and antibacterial activity of Mentha pulegium L. and Mentha spicata L. essential oils," *Der Pharm. Lett.*, vol. 3, no. 4, pp. 267–275, 2011.

[36] M. Tilaoui, H. A. Mouse, A. Jaafari, R. Aboufatima, A. Chait, and A. Zyad, "Chemical composition and antiproliferative activity of essential oil from aerial parts of a medicinal herb Artemisia herba-alba," *Rev. Bras. Farmacogn.*, vol. 21, no. 4, pp. 781–785, 2011, doi: 10.1590/S0102-695X2011005000114.

[37] M. Ghanmi *et al.*, "Effect of harvest period on yield, chemical composition and bioactiviy sagebrush's (Artemisia herba-alba) essential oils in Guercif (Eastern region of Morocco)," *Phytotherapie*, vol. 8, no. 5, pp. 295–301, 2010, doi: 10.1007/s10298-010-0578-1.

[38] J. Paolini *et al.*, "Chemical variability of Artemisia herba-alba Asso essential oils from East Morocco," *Chem. Pap.*, vol. 64, no. 5, pp. 550–556, 2010, doi: 10.2478/s11696-010-0051-5.

[39] M. M. Hudaib and T. A. Aburjai, “Composition of the essential oil from artemisia herba-alba grown in jordan,” *J. Essent. Oil Res.*, vol. 18, no. 3, pp. 301–304, 2006, doi: 10.1080/10412905.2006.9699096.

[40] M. N. & A. S. Sofía Salido, Joaquín Altarejos, “Chemical Composition of the Essential Oil of Artemisia herba-alba Asso ssp. valentina (Lam.) Marcl.,” *J. Essent. Oil Res.*, vol. 13, no. 4, pp. 221–224, Jul. 2001, doi: 10.1080/10412905.2001.9699675.

[41] I. Feuerstein, A. Danin, and R. Segal, “Constitution of the essential oil from an Artemisia herba-alba population of Spain,” *Phytochemistry*, vol. 27, no. 2, pp. 433–434, 1988, doi: 10.1016/0031-9422(88)83114-5.

[42] M. J. Mohammed, U. Anand, A. B. Altemimi, V. Tripathi, Y. Guo, and A. Pratap-Singh, “Phenolic composition, antioxidant capacity and antibacterial activity of white wormwood (Artemisia herba-alba),” *Plants*, vol. 10, no. 1, pp. 1–14, 2021, doi: 10.3390/plants10010164.

[43] S. Bourgou, S. Tammar, N. Salem, K. Mkadmini, and K. Msaada, “Phenolic Composition, Essential Oil, and Antioxidant Activity in the Aerial Part of Artemisia Herba-Alba from Several Provenances: A Comparative Study,” *Int. J. Food Prop.*, vol. 19, no. 3, pp. 549–563, 2016, doi: 10.1080/10942912.2015.1040495.

[44] T. Souhila, B. Fatma Zohra, and H. S. Tahar, “Identification and quantification of phenolic compounds of Artemisia herba-alba at three harvest time by HPLC–ESI–Q-TOF–MS,” *Int. J. Food Prop.*, vol. 22, no. 1, pp. 843–852, 2019, doi: 10.1080/10942912.2019.1614051.

[45] S. M. Salah and A. K. Jäger, “Two flavonoids from Artemisia herba-alba Asso with in vitro GABA A-benzodiazepine receptor activity,” *J. Ethnopharmacol.*, vol. 99, no. 1, pp. 145–146, 2005, doi: 10.1016/j.jep.2005.01.031.

[46] M. Laid, M. E. F. Hegazy, A. A. Ahmed, K. Ali, D. Belkacemi, and S. Ohta, “Sesquiterpene lactones from Algerian Artemisia herba-alba,” *Phytochem. Lett.*, vol. 1, no. 2, pp. 85–88, 2008, doi: 10.1016/j.phytol.2008.04.002.

[47] A. H. Al-Mustafa and O. Y. Al-Thunibat, “Antioxidant activity of some Jordanian medicinal plants used traditionally for treatment of diabetes,” *Pakistan J. Biol. Sci.*, vol. 11, no. 3, pp. 351–358, 2008, doi: 10.3923/pjbs.2008.351.358.

[48] N. Ayad and H. Hemida, “Biological activities of phenolic extracts from Artemisia herba-alba Asso grown in western Algeria Biological activities of phenolic extracts from Artemisia herba-alba Asso grown in western Algeria,” no. February, 2022, doi: 10.5281/zenodo.6172855.

[49] K. Seddik, I. Nadjet, B. Abderrahmane, H. Daoud, and A. Lekhmici, “Antioxidant and antibacterial activities of extracts from Artemisia herba alba Asso. leaves and some phenolic compounds,” *J. Med. Plants Res.*, vol. 4, no. 13, pp. 1273–1280, 2010, doi: 10.5897/JMPR09.379.

[50] S. Lakehal and M. A, “Essential Oil Composition and Antimicrobial Activity of Artemisia herba– alba Asso Grown in Algeria,” *Med. Chem. (Los. Angeles).*, vol. 6, no. 6, pp. 435–439, 2016, doi: 10.4172/2161-0444.1000382.

[51] I. Jaouadi *et al.*, “Anti-hemolytic and anti-cytotoxic effect of two artemisia species (A. campestris and A. herba-alba) essential oil against snake venom,” *Int. J. Agric. Biol.*, vol. 18, no. 4, pp. 805–812, 2016, doi: 10.17957/IJAB/15.0174.

[52] A. Boudjelal *et al.*, “Antidiabetic Effects of Aqueous Infusions of Artemisia herba-alba and Ajuga iva in Alloxan-Induced Diabetic Rats,” *Planta Med.*, vol. 81, no. 9, pp. 696–704, 2015, doi: 10.1055/s-0035-1546006.

[53] M. M. Almasad, W. S. Qazan, and H. Daradka, “Reproductive toxic effects of Artemisia herba alba ingestion in female Spague-dawley rats,” *Pakistan J. Biol. Sci.*, vol. 10, no. 18, pp. 3158–3161, 2007, doi: 10.3923/pjbs.2007.3158.3161.

[54] S. M. Abderrahman and S. Jamal Shbailat, “Genotoxic and cytotoxic effects of Artemisia herba-alba on mammalian cells,” *Caryologia*, vol. 67, no. 4, pp. 265–272, 2014, doi: 10.1080/0144235X.2014.974355.

[55] M. A. Gacem, A. Ould El Hadj-Khelil, B. Boudjemaa, and H. Gacem, “Phytochemistry, Toxicity and Pharmacology of Pistacia lentiscus, Artemisia herba-alba and Citrullus colocynthis,” no. April, 2020, pp. 57–93.

[56] D. Holland, K. Hatib, and I. Bar-ya, “Pomegranate: Botany, Horticulture, Breeding,” vol. 35, 2009, pp. 127–192.

[57] M. Erkan and A. Dogan, “Pomegranate/Roma— Punica granatum,” in *Exotic Fruits*, Elsevier Inc., 2018, pp. 355–361.

[58] G. Pande and C. C. Akoh, “Pomegranate Cultivars (Punica granatum L.),” in *Nutritional Composition of Fruit Cultivars*, Elsevier Inc., 2015, pp. 667–689.

[59] J. A. Teixeira da Silva, T. S. Rana, D. Narzary, N. Verma, D. T. Meshram, and S. A. Ranade, “Pomegranate Biology And Biotechnology: A Review,” *Sci. Hortic. (Amsterdam).*, vol. 160, pp. 85–107, 2013, doi: 10.1016/j.scienta.2013.05.017.

[60] E. Shaygannia, M. Bahmani, B. Zamanzad, and M. Rafieian-Kopaei, “A Review Study on Punica granatum L,” *J. Evidence-Based Complement. Altern. Med.*, vol. 21, no. 3, pp. 221–227, 2016, doi: 10.1177/2156587215598039.

[61] R. W. Bussmann *et al.*, “Punica granatum L. Lythraceae,” in *Ethnobotany of the Mountain Regions of Far Eastern Europe*, 2020, pp. 1–6.

[62] I. Kumari, H. Kaurav, and G. Chaudhary, “Punica granatum L. (Dadim), Therapeutic Importance of World’s Most Ancient Fruit Plant,” *J. Drug Deliv. Ther.*, vol. 11, no. 3, pp. 113–121, 2021, doi: 10.22270/jddt.v11i3.4832.

[63] N. Panth, B. Manandhar, and K. R. Paudel, “Anticancer Activity of Punica granatum (Pomegranate): A Review,” *Phyther. Res.*, vol. 31, no. 4, pp. 568–578, 2017, doi: 10.1002/ptr.5784.

[64] A. A. Altaf *et al.*, “A Review on the Medicinal Importance of Pyridine Derivatives,” *Http://Www.Sciencepublishinggroup.Com*, vol. 1, no. 1, p. 1, 2015, doi: 10.5530/rjps.2013.4.3.

[65] D. Ricci, L. Giamperi, A. Bucchini, and D. Fraternale, “Antioxidant activity of Punica granatum fruits,” *Fitoterapia*, vol. 77, no. 4, pp. 310–312, 2006, doi: 10.1016/j.fitote.2006.01.008.

[66] A. D. Khwairakpam *et al.*, “Possible use of Punica granatum (Pomegranate) in cancer therapy,” *Pharmacol. Res.*, vol. 133, no. January, pp. 53–64, 2018, doi: 10.1016/j.phrs.2018.04.021.

[67] P. Mena *et al.*, “Rapid and comprehensive evaluation of (Poly)phenolic compounds in pomegranate (Punica granatum L.) Juice by UHPLC-MSn,” *Molecules*, vol. 17, no. 12, pp. 14821–14840, 2012, doi: 10.3390/molecules171214821.

[68] F. A. P. Melgarejo, D. M. Salazar, “Organic acids and sugars composition of harvested pomegranate fruits,” pp. 186–190, 2000, doi: 10.1007/s002170050021.

[69] P. Garima and C. C. Akoh, "Antioxidant capacity and lipid characterization of six georgia-grown pomegranate cultivars," *J. Agric. Food Chem.*, vol. 57, no. 20, pp. 9427–9436, 2009, doi: 10.1021/jf901880p.

[70] E. Poyrazoğlu, V. Gökmen, and N. Artık, "Organic Acids and Phenolic Compounds in Pomegranates (Punica granatum L.) Grown in Turkey," *J. Food Compos. Anal.*, vol. 15, no. 5, pp. 567–575, 2002, doi: 10.1006/jfca.2002.1071.

[71] S. Wu and L. Tian, "Diverse Phytochemicals and Bioactivities in the Ancient Fruit and Modern Functional Food Pomegranate (Punica granatum)," *Molecules*, vol. 22, no. 10, 2017, doi: 10.3390/molecules22101606.

[72] N. Seeram, R. Lee, M. Hardy, and D. Heber, "Rapid large scale purification of ellagitannins from pomegranate husk, a by-product of the commercial juice industry," *Sep. Purif. Technol.*, vol. 41, no. 1, pp. 49–55, 2005, doi: 10.1016/j.seppur.2004.04.003.

[73] I. Tanaka, T.; Nonaka, G.-I.; Nishioka, "Tannins and related compounds. XLI.: Isolation and characterization of novel ellagitannins, punicacorteins A, B, C, and D, and punigluconin from the bark of Punica granatum L," *Chem. Pharm. Bull.*, no. 34, pp. 656–663, 1986, doi: https://doi.org/10.1248/cpb.34.656.

[74] M. M. Sharrif and H. K. Hamed, "Chemical composition of the plant Punica granatum L. (Pomegranate) and its effect on heart and cancer," *J. Med. Plants Res.*, vol. 6, no. 40, pp. 5306–5310, 2012, doi: 10.5897/jmpr11.577.

[75] M. C. P. de A. Santiago *et al.*, "Analytical standards production for the analysis of pomegranate anthocyanins by HPLC," *Brazilian J. Food Technol.*, vol. 17, no. 1, pp. 51–57, 2014, doi: 10.1590/bjft.2014.008.

[76] S. Eghbali, S. F. Askari, R. Avan, and A. Sahebkar, "Therapeutic Effects of Punica granatum (Pomegranate): An Updated Review of Clinical Trials," *J. Nutr. Metab.*, vol. 2021, pp. 1–22, 2021, doi: 10.1155/2021/5297162.

[77] P. Bagri, M. Ali, S. Sultana, and V. Aeri, "New flavonoids from punica granatum flowers," *Chem. Nat. Compd.*, vol. 46, no. 2, pp. 201–204, 2010, doi: 10.1007/s10600-010-9568-7.

[78] C. Guo, J. Yang, J. Wei, Y. Li, J. Xu, and Y. Jiang, "Antioxidant activities of peel, pulp and seed fractions of common fruits as determined by FRAP assay," *Nutr. Res.*, vol. 23, no. 12, pp. 1719–1726, 2003, doi: 10.1016/j.nutres.2003.08.005.

[79] S. Okonogi, C. Duangrat, S. Anuchpreeda, S. Tachakittirungrod, and S. Chowwanapoonpohn, "Comparison of antioxidant capacities and cytotoxicities of certain fruit peels," *Food Chem.*, vol. 103, no. 3, pp. 839–846, 2007, doi: 10.1016/j.foodchem.2006.09.034.

[80] R. P. Singh, K. N. Chidambara Murthy, and G. K. Jayaprakasha, "Studies on the antioxidant activity of pomegranate (Punica granatum) peel and seed extracts using in vitro models," *J. Agric. Food Chem.*, vol. 50, no. 1, pp. 81–86, 2002, doi: 10.1021/jf010865b.

[81] S. K. Middha, T. Usha, and V. Pande, "HPLC evaluation of phenolic profile, nutritive content, and antioxidant capacity of extracts obtained from Punica granatum fruit peel," *Adv. Pharmacol. Sci.*, vol. 2013, pp. 1–6, 2013, doi: 10.1155/2013/296236.

[82] W. Elfalleh, "Total phenolic contents and antioxidant activities of pomegranate peel, seed, leaf and flower," *J. Med. Plants Res.*, vol. 6, no. 32, pp. 4724–4730, 2012, doi: 10.5897/jmpr11.995.

[83] S. K. Devatkal, P. Jaiswal, S. N. Jha, R. Bharadwaj, and K. N. Viswas, "Antibacterial activity of aqueous extract of pomegranate peel against Pseudomonas stutzeri isolated from poultry meat," *J. Food Sci. Technol.*, vol. 50, no. 3, pp. 555–560, 2013, doi: 10.1007/s13197-011-0351-y.

[84] N. S. Al-Zoreky, "Antimicrobial activity of pomegranate (Punica granatum L.) fruit peels," *Int. J. Food Microbiol.*, vol. 134, no. 3, pp. 244–248, 2009, doi: 10.1016/j.ijfoodmicro.2009.07.002.

[85] T. Nuamsetti, P. Dechayuenyong, and S. Tantipaibulvut, "Antibacterial activity of pomegranate fruit peels and arils," *ScienceAsia*, vol. 38, no. 3, pp. 319–322, 2012, doi: 10.2306/scienceasia1513-1874.2012.38.319.

[86] S. A. Ahmed and N. H. Abood, "Antimicrobial Effect of Pomegranate Peel Extract on Some Pathogenic Microorganisms," vol. 31, no. 3, pp. 316–324, 2013.

[87] E. A. M. Khalil, "Antidiabetic effect of an aqueous extract of Pomegranate (Punica granatum L.) peels in normal and alloxan diabetic rats," *Egypt. J. Hosp. Med.*, vol. 16, no. 1, pp. 92–99, 2004, doi: 10.21608/ejhm.2004.18177.

[88] K. Kanoun, B. Abbouni, M. Lamine, B. Fatima, Z. Benmahdi, and B. Marouf, "Etude De L'Efficacite De L'Extrait Ethanolique D'Ecorces De Punica Granatum Linn Sur Deux Souches Phytopathogenes :Ascocyhta Rabiei (Pass.) Labr. Et Fusarium Oxysporum F.Sp.Radicis – Lycopersici," *Eur. Sci. J.*, vol. 10, no. 12, pp. 1857–7881, 2014.

[89] I. Glazer *et al.*, "Partial identification of antifungal compounds from Punica granatum peel extracts," *J. Agric. Food Chem.*, vol. 60, no. 19, pp. 4841–4848, 2012, doi: 10.1021/jf300330y.

[90] S. Bagal, K. Bhaurao, P. Mahavidyalaya, and M. S. Patil, "Phytochemistry , Pharmacological and Therapeutic Properties of Punica Phytochemistry , Pharmacological and Therapeutic Properties of Punica granatum," *Res. Jr. Agril. Sci.*, vol. 12, no. 5, pp. 1760–1766, 2021.

[91] O. Keta *et al.*, "Pomegranate (Punica granatum L.) peel extract: Potential cytotoxic agent against different cancer cell lines," *Rec. Nat. Prod.*, vol. 14, no. 5, pp. 326–339, 2020, doi: 10.25135/rnp.170.19.11.1477.

[92] K. B. Ajaikumar, M. Asheef, B. H. Babu, and J. Padikkala, "The inhibition of gastric mucosal injury by Punica granatum L. (pomegranate) methanolic extract," *J. Ethnopharmacol.*, vol. 96, no. 1–2, pp. 171–176, Jan. 2005, doi: 10.1016/j.jep.2004.09.007.

Chap II : OVERVIEW ON NANOPARTICLES

Chapter II: overview on nanoparticles

Nanoscale science and technology, often termed "nanoscience" or "nanotechnology," are the science and engineering performed on the nanosized materials (1-100) nm for the advancement of science.

Nanoscience and nanotechnology are now among the most promising fields of research in the material sciences. This field has proven to have an important role in many disciplines and thus has become the most innovative scientific field.

Recently, nanosized materials have attracted the attention of many researchers due to their distinctive and exceptional properties compared to the bulk form of the same material. These distinctive characteristics make the world of nanomaterials a field of research that's always developing by trying to invent new techniques for the production of these nanomaterials of controlled size and shape.

II.1 The history of nanotechnology

Many researchers are currently interested in developing materials at the nanoscale to get new characteristics and functionalities, but there is a lot of evidence that shows that ancient artisans controlled materials at the nanoscale and used them mostly in coloring decorative glass the term nanoparticles was unaware for the artisans on those days [1].

There are many instances of ancient artisans utilizing nanosized materials. For instance, analysis techniques have shown that Celtic red enamels made between 100 and 400 BC included nanoparticles of copper and cuprous oxide. Additionally, during the Roman era, metallic particles were commonly used for embellishing glass. The majority of red tesserae employed in Roman mosaics were composed of glass that had a dispersion of copper nanocrystals [2].

The most well-known example is the Lycurgus Cup (4th century AD), which was made by the Romans and consists of glass that changes color when light passes through it from green to brilliant red, the analyses revealed that the glass was made up of a very small amount of two metallic Au-Ag crystals with a crystal size of (~70 nm) and a molar ratio of (14:1), which gives it these extraordinary optical properties [3].

Figure II.1 Photograph of the famous Lycurgus Cup **[3].**

The ancient Indians and Chinese utilized soluble gold nanoparticles in a treatment called "Suvarna Bhasma" to treat various diseases, these nanosized materials have been revealed to include gold mixed with larger particles, However, ancient civilizations were unaware of the distinctive properties of their materials as we now understand them **[1]**.

In 1857, the physicist Faraday studied the preparation and properties of colloidal gold and revealed that gold nanoparticles generate distinctive colors under different lighting conditions, these findings excited a revolution in nanotechnology, creating the concept of metallic nanoparticles **[4]**.

During a famous conference held in 1959, Feynman presented a visionary concept, suggesting the development of machines capable of manufacturing objects with atomic-level precision. Furthermore, he predicted the remarkable potential for storing information at high densities. Subsequently, the term "nanotechnology" was introduced by Norio Taniguchi in 1974. **[1]**.

Table II.1 History of Nanotechnology **[1].**

Year	items
1981	Scanning tunneling electron microscope that could process single atoms.
1985	Discovery of fullerene (C_{60}).
1992	Discovery of carbon nanotubes.
1993	Discovery of quantum dots.
2000	Construction of passive nanoparticles
2005	Construction of active nanoparticles for target-directed drugs and other adaptive structures.
future	Nano systems, atomic devices, diagnostic robots, etc.

II.2 Definitions

The term "nano" refers to a Greek word that means "dwarf' or something tiny" and is utilized as the prefix for one-billionth parts (10^{-9}) **[4]**. Nanoscience is the science that is especially interested in studying, discovering, and understanding the properties of materials on the scales of nanometers ranging between 1-100 nm **[5]**.

II.2.1 Nanotechnology

Nanotechnology is defined as the ability to create new structures at the tiniest scale, utilizing tools and techniques to understand and manipulate materials on the scales of nanometers ranging from 1-100 nm, in order to take full advantage of their extraordinary properties and use them for a wide range of fields **[6]**.

II.2.2 Nanomaterials

Nanomaterials are commonly defined as materials with an average grain size of fewer than 100 nanometers. Nanomaterials have tiny sizes with at least one dimension in the nanoscale range. Nanomaterials are produced from the organization of a group of atoms or molecules or by the destruction of a macroscopic material, they can be in different forms such as (spherical, plates, tubes, polyhedrons…etc.) **[7]**. Nanomaterials have attracted the curiosity of many researchers due

to their distinctive proprieties such as mechanical, biological, electrical, and optical properties compared to their bulk counterpart [8].

II.2.3 Nanoparticles

Nanoparticles are a cluster of atoms with at least one dimension smaller than 100 nanometers. They can be made from carbon, metal, metal oxides, or organic substances [9]. compared with natural organic structures, nanoparticles are mainly in the size range corresponding to proteins [10]. Nanoparticles exhibit enhanced physical, chemical, and biological properties as compared to their counterparts at larger scales. This is owing to a higher surface area to volume ratio, increased chemical reactivity and stability, increased mechanical power, and other factors [11]. These unique properties make them extremely attractive matter for use in a variety of fields such as cosmetics, medicine, biotechnology, chemistry, and agriculture [12].

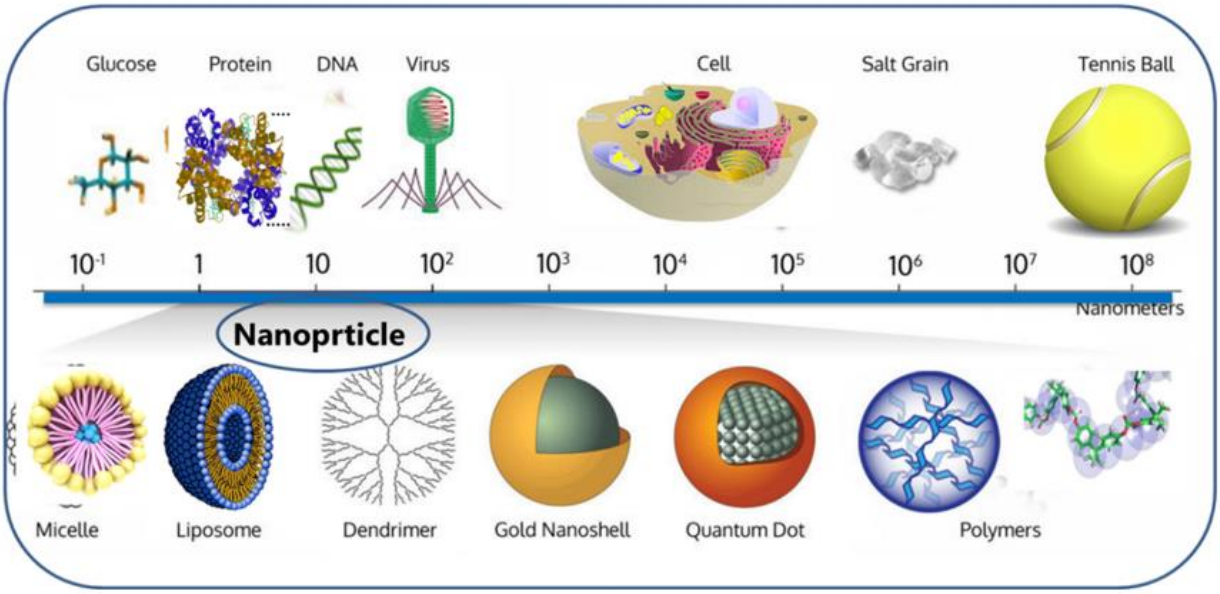

Figure II.2 The range of nanoparticle sizes compared to major chemical and biological structures [10].

II.3 General properties of nanoparticles

II.3.1 Optical properties

The optical properties of nanoparticles such as reflection, absorption, light emission, and transmission significantly differ from their same counterparts at larger scales [13]. In the nanosized materials, the electrons are not free to move as in the case of the bulk counterpart, and due to this quantum confinement of electrons, nanoparticles react to light differently compared to their bulk counterpart [14]. Many nanoparticles show a significant change in their optical properties as a function of their size and shape. For example, gold spheres of 10-20 nm in diameter exhibit red color, meanwhile gold spheres of 2-5 nm in diameter exhibit yellow color, and gold spheres with

diameters more than 20 nm exhibit a purple color. Similarly, Ag particles of 40 nm have a blue color, 100 nm have a yellow color, and prism-shaped Ag particles have a red color [15].

II.3.2 Surface properties

Nanoparticles have unique properties that can be attributed to the large proportion of atoms present at the surface compared to the number of core atoms. As a bulk material is reduced to the nanometer scale, the ratio of surface atoms increases, resulting in a high number of reactive surface sites. A cube of 1*1*1 cm size can be used as an example: if it is cut into small cubes of 0.1*0.1*0.1 mm size, the total volume of all small cubes would still be the same as the original cube, but the surface area of all small cubes would be 100 times greater than that of the original cube. Consequently, nanomaterials have a high surface area to volume ratio, making them interact more effectively with the environment than bulk materials [14]. Assuming that the nanoparticles have a spherical shape, the ratio of their surface area to volume increases as the particle size decreases.

Size (nm)	Volume (nm^3)	Surface area (nm^2)	SA : Vol Ratio
1	0.524	3.14	6
10	524	314	0.6
100	523598	31416	0.06
1000	5.24E+08	3.14E+06	0.006
10000	5.24E+11	3.14E+08	0.0006
100000	5.24E+14	3.14E+10	0.00006
1000000	5.24E+17	3.14E+12	0.000006

Table II.2 Some example calculations for volume and surface-area of nanoparticles [5].

II.3.3 Mechanical properties

The unique mechanical properties of nanoparticles allow researchers to develop new applications in many fields. Mechanical properties such as bending strength, modulus of elasticity, tensile strength, fracture properties, and impact resistance are expected to improve in the nanoscale range. The mechanical properties of nanoparticles are affected by the material base. The mechanical strength of carbon-based materials is significantly higher than other nanomaterials [16].

II.3.4 Electrical properties

Reducing the size of material particles to less than 100 nanometers improves their capacity to conduct electrical current, allowing us to use these materials to make micro-sensors and electronic devices [17].

II.3.5 Catalytic Properties

Nanoparticles have a substantial catalytic activity compared to their bulk counterparts. The size of the nanoparticles influences the catalytic activity, this is explained by the large surface-to-volume ratio which has a significant benefit on the catalytic properties involving exchanges at the interface between nanoparticles and their environment [18].

II.4 Strategies for the Synthesis of nanoparticles

Multiple methods have been used to synthesize nanoparticles with precise size, shape, structure, and dimensions. These methods are generally categorized into two classes, namely, top-down and bottom-up approaches, and are further subdivided based on their procedures and reaction conditions [9].

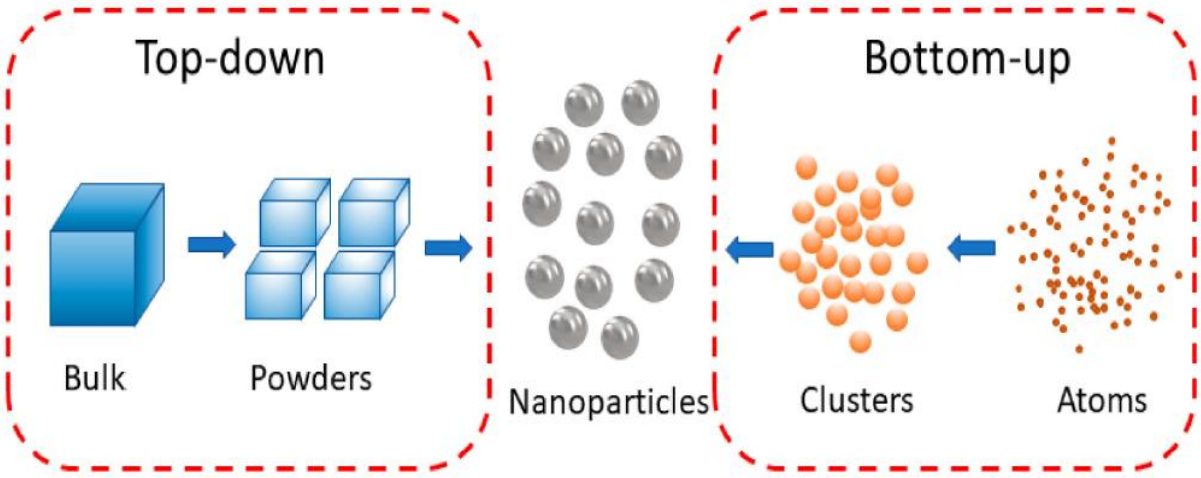

Figure II.3 Approaches for the Synthesis of nanoparticles [19].

II.4.1 Top-down approach

The top-down approach, generally known as the destructive method, is the conversion of bulk materials into nanosized materials using mechanical processes. Although the top-down approach is easy to achieve, is not proper for synthesizing the desired shape and size. The main disadvantage related to this approach is the changes in surface chemistry and physical and chemical properties of nanoparticles [20]. Laser ablation, nanolithography, Mechanical milling,

thermal decomposition, and sputtering are the most common top-down methods for nanoparticle fabrication [21].

II.4.2 The bottom-up approach

The bottom-up method, often known as the constructive method, is a build-up approach in which nanoparticles are formed from clusters, which are obtained from atoms. The Bottom-up approach is considered to be inexpensive as it has the capacity of producing less waste [9]. Sol-gel, chemical vapor deposition (CVD), biosynthesis, pyrolysis, and spinning are the most common bottom-up methods for nanoparticle fabrication [21].

II.4.1.1 Laser ablation

Laser ablation is a common method for nanoparticle synthesis from different solvents, is a method in which a high-energy laser beam is focused at a target in order to vaporize a part of the target and then condense the particles obtained onto the substrate. The nanocrystals produced are grown by condensing the emitted substances from the target in the gas phase at a well-defined pressure range. The size of nanoparticles are effected by different parameters including carrier gas, its pressure, and the intensity of the laser beam [22].

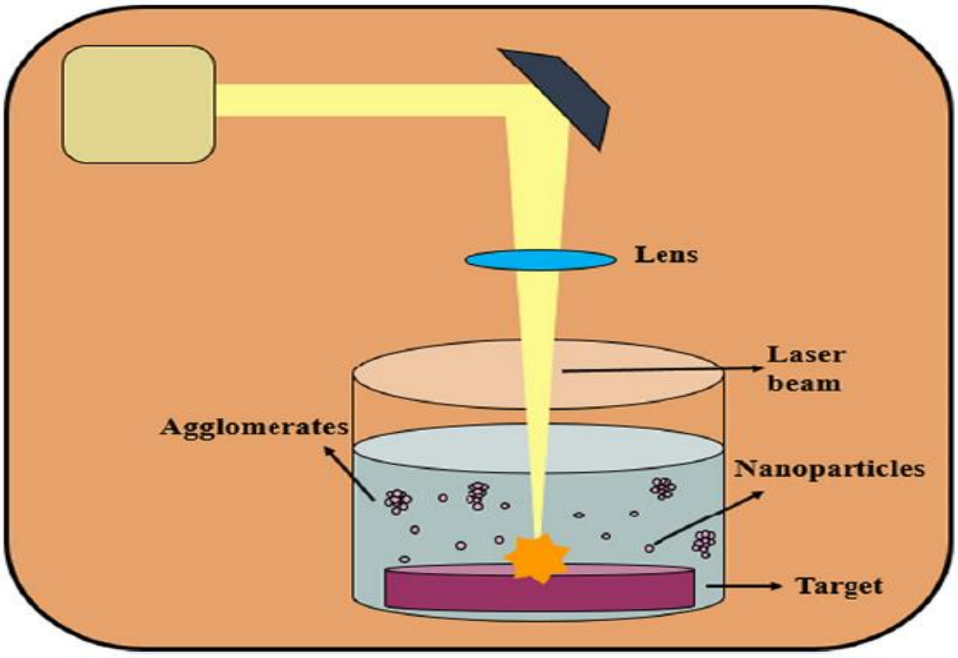

Figure II.4 laser ablation method diagram [23].

II.4.1.2 Thermal decomposition

Thermal decomposition refers to an endothermic reaction wherein the compound's chemical bonds are broken through the application of heat. The temperature at which an element

undergoes chemical decomposition is referred to as the decomposition temperature. Nanoparticles are generated through the decomposition of metals at precise temperatures, leading to a chemical reaction that produces secondary products [24].

II.4.1.3 Sputtering

The sputtering method is based on the deposition of nanoparticles on the surface by the collision of ejecting target materials with ions [25]. The obtained Nanoparticles are often deposited on the surface in the form of a thin layer, which is followed by annealing. The size and shape of nanoparticles are influenced by several parameters such as layer thickness, duration of annealing, annealing temperature, and substrate type [26].

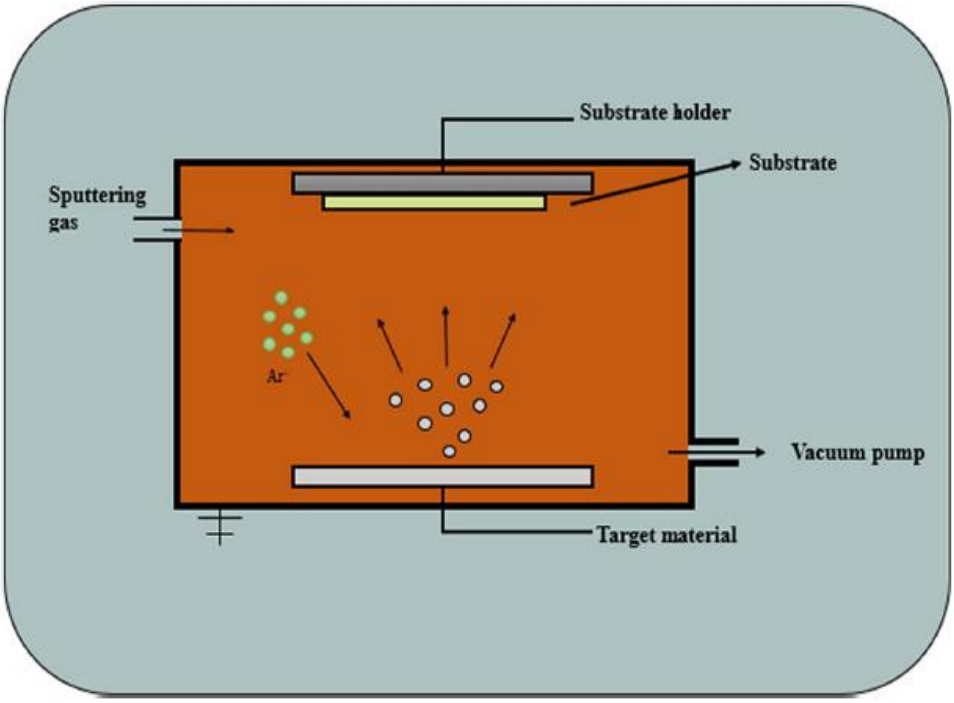

Figure II.5 Sputtering method diagram [23].

II.4.2.1 Sol-gel

The sol-gel method is frequently used to produce various nanomaterials, especially metal oxide nanoparticles. The sol-gel method involves the conversion of metal alkoxide into nanoparticles through a polycondensation reaction which is catalyzed by water or alcohol. to obtain solid and liquid phases various methods are used such as shaking, stirring, or sonication. These two phases can be separated either by filtration, centrifugation or sedimentation [27].

II.4.2.2 Biosynthesis

Biosynthesis is also termed as green synthesis method; it involves the synthesis of nanoparticles via plant extracts or microorganisms. The green synthesis method is considered

environmentally friendly, cost-effective, and non-toxic. Additionally, this method eliminates the use of hazardous chemicals and produces nontoxic and biodegradable nanoparticles **[28,29]**. Due to their distinct and enhanced properties, biosynthesized nanoparticles are extensively used in biomedical applications **[30]**.

II.5 Classifications of nanoparticles

Nanoparticles can be categorized based on their origin (natural or anthropogenic), dimensions, and chemical compositions **[31]**.

II.5.1 The classification of nanoparticles based on their dimensions

II.5.1.1 Zero-dimensional nanoparticles

0D-nanoparticles are among the most popular types of nanosized materials, in which all dimensions are smaller than 100 nanometers. Quantum dots, hollow spheres, and nano lenses are among the most common particles in this class **[13]**.

II.5.1.2 One-dimensional nanoparticles

This nanoparticle class has only one dimension more than 100 nanometers. The most famous examples of 1D-nanoparticles are nanorods, nanotubes, and nanofibers **[13]**.

II.5.1.3 Two-dimensional nanoparticles

2D-nanoparticles are materials having one dimension at the nanoscale range and two dimensions outside the nanoscale range. Nanocoating, nanofilms, and nanolayers are among the most common examples of 2D-nanoparticles **[13]**.

II.5.1.4 Three-dimensional nanoparticles

3D- nanoparticles are materials having three dimensions outside the nanoscale range (larger than 100 nm), but display internal nanoscale features. Multi nanolayers type structures, nanocomposites, and bundles of nanofibers are among the most common examples of 3D-nanoparticles **[13]**.

II.5.2 Classifications of nanoparticles based on their origin

II.5.2.1 Natural or Anthropogenic Nanoparticles

There is a significant proportion of natural nanoparticles found in the environment. Natural nanoparticles are produced by, volcanic eruptions, forest fires, lightning, and other natural processes **[32]**. They have been a main part of the environment since the origin of the planet. Anthropogenic NPs are divided into two categories accidental and engineered nanoparticles.

Incidental NPs are heterogeneous in shape and size, they can be produced by the combustion of fossil fuels (propane, diesel, gasoline, and coal) or large-scale mining [32]. Engineered NPs are particles with precisely controlled sizes, shapes, and compositions. They can even contain multiple layers, for example, gold NPs covered in drug-loaded porous silica NPs coated with specially chosen anti-bodies [1].

II.5.3 Classifications of nanoparticles based on their chemical compositions

Nanoparticles are generally classified into three main categories: organic nanoparticles, inorganic nanoparticles, and carbon-based nanoparticles.

II.5.3.1 Organic nanoparticles

Organic nanoparticles are solid particles originally made up of organic compounds (mostly lipids or polymers) with diameters ranging from 10 nm to 1 μm [33]. Among the most well-known organic nanoparticles are dendrimers, micelles, liposomes, and ferritin. This class is considered non-toxic, environment friendly, and biodegradable [28]. Both liposomes and micelles have a hollow sphere, commonly known as nano-capsules, and are sensitive to thermal and electromagnetic radiation [34]. Due to these distinct properties, organic NPs are an excellent alternative for drug delivery [35].

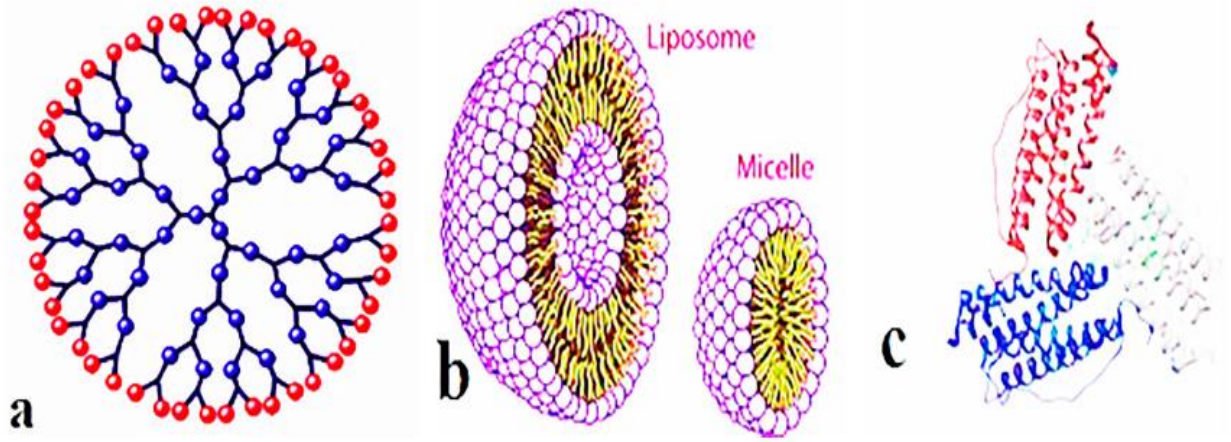

Figure II.6 Organic NPs: **(a)** Dendrimers; **(b)** Liposomes and Micelles**;** and **(c)** Ferritin [35].

II.5.3.2 Inorganic nanoparticles

Inorganic nanoparticles are particles that do not include carbon. Metals and metal oxide-based nanoparticles are classified as inorganic nanoparticles [21].

II.5.3.2.1 Metals nanoparticles

Various metals are employed to produce metal nanoparticles using a top-down or bottom-up approach. Cadmium, aluminum, copper, iron, gold, zinc, and silver are the most common metal nanoparticles [35]. Metal nanoparticles are of great interest due to their unique properties and are extensively used in a variety of fields, including medicine, catalysis, electronic sensors, etc. [5].

II.5.3.2.2 Metal oxides nanoparticles

The aim of the synthesis of metal oxides NPS is to enhance the properties of their metal counterpart such as iron NPs being converted to iron oxide NPs. It has been found that iron oxide NPs have a significant reactivity in comparison to iron NPs [35]. Various metal oxides NPs were synthesized such as Aluminum oxide, Titanium oxide, Silicon dioxide, etc. these metal oxides NPs exhibit enhanced properties compared to their metal counterpart [9].

II.5.3.3 Carbon-based nanoparticles

Carbon-based NPs are particles wholly composed of carbon [36]. They are classified as graphene, carbon nano tubes (CNT), carbon black, carbon nanofibers, and fullerenes.

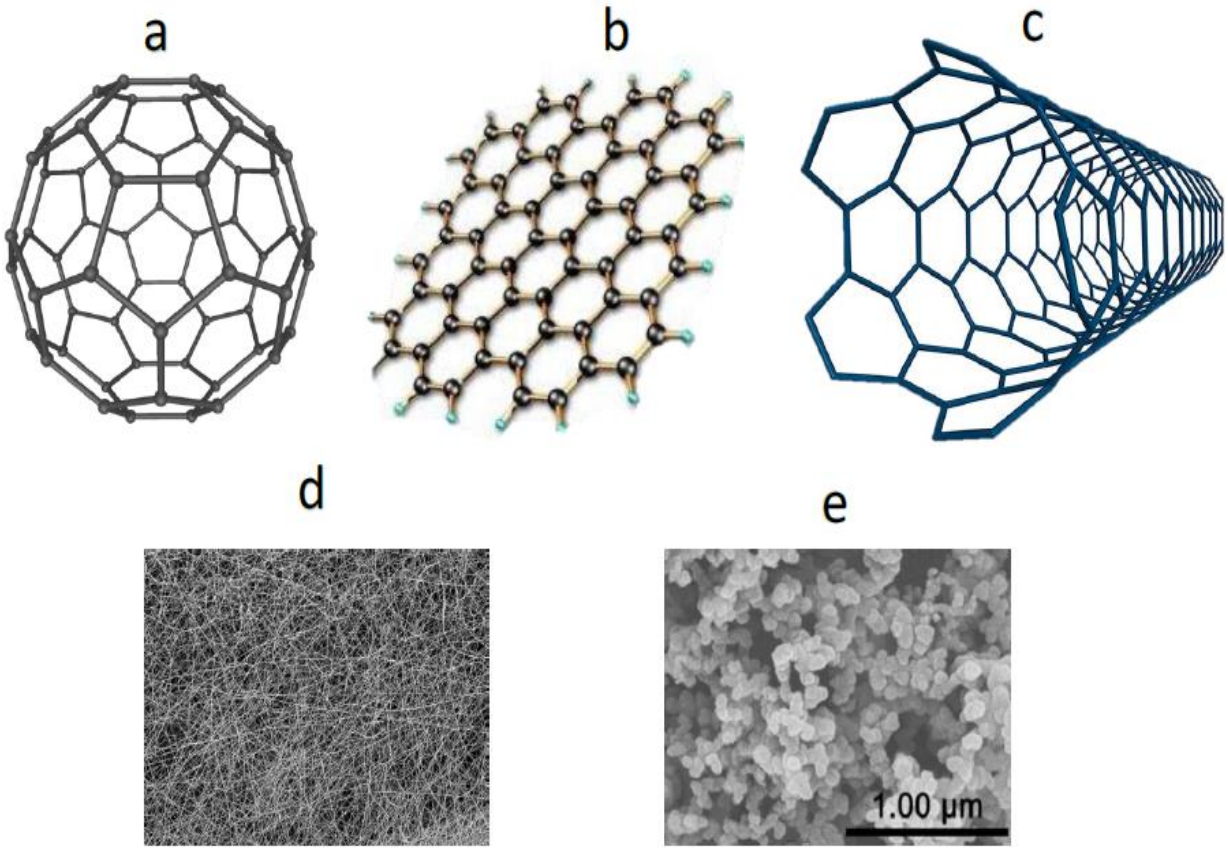

Figure II.7 carbon based NPs: **(a)** fullerenes; (**b)** graphene; **(c)** carbon nanotubes; **(d)** nanofibers; and **(e)** carbon black [5].

II.5.3.3.1 Graphene

Graphene is a two-dimensional carbon allotrope structured in a hexagonal lattice like a honeycomb. The thickness of a graphene sheet is generally around 1 nm **[23]**.

II.5.3.3.2 carbon nano tubes (CNT)

a graphene sheet that has been rolled up into a cylindrical shape is called carbon nanotubes. Carbon nanotubes are particles that have cylindrical structures built of rolled graphene sheets with diameters ranging from 1 to 2 nm **[9,35]**. They can be classified into single-walled, double-walled, and multi-walled **[35]**.

II.5.3.3.3 carbon black

Carbon black NPs are amorphous nanomaterials mainly composed of carbon atoms organized in a spherical shape with sizes ranging from 20 to 70 nm **[11]**. These particles form an agglomerate with a size of about 500 nm due the strong interaction between them **[9]**.

II.5.3.3.4 carbon nanofibers

Nano sheets of the same graphene are converted into carbon nanofibers like carbon nanotubes, however nano sheets are twisted into cups or cones form rather than elongate cylindrical tubes **[35]**.

II.6 General properties and applications of nickel oxide (NiO)

Nickel oxide is a chemical compound having the formula NiO. It crystallizes in a cubic structure (space group Fm3m) like NaCl, with octahedral Ni(II) and O^{-2} sites **[37]**. Bulk nickel oxide has a deep green color while NiO NPs have a black color **[38]**. Nickel oxide has a melting point of (1955 °C) and a molecular weight of (74.69 g/mol), Its density is (6.67 g/cm3) **[39]**. It has a refractive index of 2.1818 and magnetic susceptibility of $+660.0 \cdot 10^{-6}$ cm^3/mol **[37]**. Nickel oxide's toxicity depends on the amount inhaled **[40]**. It can exist in a variety of oxidation states such as nickel dioxide (NiO_2), nickel peroxide (NiO_4), nickelosic oxide (Ni_3O_4), nickelous oxide (NiO), and nickel trioxide (Ni_2O_3) **[41]**.

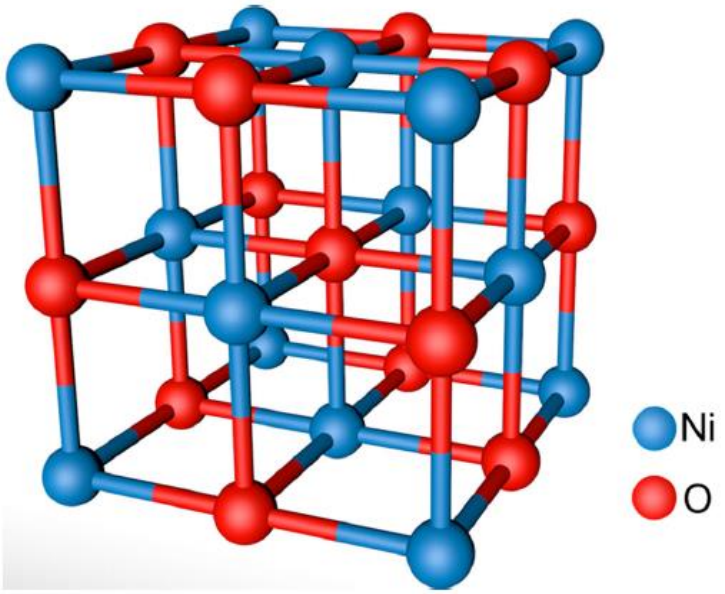

Figure II.8 crystal structure of nickel oxide (NiO) **[42]**.

Recently, the interest of researchers in the synthesis of NONPs has increased due to its importance in many applications in science and technology. NONPs are one of the most important P-type semiconducting nanomaterial classes, which has gained a lot of research interest. This is to the fact that NONPs have distinctive such as the significant degree of stability, high conductivity, electro-catalysis, ability to transfer electrons efficiently that allow them to be used in a wide range of applications such as energy efficient smart windows **[43]**, building glazing, automobile mirrors, optoelectronic devices, solar cells, and chemical sensor...etc. **[37,44]**. In addition, there is much experimental evidence has proven that NONPs have biological features as antibacterial, antioxidant, fungicide, anticancer, and as adsorbents to hazardous pollutants and dyes **[45-50]**. These interesting characteristics of $NONP_S$ including magnetic, Optical, Electrical, Catalytic activity, antibacterial, and antioxidants are strongly influenced by their size, shape, and interactions with stabilizers **[48,51-55]**. Adjusting the synthesis conditions such as concentration of metallic salts, reaction acidity, reaction duration, reaction temperature and annealing temperature, makes it possible to control and uses these characteristics more effectively.

II.7 Green synthesis of nanoparticles using plants extracts

In recent years, green synthesis has received a lot of attention from scientists because it is considered an inexpensive, environmentally friendly, and effective method. In addition, this method eliminates the use of hazardous products and produces non-toxic and biodegradable nanoparticles, making it a suitable alternative to other synthesis methods in many fields.

Synthesis of metal oxides nanoparticles is achieved by various processes such as sol-gel solvothermal, hydrothermal, thermal decomposition, and precipitation, However, these processes can be extremely costly and environmentally hazardous. This has arisen the need for a clear, inexpensive, and environmentally friendly procedure for nanoparticle creation. It has been proven that many biological systems, including fungi, yeast, bacteria, and plant extracts can change the transitional metal ions into metal oxide nanoparticles through the reductive abilities of the proteins and metabolites in these organisms.

Plant extracts are considered the most important biological systems for nanoparticle production because of their richness in polyphenols, proteins, and metabolites and their unique properties such as nucleophilia, reducing character, polarizability, ability to form hydrogen bonds, acidity, and ability to chelate metal ions **[56]**. In comparison to the mentioned biological systems, the plant-based metal oxides have higher stability and lower toxicity, which prompted scientists to manufacture nanoparticles from diverse plant extracts and use them in several applications.

II.7.1 Mechanism of green synthesis of nanoparticles by plant extracts

Generally, the mechanism of metal oxides synthesis in plant extracts is divided into three main phases; activation, growth, and termination phase **figure III. 1.**

The activation phase comprises the reduction of metal ions by biomolecules present in the plant extract, followed by the nucleation of the reduced metal atoms. the growth phase in which adjacent small NPs are immediately combined to produce larger NPs, with improved thermodynamic stability. Finally, in the termination phase, nanoparticles attain their final stable morphology. The resulting material is subsequently calcined in order to produce a pure product **[57]**.

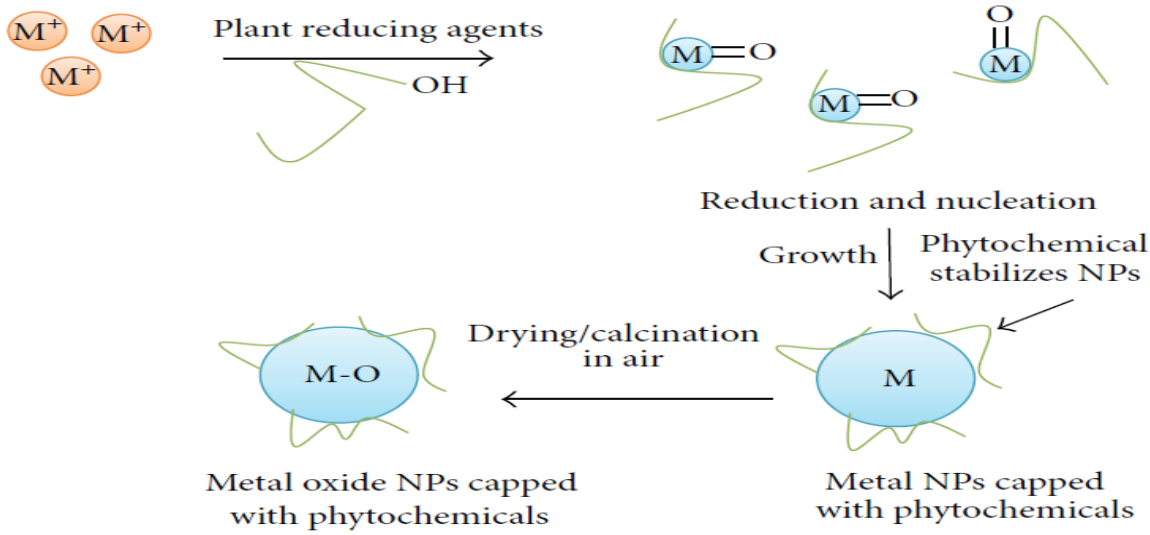

Figure II.9 Mechanism of green synthesis of metal oxide nanoparticles **[57]**.

II.7.2 The importance of plant secondary metabolites in the formation of nanoparticles

Secondary plant metabolites encompass a diverse range of chemical compounds that are synthesized by plant cells through metabolic pathways derived from primary metabolism. These secondary metabolites are of utmost importance in the process of bio-reducing metal ions, an essential step in nanoparticle production. Various plant metabolites, such as polyphenols, terpenoids, alkaloids, phenolic acids, and proteins, actively contribute to the bio-reduction process of nanoparticles. **Figure II.10** illustrates the probable biomolecules involved in the synthesis of nanoparticles.

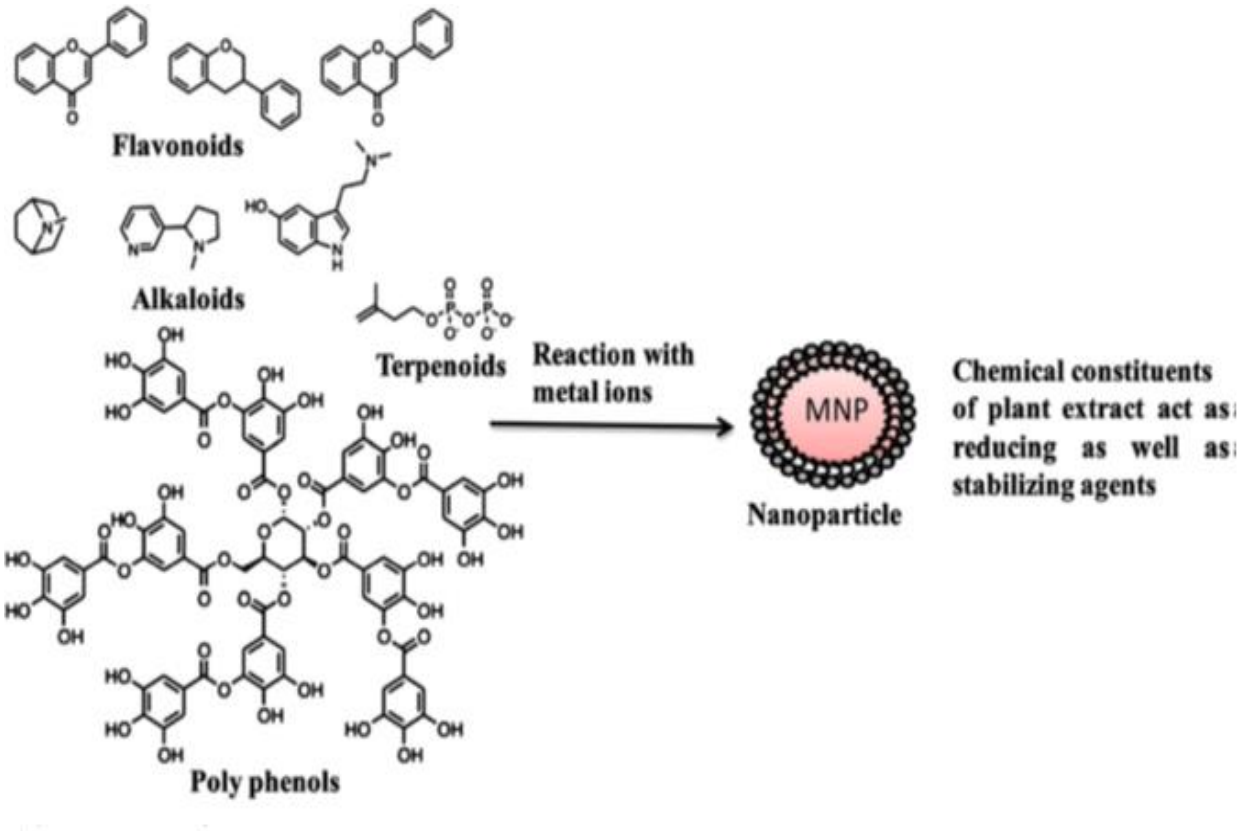

Figure II.10 Probable biomolecules involved in the synthesis of nanoparticles **[58]**.

II.8 Study of antioxidant activity

The study of the antioxidant activity of diverse materials and compounds is one of the significant research in molecular biology and biotechnology. Antioxidants serve a significant function in biosystems by combating the free radicals produced by biological processes. Hence, it is important to study the efficacy of metal oxide NPs as antioxidants due to their recent uses and applications in biological systems **[59]**.

II.8.1 Oxidative stress

II.8.1.1 Definition of oxidative stress

The term "oxidative stress" refers to a disruption in the equilibrium between reactive species or free radicals (e.g., reactive oxygen species, reactive nitrogen species) and antioxidants [60]. These antioxidants may inhibit the effects of these free radicals. The excessive production of free radicals may damage biomolecules (DNA, lipids, and proteins), ultimately leading to a variety of chronic illnesses, including diabetes, cancer, chronic inflammation, aging, cardiovascular disease, and osteoporosis [61].

II.8.1.2 Free radicals

Free radicals are chemical substances that possess unpaired electrons. Atoms and molecules are more reactive when they contain unpaired electrons. A large number of radicals are unstable and highly reactive. Therefore, they may behave as oxidants or reductants [62]. Among the free radicals responsible for several diseases are superoxide anion radical, peroxynitrite radical, hydroxyl radical, oxygen singlet, hydrogen peroxide, hypochlorite and nitric oxide radical [62].

II.8.1.3 Source of free radicals

Free radicals are produced by the human body's metabolic processes or by external sources such as cigarette smoking, air pollution, industrial contaminants, ozone, and exposure to X-rays [63]. Free radicals are produced in human cells as a consequence of two reactions: enzymatic and non-enzymatic. Enzymatic reactions, which act as a source of free radicals, include those involved in phagocytosis, the cytochrome P-450 system, respiratory chain, and prostaglandin synthesis [62]. Moreover, non-enzymatic reactions of oxygen with organic molecules, as well as ionizing reactions, can also produce free radicals.

II.8.1.4 Role of antioxidant

The human body can be protected by a variety of endogenous and exogenous antioxidants. These kinds of antioxidant inhibit the damage of cellular molecules. In the present study, all antioxidant activity assessment techniques are mainly dependent on exogenous antioxidants (synthetic antioxidants). Antioxidants are stable compounds that can donate an electron to free radicals [64].

References

References

[1] A. K. Singh, “Introduction to Nanoparticles and Nanotoxicology,” in *Engineered Nanoparticles*, Elsevier, 2016, pp. 1–18.

[2] P. Sciau, “Nanoparticles in Ancient Materials: The Metallic Lustre Decorations of Medieval Ceramics,” in *The Delivery of Nanoparticles*, InTech, 2012.

[3] P. N. Sudha, K. Sangeetha, K. Vijayalakshmi, and A. Barhoum, “Chapter 12 - Nanomaterials history, classification, unique properties, production and market,” in *Emerging Applications of Nanoparticles and Architecture Nanostructures*, no. December, Elsevier Inc., 2018, pp. 341-384.

[4] S. Bayda, M. Adeel, T. Tuccinardi, M. Cordani, and F. Rizzolio, “The history of nanoscience and nanotechnology: From chemical-physical applications to nanomedicine,” *Molecules*, vol. 25, no. 1, pp. 1–15, 2020, doi: 10.3390/molecules25010112.

[5] T. M. L. K. Abdelhamid, “Optimizing the Biosynthesis Temperature of Iron Oxide Nanoparticles Using Moringa Oleifera Extract and Study of their Biological Activities,” 2022.

[6] J. Silvestre, N. Silvestre, and J. De Brito, “Review on concrete nanotechnology,” *Eur. J. Environ. Civ. Eng.*, vol. 20, no. 4, pp. 455–485, 2016, doi: 10.1080/19648189.2015.1042070.

[7] A. M. and D. G. EL-Ghwas DE , Elkhateeb WA, “Synthèse des nanoparticules d’oxydes métalliques pour des applications photocatalytiques solaires : cas des nanoparticules d’oxyde de fer alpha,” 2015.

[8] K. Vijayaraghavan and T. Ashokkumar, “Plant-mediated biosynthesis of metallic nanoparticles: A review of literature, factors affecting synthesis, characterization techniques and applications,” *J. Environ. Chem. Eng.*, vol. 5, no. 5, pp. 4866–4883, 2017, doi: 10.1016/j.jece.2017.09.026.

[9] S. Kumari and L. Sarkar, “A Review on Nanoparticles: Structure, Classification, Synthesis & Applications,” *J. Sci. Res.*, vol. 65, no. 08, pp. 42–46, 2021, doi: 10.37398/jsr.2021.650809.

[10] D. H. Samak *et al.*, “Developmental toxicity of carbon nanoparticles during embryogenesis in chicken,” *Environ. Sci. Pollut. Res.*, vol. 27, no. 16, pp. 19058–19072, 2020, doi: 10.1007/s11356-018-3675-6.

[11] E. WA, “Nanoparticles: Characterization, Biological Synthesis and Applications,” *Open Access J. Microbiol. Biotechnol.*, vol. 6, no. 2, pp. 1–12, 2021, doi: 10.23880/oajmb-16000196.

[12] B. Uzair *et al.*, "Green and cost-effective synthesis of metallic nanoparticles by algae: Safe methods for translational medicine," *Bioengineering*, vol. 7, no. 4, pp. 1–22, 2020, doi: 10.3390/bioengineering7040129.

[13] V. Singh, P. Yadav, and V. Mishra, "Recent Advances on Classification, Properties, Synthesis, and Characterization of Nanomaterials," in *Green Synthesis of Nanomaterials for Bioenergy Applications*, no. September, 2020, pp. 83–97.

[14] A. B. Asha and R. Narain, "Nanomaterials properties," in *Polymer Science and Nanotechnology: Fundamentals and Applications*, Elsevier Inc., 2020, pp. 343–359.

[15] S. Mohan Bhagyaraj and O. S. Oluwafemi, "Nanotechnology: The Science of the Invisible," in *Synthesis of Inorganic Nanomaterials*, Elsevier, 2018, pp. 1–18.

[16] A. Reghunadhan, N. Kalarikkal, and S. Thomas, "Mechanical Property Analysis of Nanomaterials," in *Characterization of Nanomaterials*, Elsevier, 2018, pp. 191–212.

[17] C. Huang, X. Chen, Z. Xue, and T. Wang, "Effect of structure: A new insight into nanoparticle assemblies from inanimate to animate," *Sci. Adv.*, vol. 6, no. 20, pp. 1–13, 2020, doi: 10.1126/sciadv.aba1321.

[18] E. Kianfar, "Catalytic Properties of Nanomaterials and Factors Affecting it," *Importance Appl. Nanotechnol.*, vol. 5, pp. 22–25, 2020, [Online]. Available: http://meddocsonline.org/.

[19] H. Lu *et al.*, "Modular and Integrated Systems for Nanoparticle and Microparticle Synthesis—A Review," *Biosensors*, vol. 10, no. 11, pp. 1–34, 2020, doi: 10.3390/BIOS10110165.

[20] P. G. Jamkhande, N. W. Ghule, A. H. Bamer, and M. G. Kalaskar, "Metal nanoparticles synthesis: An overview on methods of preparation, advantages and disadvantages, and applications," *J. Drug Deliv. Sci. Technol.*, vol. 53, no. July, p. 101174, 2019, doi: 10.1016/j.jddst.2019.101174.

[21] A. M. Ealias and M. P. Saravanakumar, "A review on the classification, characterisation, synthesis of nanoparticles and their application," *IOP Conf. Ser. Mater. Sci. Eng.*, vol. 263, no. 3, 2017, doi: 10.1088/1757-899X/263/3/032019.

[22] J. S. M. Claude *et al.*, "Elaboration par implantation ionique de nanoparticules de cobalt dans la silice et modifications de leurs propriétés sous irradiation d'électrons et d'ions de haute énergie," 2003.

[23] N. Abid *et al.*, "Synthesis of nanomaterials using various top-down and bottom-up approaches, influencing factors, advantages, and disadvantages: A review," *Adv. Colloid Interface Sci.*, vol. 300, no. December, p. 102597, 2022, doi: 10.1016/j.cis.2021.102597.

[24] M. Salavati-Niasari, F. Davar, and N. Mir, "Synthesis and characterization of metallic copper nanoparticles via thermal decomposition," *Polyhedron*, vol. 27, no. 17, pp. 3514–3518, 2008, doi: 10.1016/j.poly.2008.08.020.

[25] P. Shah and A. Gavrin, "Synthesis of nanoparticles using high-pressure sputtering for magnetic domain imaging," *J. Magn. Magn. Mater.*, vol. 301, no. 1, pp. 118–123, 2006, doi: 10.1016/j.jmmm.2005.06.023.

[26] E. Lugscheider, S. Bärwulf, C. Barimani, M. Riester, and H. Hilgers, "Magnetron-sputtered hard material coatings on thermoplastic polymers for clean room applications," *Surf. Coatings Technol.*, vol. 108–109, pp. 398–402, 1998, doi: 10.1016/S0257-8972(98)00627-6.

[27] S. Mann *et al.*, "Sol-Gel Synthesis of Organized Matter," *Chem. Mater.*, vol. 9, no. 11, pp. 2300–2310, 1997, doi: 10.1021/cm970274u.

[28] A. Barhoum *et al.*, "Review on Natural, Incidental, Bioinspired, and Engineered Nanomaterials: History, Definitions, Classifications, Synthesis, Properties, Market, Toxicities, Risks, and Regulations," *Nanomaterials*, vol. 12, no. 2, 2022, doi: 10.3390/nano12020177.

[29] P. Kuppusamy, M. M. Yusoff, G. P. Maniam, and N. Govindan, "Biosynthesis of metallic nanoparticles using plant derivatives and their new avenues in pharmacological applications – An updated report," *Saudi Pharm. J.*, vol. 24, no. 4, pp. 473–484, 2016, doi: 10.1016/j.jsps.2014.11.013.

[30] S. Hasan, "A Review on Nanoparticles : Their Synthesis and Types," *Res. J. Recent Sci. Res . J . Recent . Sci . Uttar Pradesh (Lucknow Campus)*, vol. 4, no. February, pp. 1–3, 2014.

[31] R. Garg, P. Rani, R. Garg, and N. O. Eddy, "Study on potential applications and toxicity analysis of green synthesized nanoparticles," *Turkish J. Chem.*, vol. 45, no. 6, pp. 1690–1706, 2021, doi: 10.3906/kim-2106-59.

[32] C. Buzea, I. I. Pacheco, and K. Robbie, "Nanomaterials and nanoparticles: Sources and toxicity," *Biointerphases*, vol. 2, no. 4, pp. MR17–MR71, 2007, doi: 10.1116/1.2815690.

[33] R. K. Shatrohan Lal, "Synthesis of Organic Nanoparticles and their Applications in Drug Delivery and Food Nanotechnology: A Review," *J. Nanomater. Mol. Nanotechnol.*, vol. 03, no. 04, 2014, doi: 10.4172/2324-8777.1000150.

[34] S. Singh, V. Kumar, R. Romero, K. Sharma, and J. Singh, "Applications of Nanoparticles in Wastewater Treatment," *Nanotechnol. Life Sci.*, vol. 3, no. 3, pp. 395–418, 2019, doi: 10.1007/978-3-030-17061-5_17.

[35] I. Ijaz, E. Gilani, A. Nazir, and A. Bukhari, "Detail review on chemical, physical and green synthesis, classification, characterizations and applications of nanoparticles," *Green Chem. Lett. Rev.*, vol. 13, no. 3, pp. 59–81, 2020, doi: 10.1080/17518253.2020.1802517.

[36] S. Bhaviripudi *et al.*, "CVD synthesis of single-walled carbon nanotubes from gold nanoparticle catalysts," *J. Am. Chem. Soc.*, vol. 129, no. 6, pp. 1516–1517, 2007, doi: 10.1021/ja0673332.

[37] K. O. Ukoba, A. C. Eloka-Eboka, and F. L. Inambao, "Review of nanostructured NiO thin film deposition using the spray pyrolysis technique," *Renew. Sustain. Energy Rev.*, vol. 82, no. July, pp. 2900–2915, 2018, doi: 10.1016/j.rser.2017.10.041.

[38] R. K. Yadav, "Modern Trends in Chemical Sciences," in *Modern Trends in Chemical Sciences*, no. April, D. M. Hait and D. M. Hait, Eds. AkiNik Publications, 2022.

[39] N. A. Bakr, S. A. Salman, and A. M. Shano, "Effect of Co Doping on Structural and Optical Properties of NiO Thin Films Prepared by Chemical Spray Pyrolysis Method," *Int. Lett. Chem. Phys. Astron.*, vol. 41, no. January, pp. 15–30, 2014, doi: 10.18052/www.scipress.com/ilcpa.41.15.

[40] M. Horie, M. Stowe, M. Tabei, and E. Kuroda, "Metal Ion Release of Manufactured Metal Oxide Nanoparticles Is Involved in the Allergic Response to Inhaled Ovalbumin in Mice," *Occup. Dis. Environ. Med.*, vol. 04, no. 02, pp. 17–26, 2016, doi: 10.4236/odem.2016.42003.

[41] B. Subramanian *et al.*, "Optoelectronic and electrochemical properties of nickel oxide (NiO) films deposited by DC reactive magnetron sputtering," *Phys. B Condens. Matter*, vol. 403, no. 21–22, pp. 4104–4110, 2008, doi: 10.1016/j.physb.2008.08.014.

[42] X. Yin, Y. Guo, H. Xie, W. Que, and L. B. Kong, "Nickel Oxide as Efficient Hole Transport Materials for Perovskite Solar Cells," *Sol. RRL*, vol. 3, no. 5, pp. 1–27, 2019, doi: 10.1002/solr.201900001.

[43] A. M. Abdallah, H. Basma, and R. Awad, "Preparation, Characterization, and Application of Nickel Oxide Nanoparticles in Glucose and Lactose Biosensors," *Mod. Appl. Sci.*, vol. 13, no. 6, p. 99, 2019, doi: 10.5539/mas.v13n6p99.

[44] Sani Garba Danjumma, "Nickel Oxide (NiO) Devices and Applications: A Review," *Int. J. Eng. Res.*, vol. V8, no. 04, 2019, doi: 10.17577/ijertv8is040281.

[45] K. Lingaraju, H. Raja Naika, H. Nagabhushana, K. Jayanna, S. Devaraja, and G. Nagaraju, "Biosynthesis of Nickel oxide Nanoparticles from Euphorbia heterophylla (L.) and their biological application," *Arab. J. Chem.*, vol. 13, no. 3, pp. 4712–4719, 2020, doi: 10.1016/j.arabjc.2019.11.003.

[46] A. A. Ezhilarasi, J. J. Vijaya, K. Kaviyarasu, M. Maaza, A. Ayeshamariam, and L. J. Kennedy, "Green synthesis of NiO nanoparticles using Moringa oleifera extract and their biomedical applications: Cytotoxicity effect of nanoparticles against HT-29 cancer cells," *J. Photochem. Photobiol. B Biol.*, vol. 164, no. November, pp. 352–360, 2016, doi: 10.1016/j.jphotobiol.2016.10.003.

[47] M. S. S. Kumar *et al.*, "Multifunctional applications of Nickel oxide (NiO) nanoparticles synthesized by facile green combustion method using Limonia acidissima natural fruit juice," *Inorganica Chim. Acta*, vol. 515, no. January, p. 120059, 2021, doi: 10.1016/j.ica.2020.120059.

[48] B. A. Abbasi, J. Iqbal, T. Mahmood, R. Ahmad, S. Kanwal, and S. Afridi, "Plant-mediated synthesis of nickel oxide nanoparticles (NiO) via Geranium wallichianum: Characterization and different biological applications," *Mater. Res. Express*, vol. 6, no. 8, 2019, doi: 10.1088/2053-1591/ab23e1.

[49] J. Iqbal, B. A. Abbasi, T. Mahmood, S. Hameed, A. Munir, and S. Kanwal, "Green synthesis and characterizations of Nickel oxide nanoparticles using leaf extract of Rhamnus virgata and their potential biological applications," *Appl. Organomet. Chem.*, vol. 33, no. 8, pp. 0–2, 2019, doi: 10.1002/aoc.4950.

[50] A. K. H. Bashir *et al.*, "Biosynthesis of NiO nanoparticles for photodegradation of free cyanide solutions under ultraviolet light," *J. Phys. Chem. Solids*, vol. 134, no. June, pp. 133–140, 2019, doi: 10.1016/j.jpcs.2019.05.048.

[51] M. I. Din, M. Tariq, Z. Hussain, and R. Khalid, "Single step green synthesis of nickel and nickel oxide nanoparticles from Hordeum vulgare for photocatalytic degradation of methylene blue dye," *Inorg. Nano-Metal Chem.*, vol. 50, no. 4, pp. 292–297, 2020, doi: 10.1080/24701556.2019.1711401.

[52] R. Barir, B. Benhaoua, S. Benhamida, A. Rahal, T. Sahraoui, and R. Gheriani, "Effect of Precursor Concentration on Structural Optical and Electrical Properties of NiO Thin Films Prepared by Spray Pyrolysis," *J. Nanomater.*, vol. 2017, 2017, doi: 10.1155/2017/5204639.

[53] Z. N. Kayani, M. Z. Butt, S. Riaz, and S. Naseem, "Synthesis of NiO nanoparticles by sol-gel technique," *Mater. Sci. Pol.*, vol. 36, no. 4, pp. 547–552, 2018, doi: 10.2478/msp-2018-0088.

[54] Z. Sabouri *et al.*, "Plant-based synthesis of NiO nanoparticles using salvia macrosiphon Boiss extract and examination of their water treatment," *Rare Met.*, vol. 39, no. 10, pp. 1134–1144, 2020, doi: 10.1007/s12598-019-01333-z.

[55] M. Perachiselvi *et al.*, "Fabrication of Nickel Oxide Nanoparticles for Ntibacterial and Photocatalytic Activity," *Res. J. Pharm. Biol. Chem. Sci.*, vol. 4, no. 6, pp. 749–460, 2018, doi: 10.26479/2018.0406.59.

[56] M. F. Zayed and W. H. Eisa, "Phoenix dactylifera L. leaf extract phytosynthesized gold nanoparticles; Controlled synthesis and catalytic activity," *Spectrochim. Acta - Part A Mol. Biomol. Spectrosc.*, vol. 121, pp. 238–244, Mar. 2014, doi: 10.1016/j.saa.2013.10.092.

[57] M. Imran Din and A. Rani, "Recent Advances in the Synthesis and Stabilization of Nickel and Nickel Oxide Nanoparticles: A Green Adeptness," *Int. J. Anal. Chem.*, vol. 2016, no. 4, pp. 1–14, 2016, doi: 10.1155/2016/3512145.

[58] A. K. Mittal, Y. Chisti, and U. C. Banerjee, "Synthesis of metallic nanoparticles using plant extracts," *Biotechnol. Adv.*, vol. 31, no. 2, pp. 346–356, 2013, doi: 10.1016/j.biotechadv.2013.01.003.

[59] J. P. Saikia, S. Paul, B. K. Konwar, and S. K. Samdarshi, "Nickel oxide nanoparticles: A novel antioxidant," *Colloids Surfaces B Biointerfaces*, vol. 78, no. 1, pp. 146–148, 2010, doi: 10.1016/j.colsurfb.2010.02.016.

[60] Z. Maroua, S. Iman, M. Zineb, D. S.-W. J. Of, and U. 2018, "Evaluation of in-vitro Antioxidant and Anti-diabetic activities of leave aqueous extracts of Oudneya Africana," *Wjpsonline.Com*, vol. 6, no. 5, pp. 48–53, 2018.

[61] N. E.-H. Haddig, A. Zerzour, and S. Derouiche, "A study of the role of calcium and oxidative stress in pathophysiology of osteoporosis in postmenopausal women-a review," *JINAV J. Inf. Vis.*, vol. 1, no. 2, pp. 60–66, Dec. 2020, doi: 10.35877/454ri.jinav255.

[62] V. Lobo, A. Patil, A. Phatak, and N. Chandra, "Free radicals, antioxidants and functional foods: Impact on human health," *Pharmacogn. Rev.*, vol. 4, no. 8, pp. 118–126, 2010, doi: 10.4103/0973-7847.70902.

[63] K. Bagachi, S, Puri, "Free radicals and antioxidants in human health and diseases," *EMHJ - East. Mediterr. Heal.*, vol. 4, no. 2, pp. 350–360, 1998.

[64] K. Shankar and H. M. Mehendale, “Oxidative Stress,” in *Encyclopedia of Toxicology: Third Edition*, Third Edit., vol. 3, Elsevier, 2014, pp. 735–737.

Chapter III: MATERIALS AND METHODS

Chapter III: Materials and methods

This chapter explains the steps for the green synthesis of nickel oxide nanoparticles, the principal characterization techniques, and the methods used to evaluate the antioxidant activity of the different samples.

III.1 Materials and methods

The study was carried out at the Laboratory of Valorization and Technology of Sahara Resources (VTRS) at Echahid Hamma Lakhdar University in El Oued, Algeria. This study is focused on the green synthesis and characterization of nickel oxide nanoparticles using different plant extracts and the study of their biological activities.

III.1.1 The Collection and preparation of plant extracts

❖ **The collection of samples**

In order to carry out a green synthesis of nickel oxide nanoparticles, *Artemisia herba alba*, and *Punica granatum L* were chosen as reducing and capping agents and collected from the Tebessa region (Eastern of Algeria). This selection is based on studies conducted on these plants in many laboratories. All these studies have confirmed the presence of bioactive compounds such as flavonoids, alkaloids, etc.

❖ **The preparation of plant extracts**

The leaves of *Artemisia herba alba* were collected in March 2020, while the peel of *Punica granatum L* fruit was collected in September 2020 from local farms in the Tebessa region (eastern Algeria). The leaves and fruit rind were washed with distilled water and dried in the shade. then using a blender, the leaves, and fruit peel were crushed to obtain a fine powder. The extraction was done by mixing 10 g of each powder with 100 ml of H2O and stirring for 24 h at room temperature. The resulting extracts were filtered using Whatman No. 42 filter paper and stored in a refrigerator at 4 °C for further use.

❖ **Synthesis conditions**

The size and shape of nanoparticles are strongly influenced by many factors such as concentration of metallic salts, reaction acidity, reaction duration, reaction temperature, annealing temperature, and interactions with stabilizers.

In this work, we have focused mainly on the study of the effect of the following factors:

- The plant species (*Punica granatum L* fruit peel, *Artemisia herba alba* leaves).
- The concentration of metallic salt (0.01, 0.025,0.05, and 0.075M).

III.1.2 The biosynthesis of NONPs

Nickel oxide nanoparticles were prepared by the reduction of nickel ions presented in the aqueous solution with the help of phenolic compounds of the plant extracts. First, 50 ml of each plant extract was added to 200 ml of different concentrations of nickel nitrate solution (0.01 to 0.07 M). The mixture was kept under stirring for 60 minutes at 75°C. UV-Vis analysis was performed for each sample to confirm the formation of NONPs. Thereafter NONPs were followed by centrifugation and several washes with H_2O and dried at 100 °C to obtain a fine powder. Finally, NONPs pure powder was obtained after keeping the samples at 500 ° C for 2 hours. After the green synthesis process, the different samples were characterized by several analytical techniques.

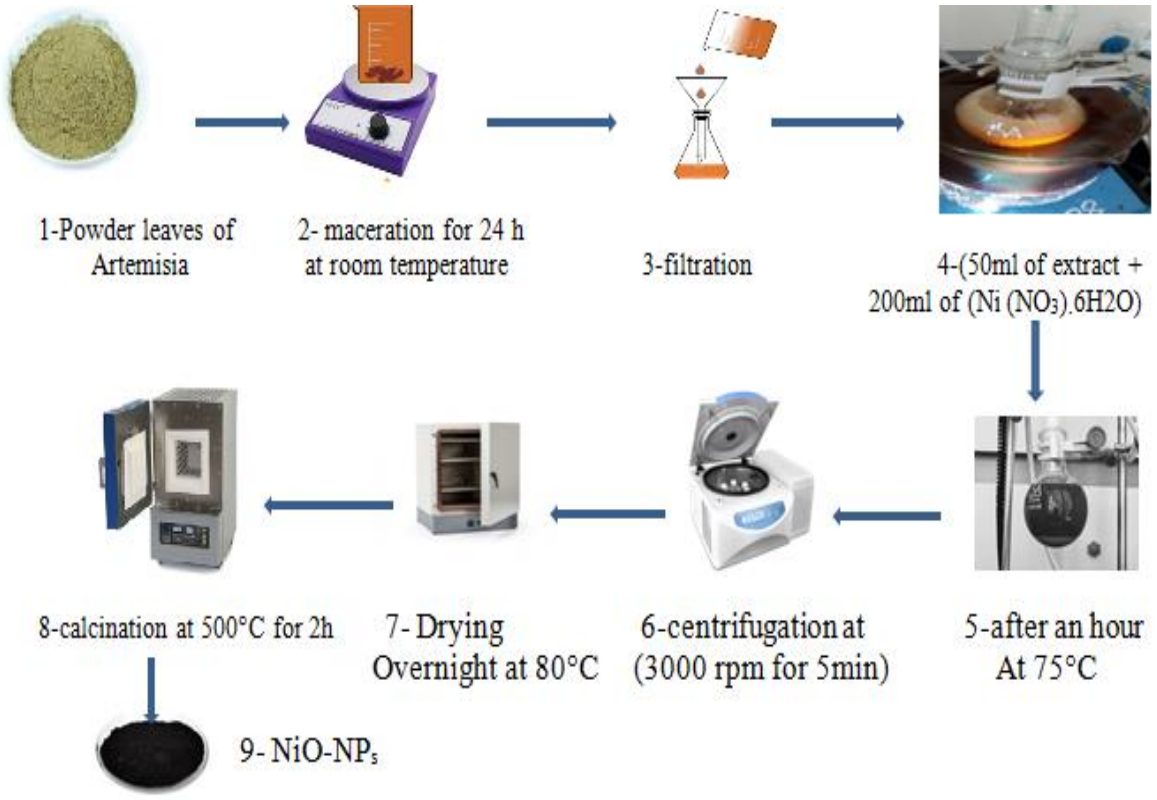

Figure III.1 Steps for the green synthesis of NONPs.

III.1.3 Characterization techniques

III.1.3.1 X Ray Diffractions (XRD)

X-rays are a form of electromagnetic radiation with wavelengths ranging from 0.01 to 10°A. This non-destructive technique is extensively used for determining crystal structure, average crystallite size, lattice parameters, as well as crystalline phase. This technique based on focusing of a monochromatic beam on the target material in order to determine its crystallographic properties. When an X-ray beam interact with the target material, the atom's electrons emit electromagnetic radiation of the same wavelength in all directions. These scattered waves are organized in the form of a crystal lattice. The interference of these waves causes diffraction by the crystal plane. Consequently, each crystalline material scatters X-rays as diffraction pattern in accordance with its atomic and molecular structure. The resultant diffraction pattern is recorded, and the structural properties are determined. The interference of the ray is either constructive or destructive. The directions in which the interferences are constructive termed diffraction peaks, which are determined by Bragg's law Equation (III.1) **Figure III.2**.

$$n\lambda = 2d \sin\theta \qquad \textbf{(III.1)}$$

where λ is the wavelength of the monochromatic X-ray beam, n is an integer, θ is the diffraction angle, and d is the interplanar spacing.

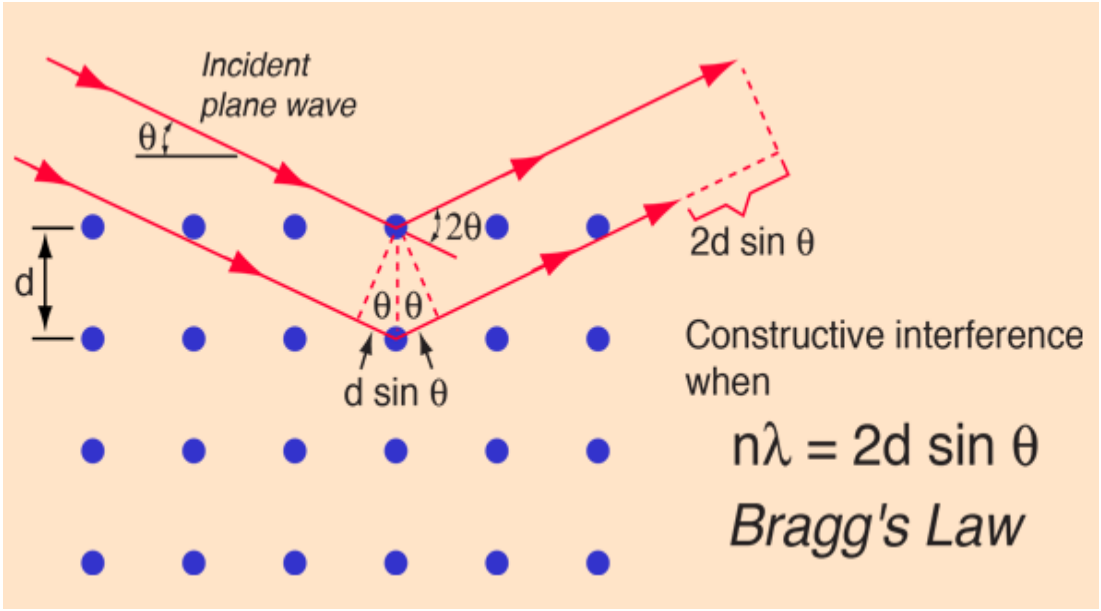

Figure III.2 Schematic representation of Bragg's law principle.

A great deal of information about the material prepared can be extracted from X-ray patterns such, as crystal structure, crystalline quality, and crystallite sizes.

Despite the existence of other approaches for determining crystallite size based on XRD patterns, Scherrer's equation is considered one of the most widely used and efficient methods for measuring crystallite size.

$$D = \frac{0.9\lambda}{B\cos\theta} \qquad \textbf{(III.2)}$$

Where D agrees with the crystal size, λ indicates the wavelength of (XRD), β represents (FWHM) of peaks, and θ is the peak position's angular **[1]**.

III.1.3.2 Scanning Electron Microscopy (SEM)

Scanning Electron Microscope (SEM) is a powerful magnification instrument based on focusing an electron beam to obtain a variety of information. The high-resolution, 3(D) images obtained by SEM provide detailed surface information, making them important in a wide range of scientific and industrial applications **[2]**.

The scanning electron microscope is composed of a high-energy electron source known as an electron gun, which generates a beam of electrons. The produced electron beam is accelerated by a high voltage system and narrowed after passing through condenser lenses and apertures **[3]**. Then after, the electron beam scans the surface of the target material with the help of scan coils. The interaction between the sample and electron beam produces many form of signals in the form of backscattered electrons, secondary electrons, and characteristic X-rays, which are detected by a variety of detectors. These prementioned detectors provides final images which are displayed on a computer screen **[4]**.

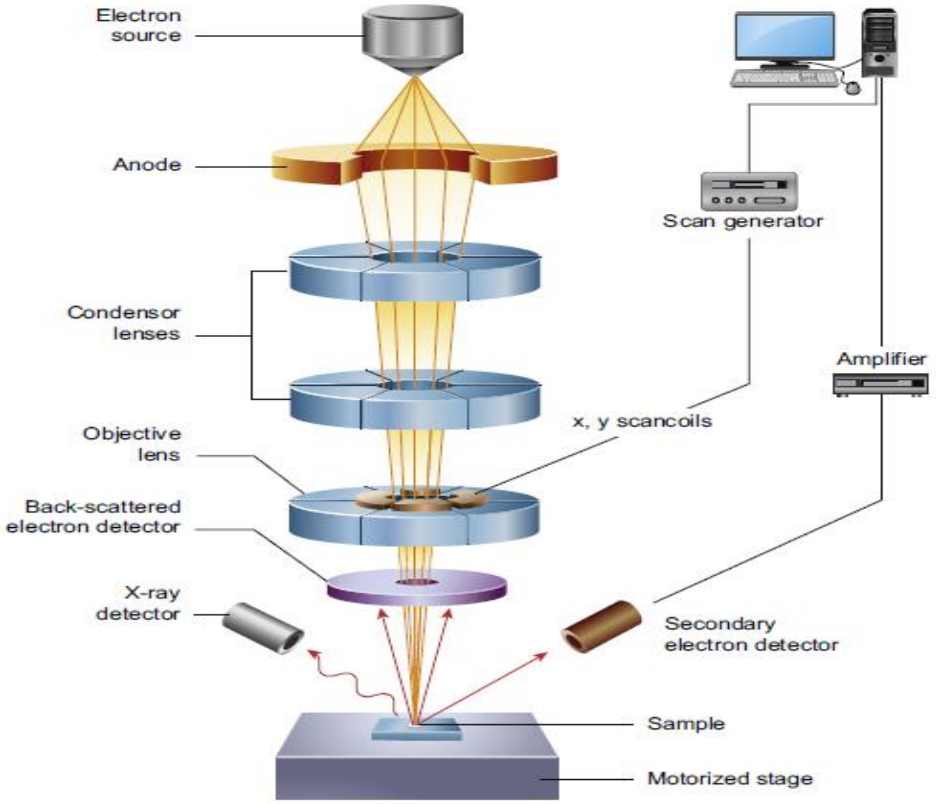

Figure III.3 Schematic representation of scanning electron microscope (SEM) [5].

III.1.3.3 UV-visible absorption spectroscopy

UV-visible absorption spectroscopy plays a critical role in the examination of the optical characteristics of nanoparticles. This method studies the interactions between electromagnetic radiation and materials.

This technique based on the transition of valence electrons from their ground state to their excited state upon absorption of a UV-visible photon.

When electrons interact with the photon with a frequency similar to their vibratory frequencies, the electrons absorb the photon's energy and acquire vibrational motion. These vibrating electrons interact with the other adjacent electrons and turns the vibration to thermal energy. Absorption spectroscopy refers to spectroscopic method which measures the absorption of photons as a function of wavelength as a result of its interaction with a material [6].

This spectrophotometer functions in accordance with the Beer-Lambert principle, which state that the fraction of incident light that is absorbed by a substance depends on:

- The path length (l).
- The concentration of the absorbing compound.

The relation between the sample's concentration, path length, and amount of light absorbed by a sample is expressed mathematically by beer-lambert law (equation 03) **[7]**.

$$A = \log_{10}\left(\frac{I_0}{I}\right) = \varepsilon lc \qquad \textbf{(III.3)}$$

Where A is the absorbance value measured by a spectrophotometer, c represents the molar concentration of the chemical identified, l is the path length (cm), ε is the absorptivity (molar $^{-1}$/cm^{-1}), I is the intensity of transmitted light, and I_0 is the intensity of incident light.

III.1.3.4 Fourier Transform Infrared (FTIR) spectroscopy

This technique is used to determine the different functional groups that exist in a substance based on the band position in the spectrum. Additionally, this analytical method may reveal the functional groups involved in the production of nanoparticles.

FTIR spectroscopy is based on the absorption of infrared radiation by the analyzed substance. By means the detection of the characteristic vibration frequencies of chemical bonds, the chemical functions present in the material can be identified. The different modes of vibrations of most particles are shown in **figure III.4**.

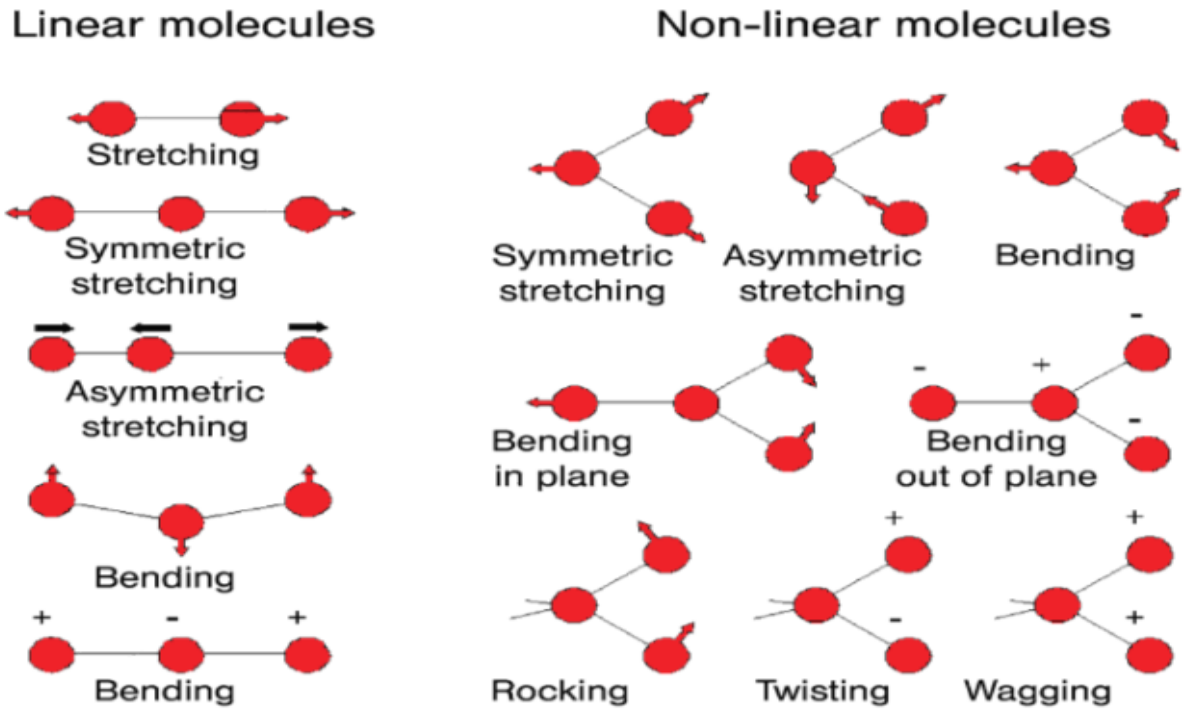

Figure III.4 The different modes of vibration of the most particles **[8]**.

III.1.2 Evaluation of antioxidant activity

The antioxidant activity of a substance is related to its ability to inhibit free radicals in the human body. Currently, many researchers are interested in the synthesis of several nanoparticles owing to their characteristics and the significant ability to inhibit free radicals.

In this study, the antioxidant activity of NONPs samples biosynthesized using *Artemisia herba alba* leaves and *Punica granatum L* peel extract at different molarities was evaluated using three different techniques: the total antioxidant capacity (CAT), the reducing power of iron ions (FRAP) and the trapping of free radical's DPPH•. Each test was performed in triplicate, and the results were calculated based on the average of three tests.

III.1.2.1 Chemicals

Hydrochloric acid, Methanol, Ascorbic acid, Sulfuric Acid, Acetic Acid, Iron Sulfate, Ferric chloride, Sodium Acetate, ammonium molybdate and Sodium Phosphate were purchased from (BIOCHEM Chemopharma). TPTZ and DPPH were bought from (ALFA AESAR). H_2O was employed in all investigations.

III.1.2.2 DPPH• scavenging assay

Since NONPs are insoluble in CH3OH, we used a modified DPPH approach for insoluble substances, as given by **[9,10]**.

❖ **Principle**

The principle of this method is the reduction of purple DPPH• (2,2-diphenyl-1-picrylhydrazyl) into yellow 2,2-diphenyl-picrylhydrazine. DPPH absorbs at 517 nm. However, its absorption is decreased by the action of an antioxidant.

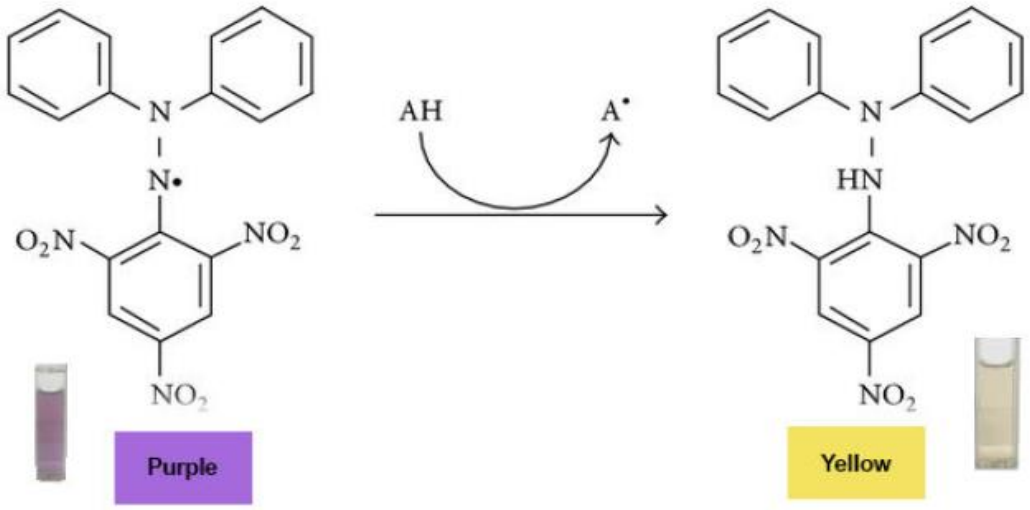

Figure III.5 Schematic diagram of the reaction between DPPH• and antioxidants [11].

❖ **Method**

Briefly, several concentrations of each sample were prepared and mixed with a methanol solution of DPPH• (2 mL, 0.1 M). using an ultrasonic device, the mixture was dispersed in a dark for 60 min to enhance the surface reaction between NONPs samples and DPPH• [12]. Thereafter The mixture was centrifuged and readings were recorded at 517 nm. Similar conditions were applied to the blank as the samples. The results were compared with ascorbic acid. The following equation was used to calculate the percentage inhibition of DPPH•.

$$\% \text{ inhibition} = \frac{A_{1-A_2}}{A1} \times 100 \quad \textbf{(III.4)}$$

A_1: the absorbance of the mixture containing only DPPH•.

A_2**:** the absorbance of the mixture containing DPPH• and NONPs sample.

$IC_{50\%}$ values was measured using % inhibition curve for each sample.

III.1.2.3 Total antioxidant activity (TAC)

❖ **Principle**

The total antioxidant capacity (TAC) of the samples was evaluated by the phosphomollybdenum method [13]. This method is based on the reduction of molybdenum Mo (VI) in the form of molybdate $MoO4^{2-}$ to molybdenum ions Mo (V) MoO^{2+} in the presence of an antioxidant to produce a green phosphate/Mo (V) complex at an acidic PH [14].

❖ **Method**

The mixture was prepared by mixing 1mg/ml of each sample with 2ml of the reactant that consists (of sodium phosphate (28 mM), ammonium molybdate (4 mM), and sulfuric acid (0.6 M)). the latter was dispersed for an hour using an ultrasonic device, thereafter centrifuged and heated for 90 minutes at 95°C. After cooling to ambient temp the mixture's readings were measured at 695 nm against blank. The blank was immersed under the same condition as the samples. TAC results are represented as mg of ascorbic acid equivalent /g $NONP_S$ (mg AAE/g NPs).

❖ **Calibration curve of ascorbic acid**

In this test, ascorbic acid was used as a standard. The calibration curve of ascorbic acid is shown in **Figure III. 6**.

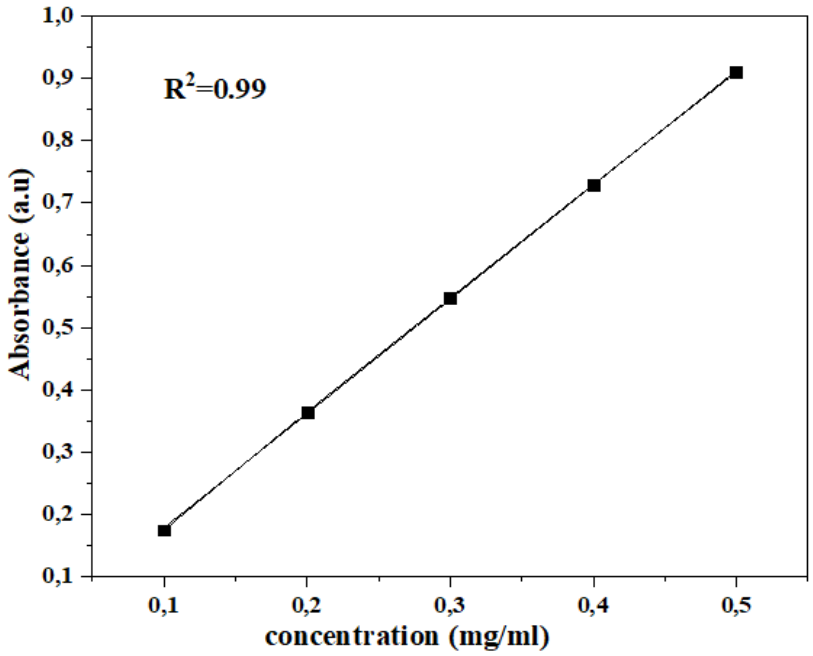

Figure III. 6 Calibration curve of ascorbic acid for evaluation of total antioxidant capacity.

III.1.2.4 Ferric reducing antioxidant power (FRAP) assay

Ferric reducing antioxidant power (FRAP) assay was carried out using a method as described by **[15]**.

❖ **Principle**

The principle of this method is the reduction of the colorless Fe3+ -TPTZ complex into the blue-colored Fe2+-TPTZ complex by an antioxidant. The increase in absorbance indicates the increase in the reducing power of the samples tested.

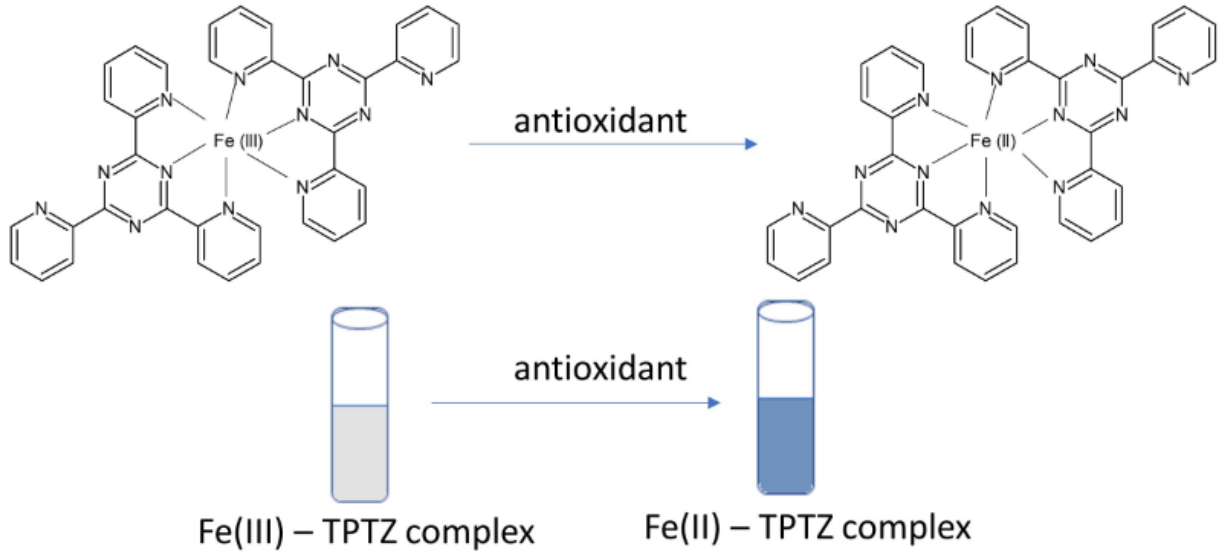

Figure III. 7 Schematic diagram of the reaction of FRAP test **[16]**.

❖ **Method**

The FRAP reagent was obtained by mixing 25 ml of an acetate buffer solution (3 mM, pH 3.6), 2.5 ml of TPTZ (10 mM) which prepared in a 40 mM HCl solution, 2.5 ml of ferric chloride (FeCl3.20 mM), and 3 ml of distilled water. 2ml of the prementioned reactant was added to 1mg/ml of each sample. The resultant mixture was dispersed for an hour at 37°C. The mixture's readings were measured at 593 nm and FRAP results are represented as mg of FeSO4 equivalent /gram of $NONP_S$ (mg FeSO4E/g NPs).

❖ Calibration curve of ascorbic acid

In this test, iron sulfate (FeSO4) was used as a standard. The calibration curve of iron sulfate is shown in **Figure III. 8**.

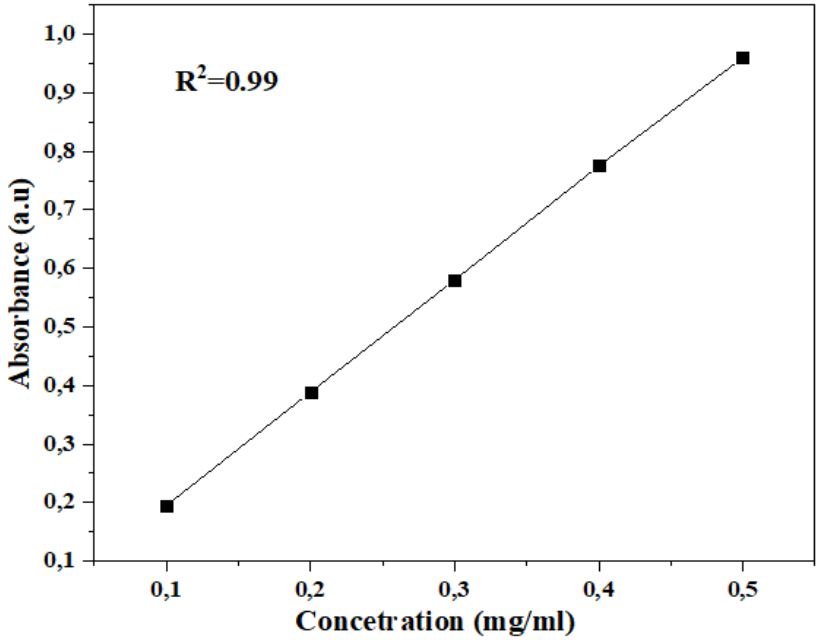

Figure III.8 Calibration curve of iron sulfate.

References

References

[1] D. Suresh, P. C. Nethravathi, Udayabhanu, H. Rajanaika, H. Nagabhushana, and S. C. Sharma, "Green synthesis of multifunctional zinc oxide (ZnO) nanoparticles using Cassia fistula plant extract and their photodegradative, antioxidant and antibacterial activities," *Mater. Sci. Semicond. Process.*, vol. 31, no. March, pp. 446–454, Mar. 2015, doi: 10.1016/j.mssp.2014.12.023.

[2] O. P. Choudhary and P. Ka, "Scanning Electron Microscope: Advantages and Disadvantages in Imaging Components," *Int. J. Curr. Microbiol. Appl. Sci.*, vol. 6, no. 5, pp. 1877–1882, 2017, doi: 10.20546/ijcmas.2017.605.207.

[3] N. Raval, R. Maheshwari, D. Kalyane, S. R. Youngren-Ortiz, M. B. Chougule, and R. K. Tekade, "Importance of physicochemical characterization of nanoparticles in pharmaceutical product development," in *Basic Fundamentals of Drug Delivery*, Elsevier, 2018, pp. 369–400.

[4] Q. Luo, "Electron microscopy and spectroscopy in the analysis of friction and wear mechanisms," *Lubricants*, vol. 6, no. 3, pp. 20–25, 2018, doi: 10.3390/lubricants6030058.

[5] B. J. Inkson, "Scanning Electron Microscopy (SEM) and Transmission Electron Microscopy (TEM) for Materials Characterization," in *Materials Characterization Using Nondestructive Evaluation (NDE) Methods*, Elsevier Ltd, 2016, pp. 17–43.

[6] G. George, R. Wilson, and J. Joy, "Ultraviolet Spectroscopy: A Facile Approach for the Characterization of Nanomaterials," in *Spectroscopic Methods for Nanomaterials Characterization*, vol. 2, Elsevier, 2017, pp. 55–72.

[7] W. Mäntele and E. Deniz, "UV–VIS absorption spectroscopy: Lambert-Beer reloaded," *Spectrochim. Acta - Part A Mol. Biomol. Spectrosc.*, vol. 173, pp. 965–968, Feb. 2017, doi: 10.1016/j.saa.2016.09.037.

[8] R. A. Ulwali, H. K. Abbas, N. Yasoob, and H. A. Alwally, "Nanotechnology and the Most Important Characterization Techniques for Nanomaterial's: A Review," *NeuroQuantology*, vol. 19, no. 8, pp. 42–52, 2021, doi: 10.14704/nq.2021.19.8.nq21111.

[9] A. Serpen, E. Capuano, V. Fogliano, and V. Gökmen, "A new procedure to measure the antioxidant activity of insoluble food components," *J. Agric. Food Chem.*, vol. 55, no. 19, pp. 7676–7681, 2007, doi: 10.1021/jf071291z.

[10] G. Madhu, V. C. Bose, A. S. Aiswaryaraj, K. Maniammal, and V. Biju, "Defect dependent antioxidant activity of nanostructured nickel oxide synthesized through a novel chemical method," *Colloids Surfaces A Physicochem. Eng. Asp.*, vol. 429, pp. 44–50, 2013, doi: 10.1016/j.colsurfa.2013.03.055.

[11] M. MR and Z. A, "Antioxidant Activity of Methanol Extract/Fractions of Senggani Leaves (Melastoma candidum D. Don)," *Pharm. Anal. Acta*, vol. 08, no. 08, pp. 1–6, 2017, doi: 10.4172/2153-2435.1000557.

[12] G. Madhu and V. Biju, "Nanostructured amorphous nickel oxide with enhanced antioxidant activity," *J. Alloys Compd.*, vol. 637, no. February, pp. 62–69, 2015, doi: 10.1016/j.jallcom.2015.02.157.

[13] F. Ijaz, S. Shahid, S. A. Khan, W. Ahmad, and S. Zaman, "Green synthesis of copper oxide nanoparticles using abutilon indicum leaf extract: Antimicrobial, antioxidant and photocatalytic dye degradation activities," *Trop. J. Pharm. Res.*, vol. 16, no. 4, pp. 743–753, 2017, doi: 10.4314/tjpr.v16i4.2.

[14] A. Ardestani and R. Yazdanparast, "Inhibitory effects of ethyl acetate extract of Teucrium polium on in vitro protein glycoxidation," *Food Chem. Toxicol.*, vol. 45, no. 12, pp. 2402–2411, 2007, doi: 10.1016/j.fct.2007.06.020.

[15] I. F. F. Benzie and J. J. Strain, "The Ferric Reducing Ability of Plasma (FRAP) as a Measure of '"Antioxidant Power"': The FRAP Assay," *Analy. Biochem*, vol. (1), no. 239, pp. 70–76., 1996, doi: 10.1039/c6ay01739h.

[16] K. A. Wojtunik-Kulesza, "Approach to Optimization of FRAP Methodology for Studies Based on Selected Monoterpenes," *Molecules*, vol. 25, no. 22, pp. 1–11, 2020, doi: 10.3390/MOLECULES25225267.

Chap IV : Results and discussion

Chapter IV: Results and discussions

This chapter presents the results of characterizations and antioxidant activities of nickel oxide nanoparticles prepared by green synthesis method using two plant extracts (*Artemisia herba alba* leaves, and *Punica granatum L* peel).

IV.1 Visual observations

Initially, the synthesis of NONPs was visually confirmed by the immediate change of the mixture's color from brown to greenish-black after mixing nickel nitrate solution with plant extracts (*Artemisia herba alba* leaves, and *Punica granatum L* peel). This result is consistent with prior research which used *Rhamnus triquetra* (Wall.) and *Rhamnella gilgitica* leaves extract for NONPs production **[1,2]**. This immediate change of the mixture's color is a clear indication of bio-reduction of the nickel ion and the formation of nickel oxide nanoparticles **[3]**. The immediate change of the mixture's color can be explained by the presence of bioactive compounds in the plant extracts which are responsible for the reduction of nickel ions.

Punica granatum L, and *Artemisia herba alba* are rich in bioactive compounds such as (polyphenols, alkaloids, flavonoids, saponins, tannins, etc.) which can act as a reducing, stabilizing, and capping agent during green synthesis process of NONPs. When nickel nitrate is dissolved in water, the nickel and nitrate ions are separated, resulting in a solution containing a combination of nickel and nitrate ions. Upon mixing the ionic solution with *Punica granatum L*, and *Artemisia herba alba* extracts, biomolecules that exist in plant extracts act as a chelating agent to reduce nickel cation into zero-valent nanoparticles. Thereafter, the resultant is stabilized and capped by the other bioactive compounds. The final product (NONPs) is then air-dried or calcined in air to obtain final NONPs.

IV.2 Characterization of NONPs

IV.2.1 UV/visible spectroscopy analysis

The optical properties of the different samples were analyzed by UV-Vis absorption spectrum in a device (Shimadzu 1800) which functions in the range of 200-900 nm. The analysis was carried out in a quartz cuvette, using distilled water as the reference solvent.

Figures (IV. 1), **(IV. 2)** show UV/Vis absorption spectrum of $NONP_S$ synthesized using two plant extracts (*Artemisia herba alba* leaves, and *Punica granatum L* peel) at different molarities of nickel nitrate. As can be seen, all of samples exhibit maximal absorption peaks at 300 nm. These absorption peaks are attributed to the characteristic surface plasmon resonance

absorption band of NONPs [4-6]. Consequently, the UV/Vis absorption spectrum confirms the formation of NONPs.

On the other side, an increase in peaks intensity was observed with an increase in the concentration of nickel nitrate, which can be explained by the increasing number of nanoparticles formed due to the reduction of nickel ions.

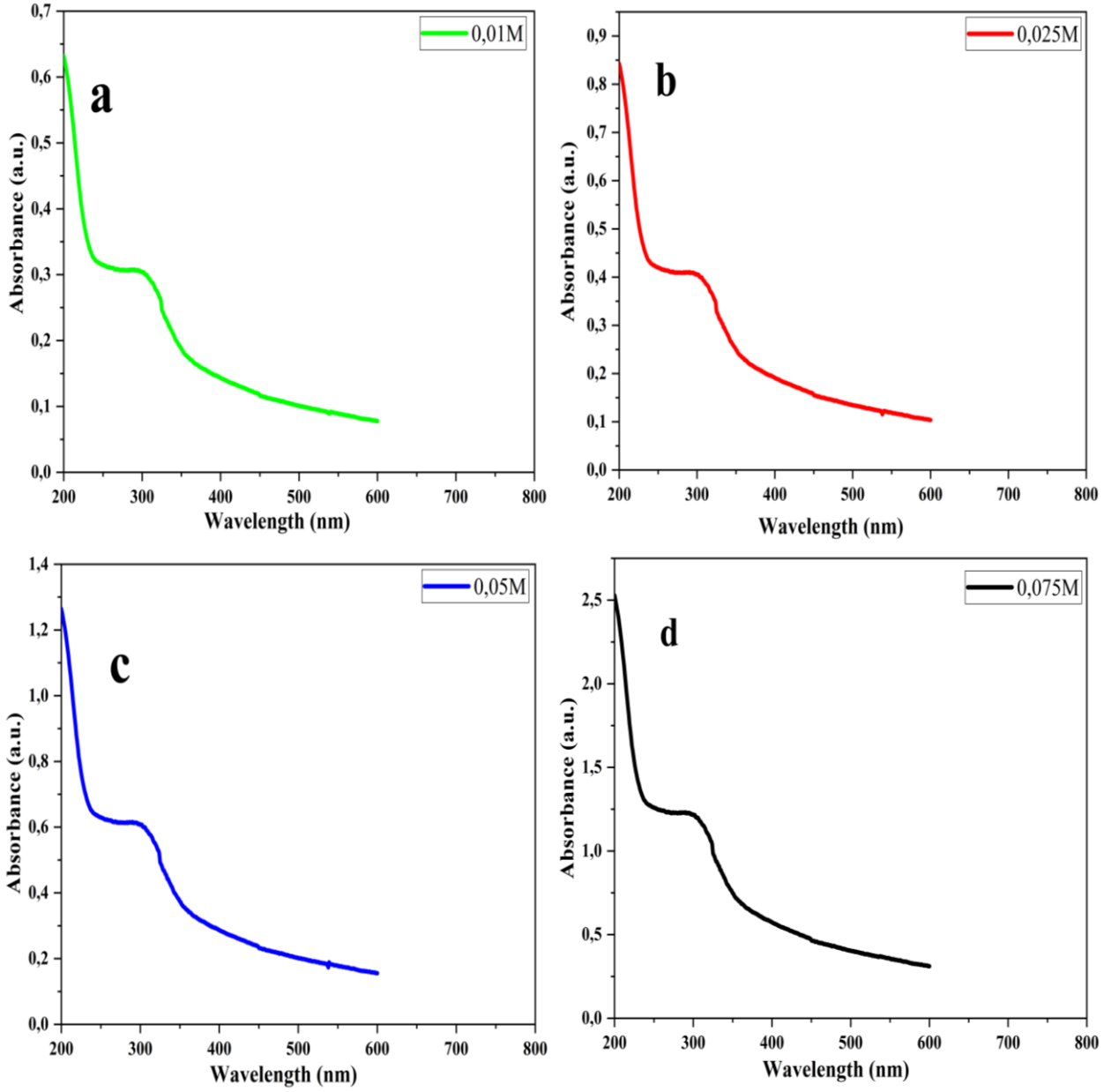

Figure IV. 1 UV/Vis absorption spectra of $NONP_S$ prepared from *A. herba alba* leaves extract at different molarities**: (a)** 0.01M; **(b)** 0.025M; **(c)** 0.05M; and **(d)** 0.075 M.

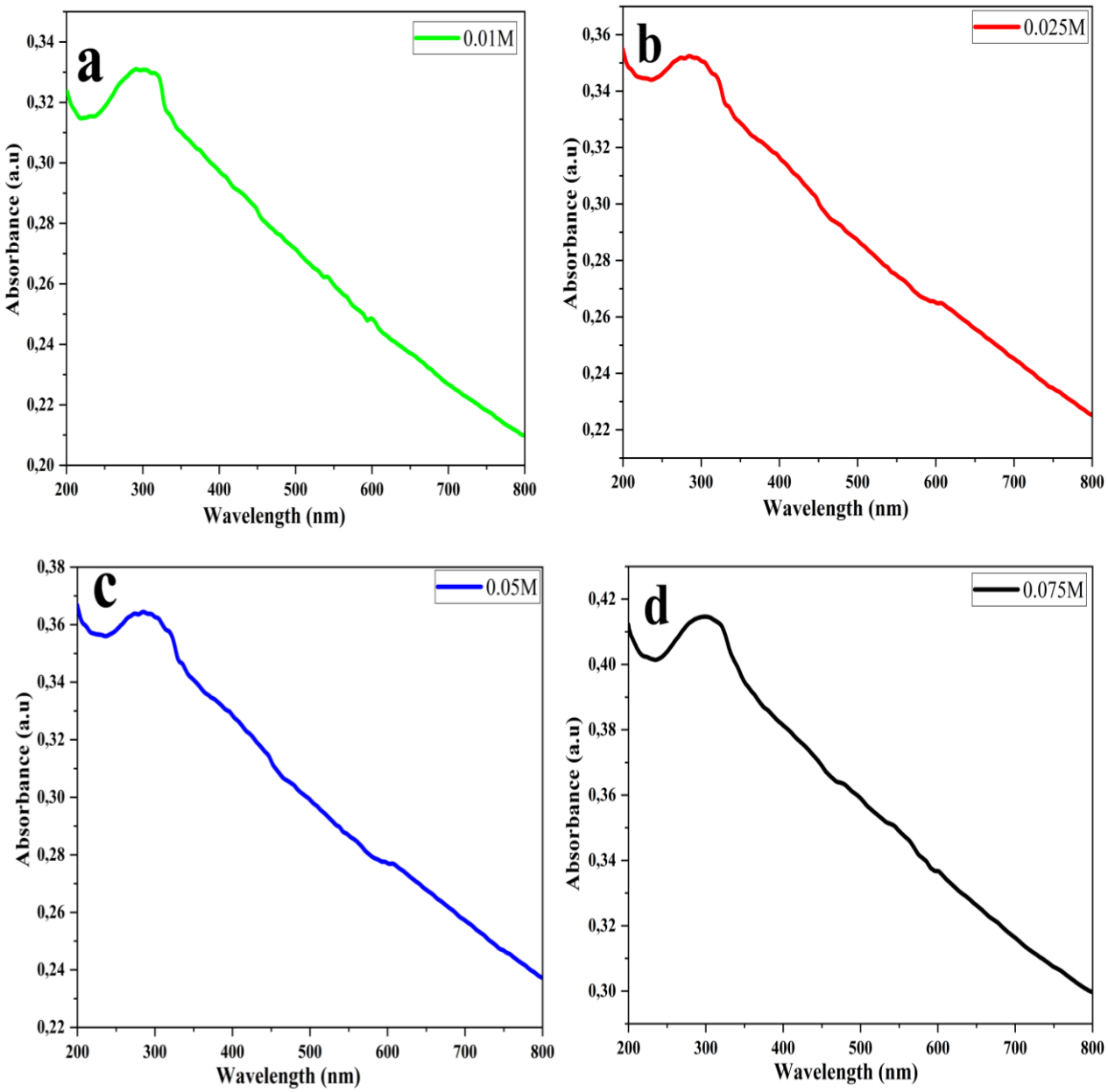

Figure IV. 2 UV/Vis absorption spectra of NONPs prepared from *P. granatum L* peel extract at different molarities**: (a)** 0.01M; **(b)** 0.025M; **(c)** 0.05M; and **(d)** 0.075 M.

The optical band gap of synthesized NONPs was determined from UV/Vis absorption spectrum and using the following equation **(1) [7,8].**

$$(\alpha h\nu)^{n} = A\,(h\nu - E_g) \qquad \textbf{(IV.1)}$$

Where α agree with the absorption coefficient, A is constant, hν is the photon energy, Eg is the optical band gap. Considering n = 2, the direct band gap was estimated by plotting of $(\alpha h\nu)^2$ as a function of photon energy (hν) **[9,10]**. **Figures (IV.3), (IV.4)** show the optical band gap of NONPS synthesized at various molarities using different plant extracts (*A. herba alba* leaves and *P. granatum L* peel). The optical band gap values (Eg) of the different samples are shown in **table IV. 1**.

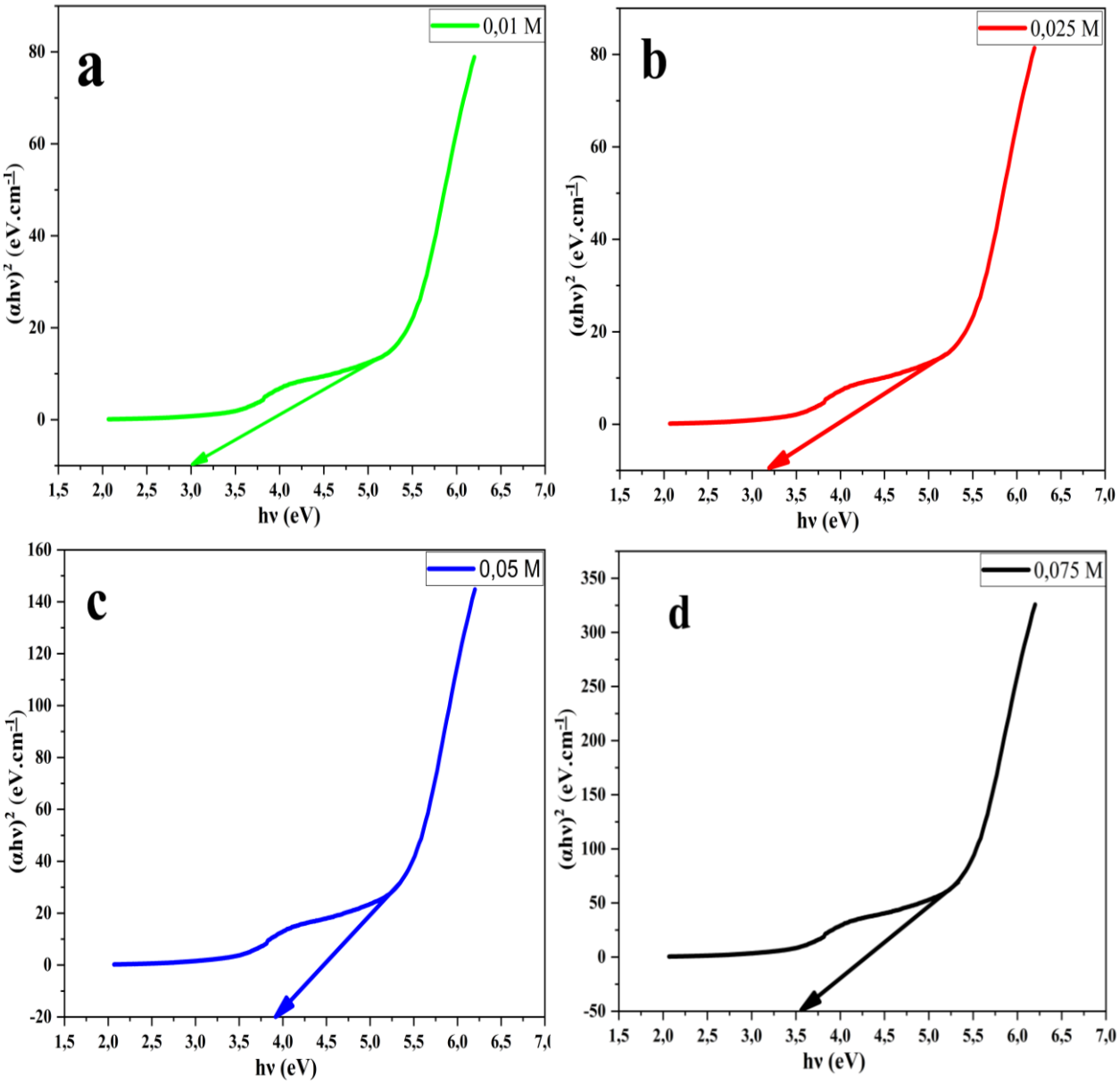

Figure IV.3 Optical properties of NONPs prepared from *A. herba alba* leaves extract at different molarities: **(a)** 0.01M; **(b)** 0.025M; **(c)** 0.05M; and **(d)** 0.075 M.

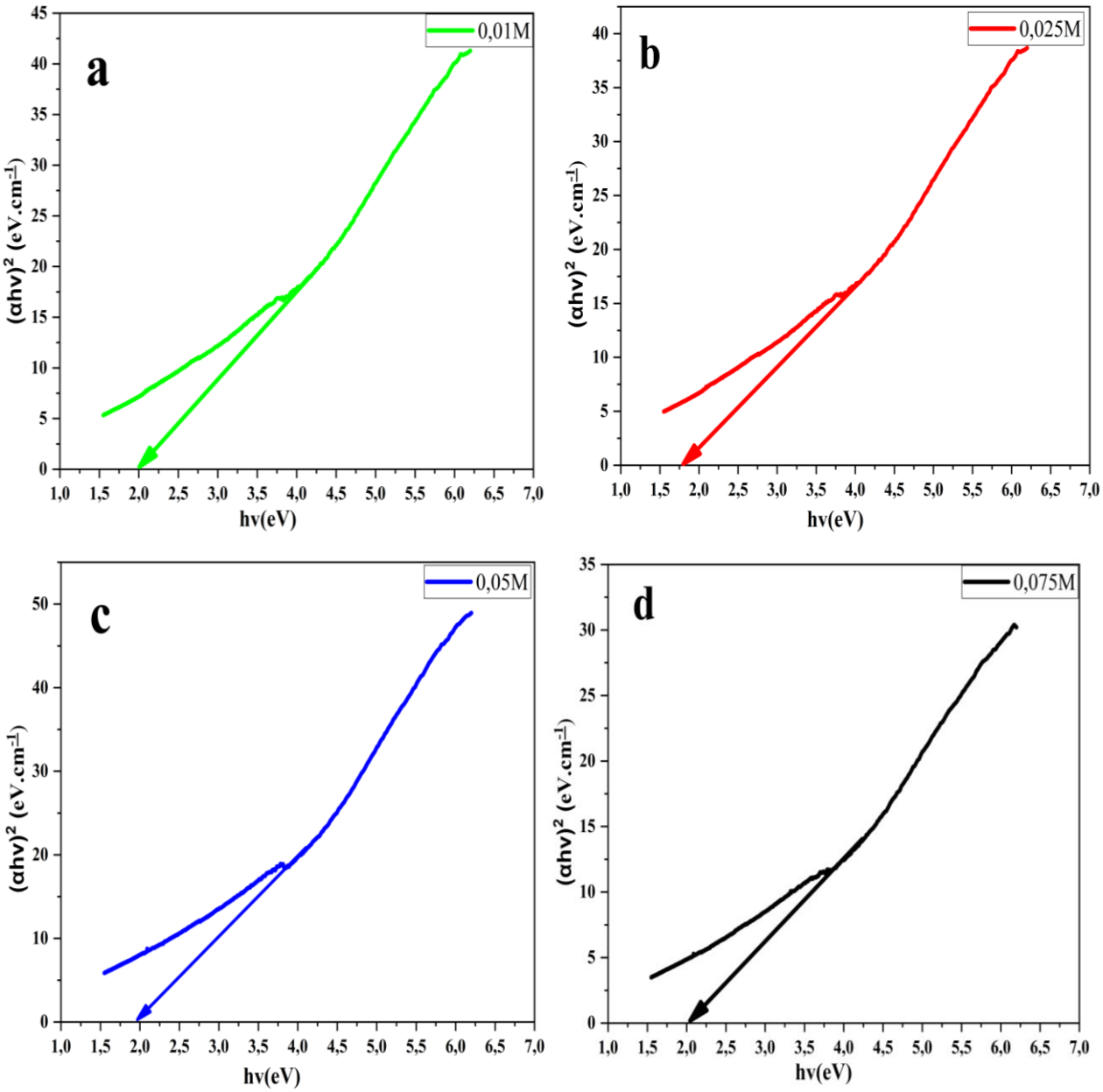

Figure IV.4 Optical properties of NONPs prepared from *P. granatum L* peel extract at different molarities: **(a)** 0.01M; **(b)** 0.025M; **(c)** 0.05M; and **(d)** 0.075 M.

Table IV. 1 shows the band gap values of NONPs synthesized using two plant extracts (*Artemisia herba alba* leaves, and *Punica granatum L* peel) at different molarities. As shown in the **table IV.1**, the samples synthesized using *Artemisia herba alba* leaves extract exhibit higher band gap values compared to the samples synthesized by *Punica granatum L* peel extract. In addition, band gap values of samples synthesized using *Artemisia herba alba* leaves extract increased with increasing concentration. While the band gap values of samples synthesized using *Punica granatum L* peel extract decreased with increasing concentration with the exception of 0.075 M, where the value increased. The results obtained reveals that band gap is affected by change in precursor concentration and from a plant to another.

Samples	0.01 M	0.025 M	0.05 M	0.075 M
The band gap values (eV) of NONPs synthesized by *A. herba alba* leaves extract	3.00 ±0.002	3.13 ± 0.018	3.90 ±0.014	3.61 ± 0.011
The band gap values (eV) of NONPs synthesized by *P. granatum L* peel extract	2.00±0.004	1.85±0.002	1.95±0.006	2.13±0.118

IV.2.2 FTIR spectroscopy analysis

The infrared spectrums of the different NONPs samples and plant extracts were recorded using an ATR-type device operating between 500-4000 cm^{-1}.

FTIR analysis was used to determine the chemical functional groups present in plant extracts, confirm the formation of the Ni-O band, and identify the components involved in the reduction and stability of NONPs. This was performed by comparing the spectrums of plant extracts with the spectrums of the synthesized NONPs.

FTIR spectra of leaves and peel extract **Figures (IV.5a)**, **(IV.6a)** revealed multiple bands at 3303, 3280, 2348, 1641, and 1635 cm^{-1}. The two broad bands that appeared at 3303 and 3280 cm^{-1} correspond to O-H stretching vibration mode **[11,12]**. The weak band located at 2348 cm^{-1} is related to C≡N or C≡C stretching vibration mode **[13]**. In addition, the bands centered at 1641 cm^{-1} and 1635 cm^{-1} correspond to the C = C stretching vibration mode of the aromatic molecules, the N–H amines vibration, the C = O vibration of the carboxyl groups, and the amides **[14,15]**. The broadbands shown in the extracts' spectra confirm that the extracts are rich in bioactive compounds which may act as reducers and stabilizers during biosynthesis process of NONPs.

By comparing the plant extracts spectrums **Figures (IV.5a), (IV.6a)** with the NONPs spectrums **Figures (IV.5b), (IV.6b)**, we observe a significant decrease in the intensity of the broadbands found at 3303 and 3280 cm^{-1}. This confirms the importance of polyphenolic compounds in the bioreduction of nickel ions and the stabilization of NONPs.

The spectrums of biosynthesized NONPs using two plant extracts at different molarities are shown in **Figures (IV.5b), (IV.6b)** and **Figures (IV.5d), (IV.6d),** as shown, all spectrums revealed one common bond in the range of 400-1000 cm^{-1} which is related to the Ni-O stretching vibration mode **[10,16]**. The FTIR spectra were in excellent agreement with XRD results and no impurities were detected.

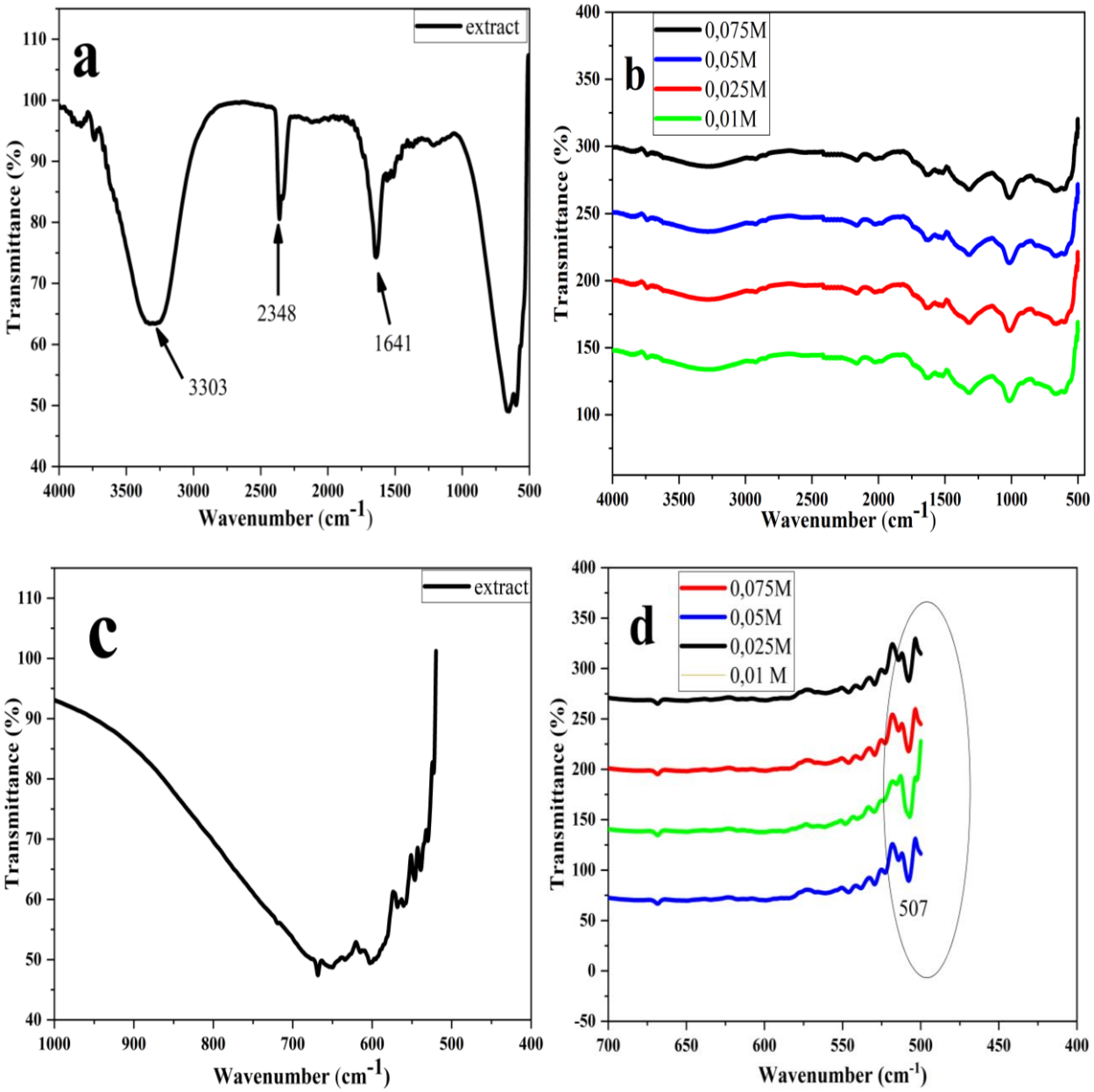

Figure IV.5: **(a)** FTIR spectrum of *Artemisia herba alba* leaves extract; **(b)** FTIR spectrums of NONPs samples; **(c)** and **(d)** FTIR spectrums illustrative for the extract, and NONPs samples.

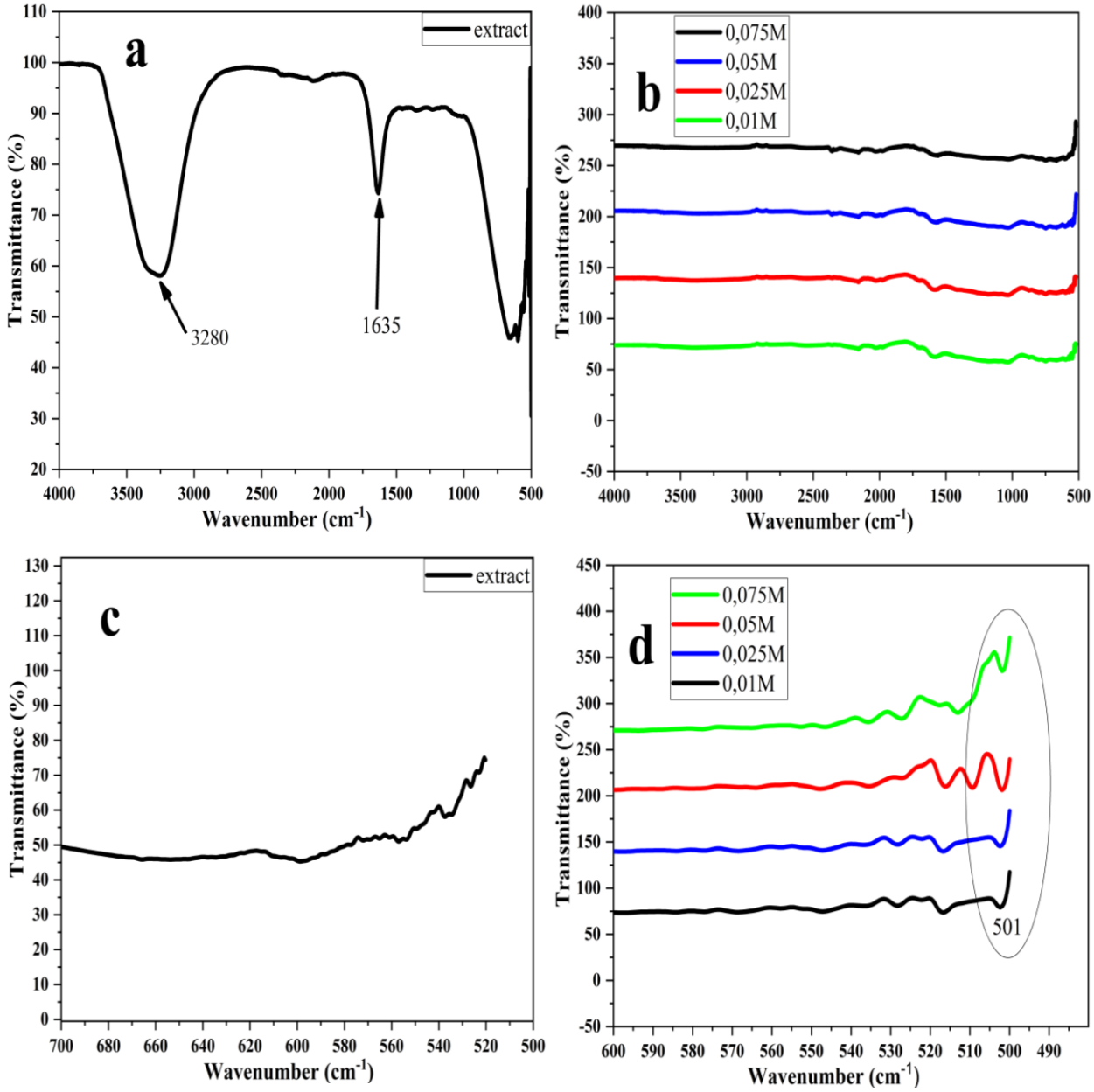

Figure IV.6: **(a)** FTIR spectrum of *Punica granatum L* peel extract; **(b)** FTIR spectrums of NONPs samples; **(c)** and **(d)** FTIR spectrums illustrative for the extract, and NONPs samples.

IV.2.3 X-ray diffraction (XRD)

The crystallite structure, phase purity, and crysttalite size of NONPs samples were studied by XRD technique using an X-ray diffractometer (Rigaku Miniflex 600) with a Cu-Kα ($\lambda = 1.5406$ Å) in the 2θ angles ranging from 10° to 80°.

Figure IV.7 displays the XRD patterns of the biosynthesized NONPs using *Artemesia herba alba* leaves extract at different molarities and annealed at 500 °C. As shown, the XRD patterns of the biosynthesized NONPs exhibit sharp and intense peaks, indicating their high crystallinity. In addition, no impurity-characteristic peaks were detected, confirming the high

purity of samples [17]. Moreover, no different phases were found, indicating that the synthesized NONPs are of great purity. The observed peaks at 2θ values 37.29°, 43.36°,62.96°, and 75.43° correspond respectively to the crystal planes of (111), (200), (220), (311) [18,19]. According to the standard data (JCPDS card no: 01-075-0269), the crystal structure of the samples corresponds to the cubic pure phase of NONPs with lattice parameters a= b= c= 4.1762 Å and space group (fm-3m) [18,20-21].

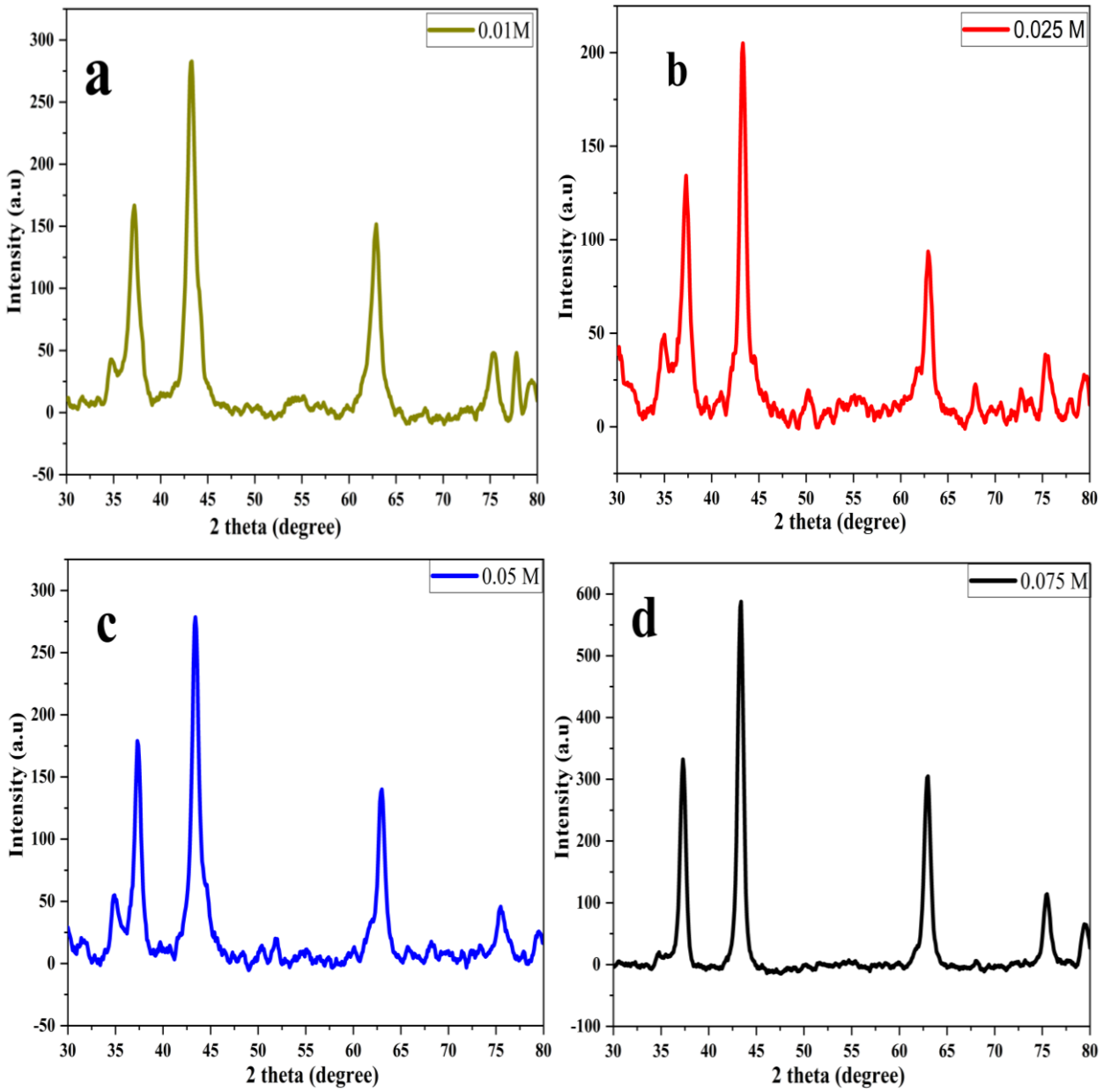

Figure IV.7 XRD analysis of $NONP_S$ prepared from *Artemesia herba alba* leaves extract at different molarities: **(a)** 0.01M; **(b)** 0.025M; **(c)** 0.05M; and **(d)** 0.075 M.

Figure IV.8 shows the XRD patterns of NONPs biosynthesized from *Punica granatum L* peel extract at four different molarities and annealed at 500 °C. All of the XRD patterns of the different samples show common peaks at 2θ values of 37.24°, 43.29°, 62.87°, and 75.47° which correspond to crystal planes (003), (012), (104), (012) respectively. These peaks are in excellent concordance with prior studies and are well-matched with standard data (JCPDS card no: 00-022-1189) **[22,23]**. The crystal structure of NONPs samples are related to rhombohedral geometry with lattice parameters a=b= 2.95 Å, and c=7.23 Å and space group (R-3m) **[24,25]**. No additional peaks were detected in the XRD patterns, indicating the pure crystallinity of NONPs.

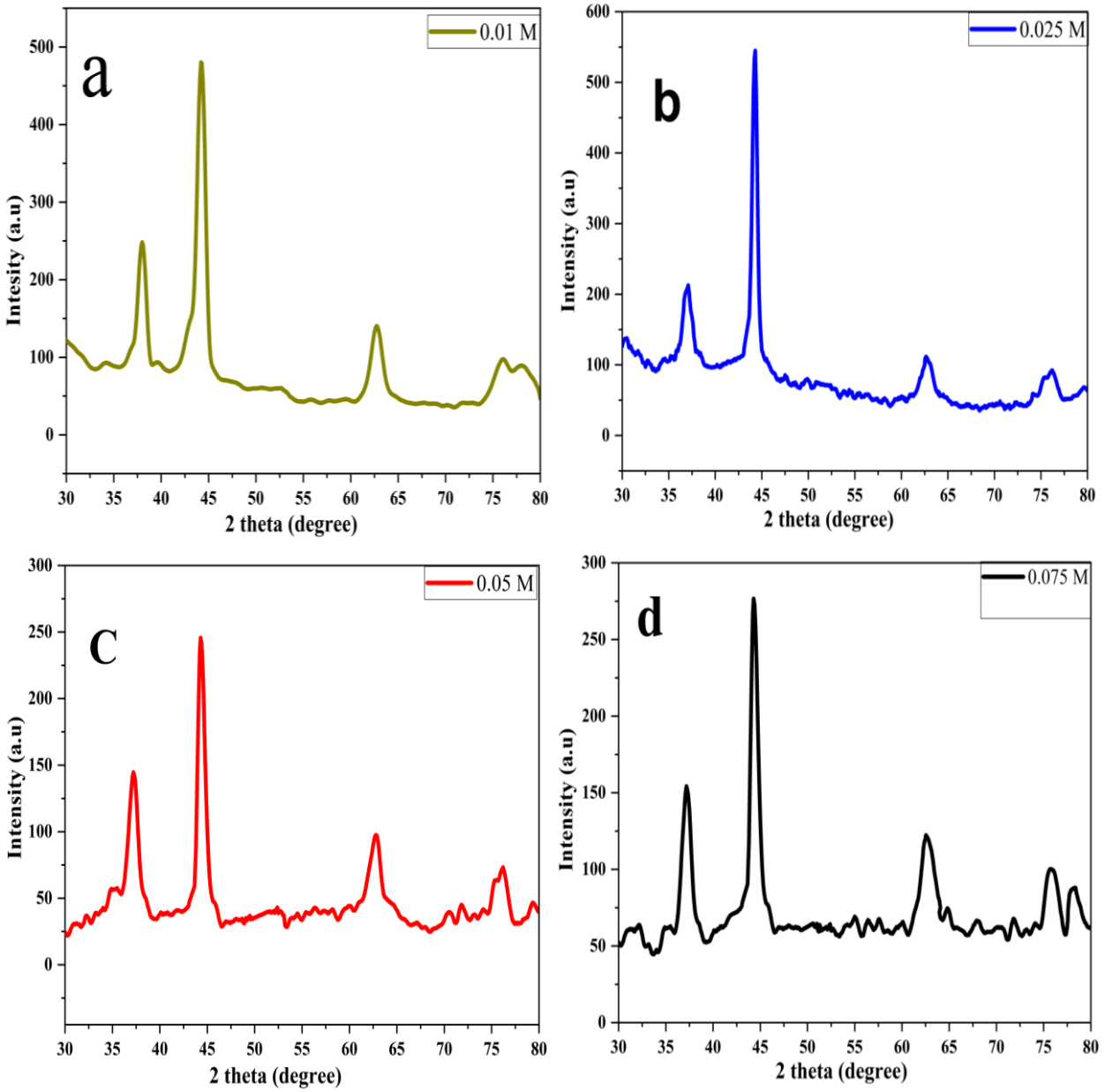

Figure IV.8 XRD analysis of $NONP_S$ prepared from *Punica granatum L* peel extract at different molarities: **(a)** 0.01M; **(b)** 0.025M; **(c)** 0.05M; and **(d)** 0.075 M.

❖ **Crystallite sizes**

The average crystallite sizes of greenly synthesized NONPs from the extract of *Artemesia herba alba* leaves and *Punica granatum L* peel at different molarities were measured using Debye Scherer equation **[26,27]**.

$$D = \frac{0.9\lambda}{B\cos\theta} \qquad \textbf{(IV.2)}$$

Where D agree with the average crystallite size, λ represents the wavelength of the incident radiation (λ=1.5406 Å), B represents the full width at half maximum (FWHM) of the most intense diffraction peak, and θ is the peak position's angular. The results obtained are listed in **table IV.2**

Samples	The average crystallite size (nm) of NONPs prepared by *Artemesia herba alba* leaves extract	The average crystallite size (nm) of NONPs prepared by *Punica granatum L* peel extract
0.01 M	7.49 ± 0.0005	14.51±0.5
0.025 M	8.58 ± 0.0001	10.66±0.38
0.05 M	8.13 ± 0.0001	09.02±1.05
0.075 M	10.7 ± 0.0002	08.88±0.35

According to these results, the average crystallite size of NONPs samples biosynthesized using *Artemesia herba alba* leaves extract increases with the increase in the concentrations of $NiNO_3$ from 0.01 to 0.07 M, except 0.05 M, where the size decreases. On other hand, it was observed that the average crystallite sizes of NONPs samples biosynthesized using *Punica granatum L* peel extract decrease when the concentration of NiNO3 increases.

The correlation between crystallite size and precursor concentration observed in NONPs prepared by *Artemesia herba alba* leaves and *Punica granatum L* peel extract is in accord with recent studies. These studies indicate that when the precursor concentration is increased in the presence of sufficient surfactants, it leads to a higher concentration of monomers by increasing the number of growth species at the same volume. Consequently, the diffusion distance between monomers decreases, resulting in higher mass transfer and growth. Consequently, the crystallite size experiences , and vice versa **[28]**.

IV.2.4 Scanning Electron Microscopy (SEM)

The surface morphological features of the different samples were studied by scanning electron microscopy (SEM: JEOL-JSM-6390) propped with a dispersive energy X-ray (EDX).

Figure IV.9 displays the SEM images of NONPs prepared using *Artemesia herba alba* leaves extract at different molarities, (a, b, c, d) related to samples obtained at (0.01, 0.025, 0.05, and 0.075 M) respectively. As shown in this figure, all samples seem spherical in shape with a high degree of agglomeration. This result is consistent with earlier studies **[29-31]**. The high degree of agglomeration can be attributed to the fact that NONPs have high surface energy and high surface tension **[32-34]**.

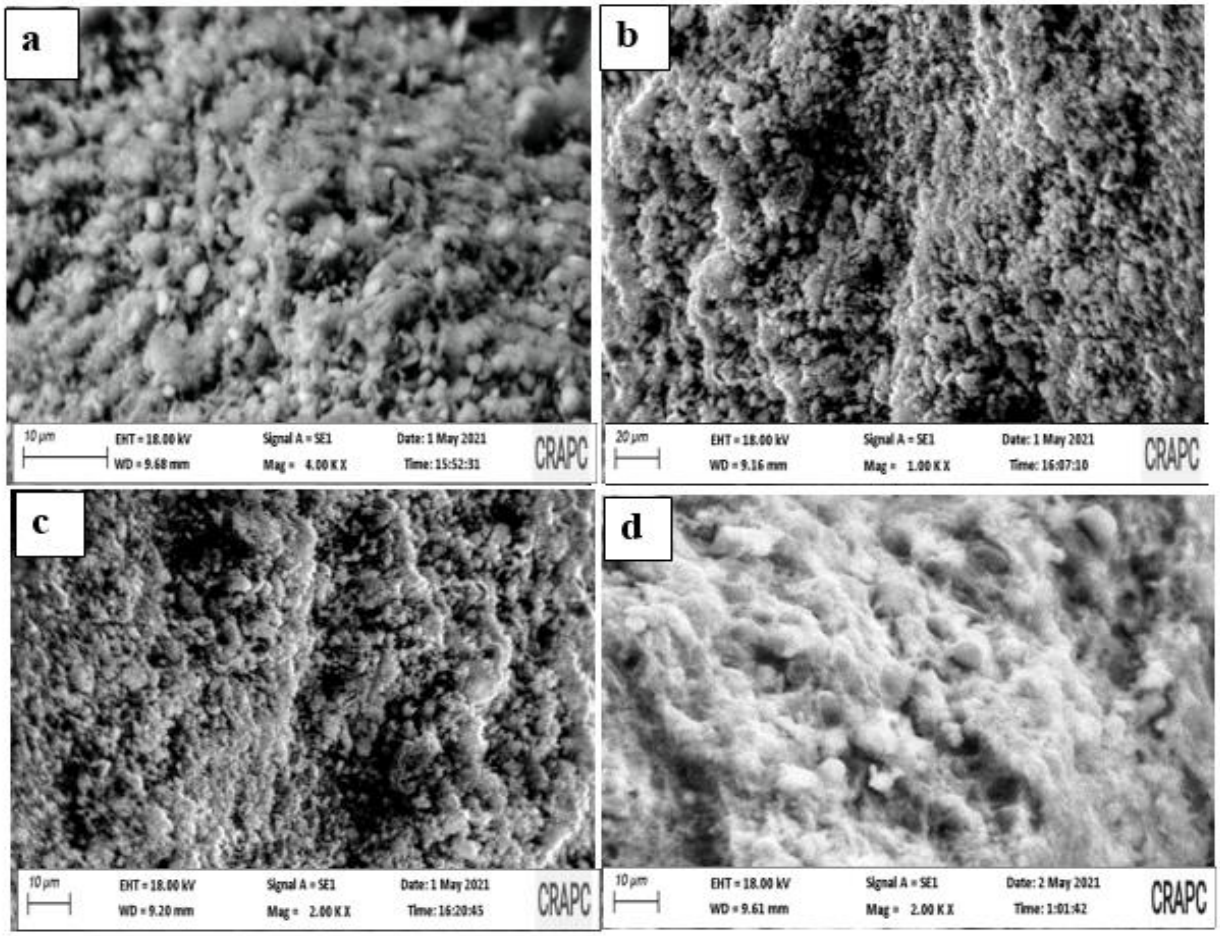

Figure IV.9 SEM images of NONPs biosynthesized using *Artemesia herba alba* leaves extract at different molarities: (**a)** 0.01M; (**b)** 0.025M; (**c)** 0.05M; and **(d)** 0.075 M.

Figure IV.10 shows SEM images of NONPs samples biosynthesized by *Punica granatum L* peel extract at different molarities, (a, b, c, d) correspond to samples synthesized at (0.01, 0.025, 0.05, and 0.075 M) respectively. From this image, it's seen that NiONPs samples are mostly irregular in shape.

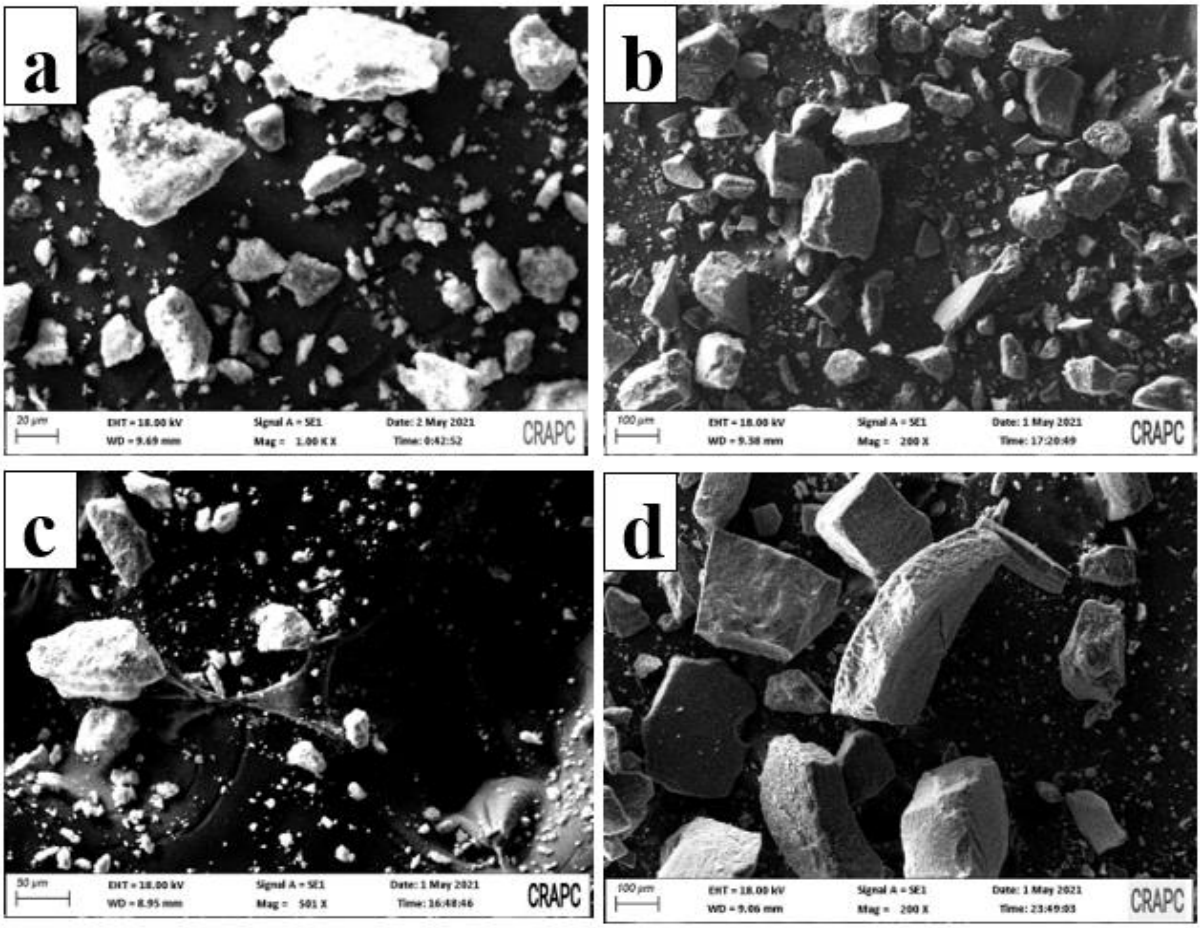

Figure IV.10 SEM images of NONPs biosynthesized using *Punica granatum L* peel extract at different molarities: (**a)** 0.01M; (**b)** 0.025M; (**c)** 0.05M; and **(d)** 0.075 M.

IV.2.5 The Energy Dispersive X-ray analysis (EDX)

EDX analysis was used to verify the chemical elements found in the biosynthesized NONPs **(Figure IV.11)**. The EDX spectrum confirm that NONPs contain both oxygen (O) and nickel (Ni) with a weight percentage of approximately 75.17 % and 24.83 % respectively. This finding agrees well with previous work **[1]**.

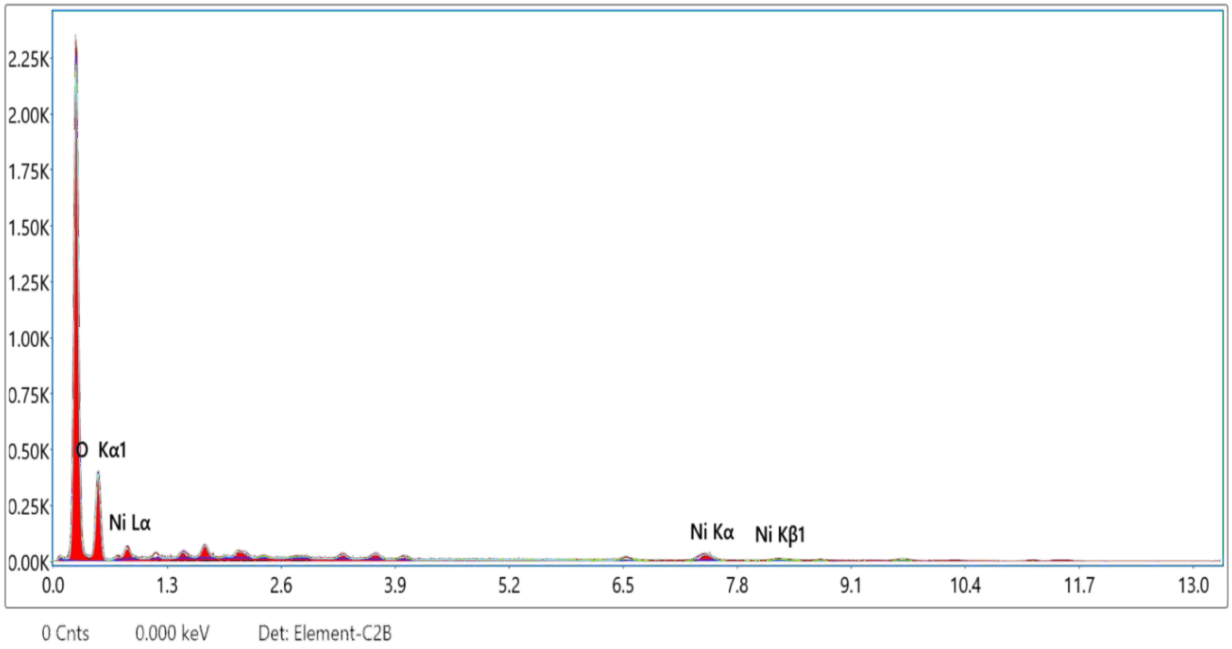

Figure IV.11 EDX analysis of NONPs prepared using *Artemesia herba alba* leaves extract.

The EDX spectrum of NONPs is shown in **Figure IV.12**. The EDX spectrum revealed that NiONPs are composed of nickel and oxygen, with weight percentages of 20.95 % and 79.05% for nickel and oxygen respectively. Furthermore, the existence of only nickel and oxygen confirms that NONPS are of high purity.

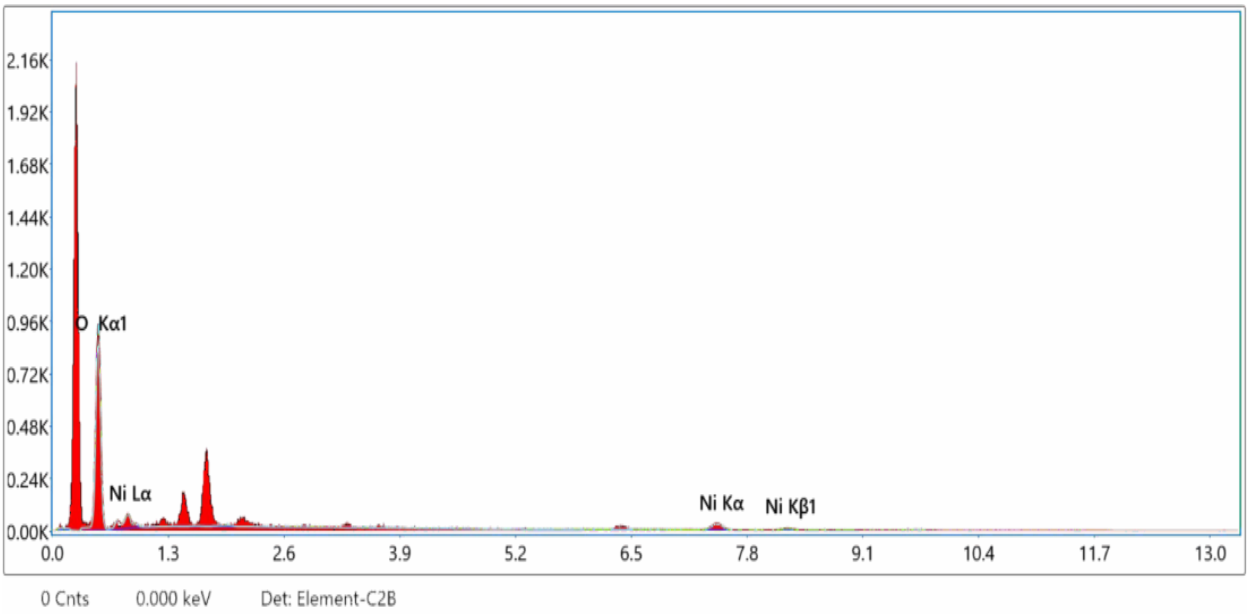

Figure IV.12 EDX analysis of NONPs prepared using *Punica granatum L* peel leaves extract.

IV.3 The results of the antioxidant activity test of NONPs

Due to the complexities of oxidation processes, no particular approach can accurately represent the antioxidant activity profile of a sample. As a result, the antioxidant activity of NONPS prepared using two plant extracts (*Artemisia herba alba* leaves, and *Punica granatum L* peel) at different molarities (0.01, 0.025, 0.05, and 0.075 M) was evaluated in vitro using three different assays the free radical scavenging (DPPH•), (TAC), and (FRAP).

IV.3.1 Total Antioxidant Capacity (TAC)

The absorbance value of each mixture was determined using a spectrophotometer. The total antioxidant capacity value of the biosynthesized NONPs samples was determined using the ascorbic acid standard curve.

Figures (IV.13a), and (**IV.13b)** show the results of the total antioxidant capacity of the different samples of NONPs prepared using the two plant extracts (*Artemisia herba alba* Leaves, and *Punica granatum L* peel) at different concentrations of nickel nitrate. As demonstrated, all of the samples exhibit a significant total antioxidant capacity.

Figure IV.13a shows the TAC values of NONPs samples biosynthesized using *Artemisia herba alba* leaves extract at different molarities. As demonstrated, the 0.05 M sample exhibited the highest total antioxidant capacity with a value of 359.8 ± 3.286 mg AAE/gNPs, the 0.025 M and 0.075 M samples showed fewer values compared to the 0.05 M sample, with values equal to 261 ± 0.547, 246.17 ± 2.741 mg AAE/g NPs respectively, they are followed by a minimum value equal to 190 ± 1.065 mg AAE/g NPs, which belongs to 0.01 M samples.

Figure IV.13b displays the TAC values of NONPs samples biosynthesized using *Punica granatum L* peel extract at different molarities. According to these results, a maximum value in terms of AAE/g NPS was found as 422.13±0.58 mg for 0.075 M sample. The 0.025 M and 0.01 M samples showed fewer values compared to 0.075 M, with values equal to 324.86±0.59, and 231.96±1.09 mg AAE/g NPS respectively, lastly a minimum value equal to 228.68±1.1 mg AAE/g NPS, which found in the 0.05 M samples.

In addition, the TAC values of samples biosynthesized using *Punica granatum L* peel extract were higher compared to those of samples biosynthesized using *Artemisia herba alba* leaves extract, except 0.05 M sample.

These findings suggest that the crystallite size of NONPs, the precursor concentration, and the type of extract used in the synthesis process affect the antioxidant activity of NONPs.

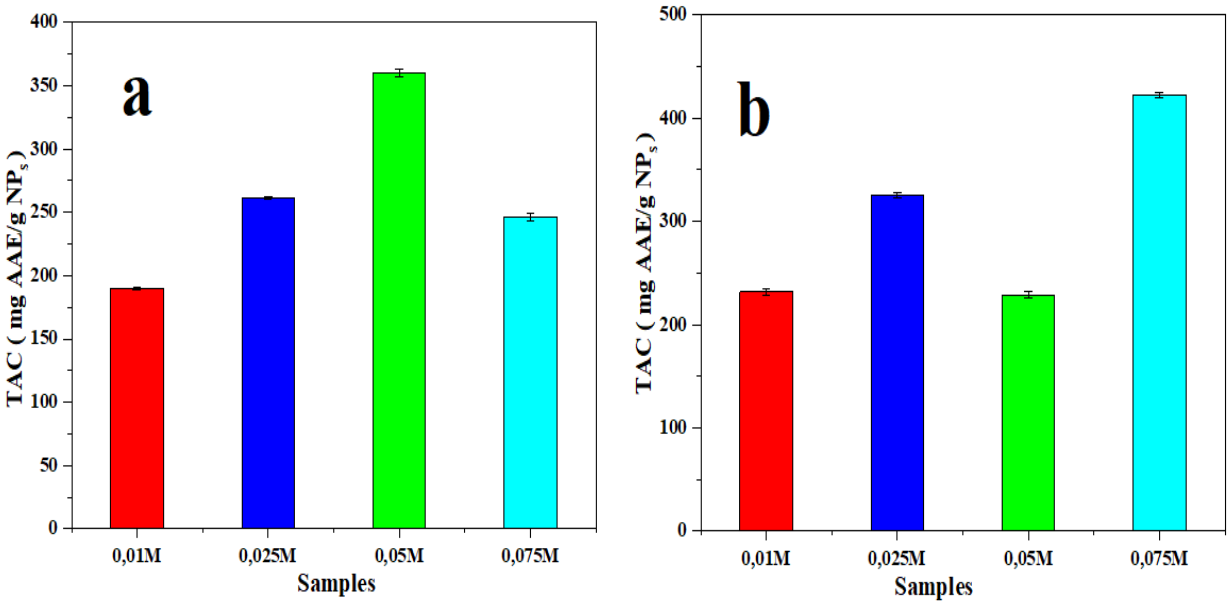

Figure IV.13 The total antioxidant capacity of NONPs samples biosynthesized at different molarities: **(a)** using *Artemisia herba alba* leaves extract, and **(b)** using *Punica granatum L* peel extract.

IV.3.2 Ferric Reducing Antioxidant Power

The antioxidant activity of the NONPs samples was evaluated using the iron reduction (FRAP) method. This method is fast, repeatable, and easy to achieve. It is based on measuring the ability of a substance to reduce Fe^{3+} to Fe^{2+} and gives important details about the tested substance's ability to donate an electron **[35]**.

Figures (IV.14a), and (IV.14b) display the results of reducing power for the different samples of NONPs prepared using the two plant extracts (*Artemisia herba alba* Leaves, and *Punica granatum L* peel) at different concentrations of nickel nitrate. According to the findings, all of the samples showed a significant potential to reduce Fe^{3+} to Fe^{2+}.

Figure IV.14a shows the results of reducing power of NONPs samples biosynthesized using *Artemisia herba alba* leaves extract at different molarities. As shown, the 0.025 M sample exhibited the highest reducing power with a value of 529.84 ± 0.611 mg FeSO4E/g NPs, followed by the 0.05, and 0.01 M samples with values of 503.61 ± 0.624, and 494.52 ± 0.173 mg FeSO4E/g NPs respectively. The lowest reducing power was found in 0.075 sample with a value of 199.6 ± 1.05 mg FeSO4E/g NPs.

Figure IV.14b displays the results of reducing power of NONPs samples biosynthesized using *Punica granatum L* peel extract at different molarities. The maximum value in terms of FeSO4E/g NPS was found as 689.58±2.16 mg for the 0.025 M sample, on other hand, the 0.05,

0.075M samples showed fewer values in comparison to the 0.025 M sample, with values of 598.15±0.62, and 519.37±0.17 mg FeSO4E/g NPS respectively, thereafter the 0.01 M sample with the lowest value of 512.96±0.52 mg FeSO4E/g NPS.

In addition, the results of reducing power of samples biosynthesized using *Punica granatum L* peel extract were higher compared to those of samples biosynthesized using *Artemisia herba alba* leaves extract.

These findings suggest that the crystallite size of NONPs, the precursor concentration, and the type of extract used in the synthesis process affect the antioxidant activity of NONPs.

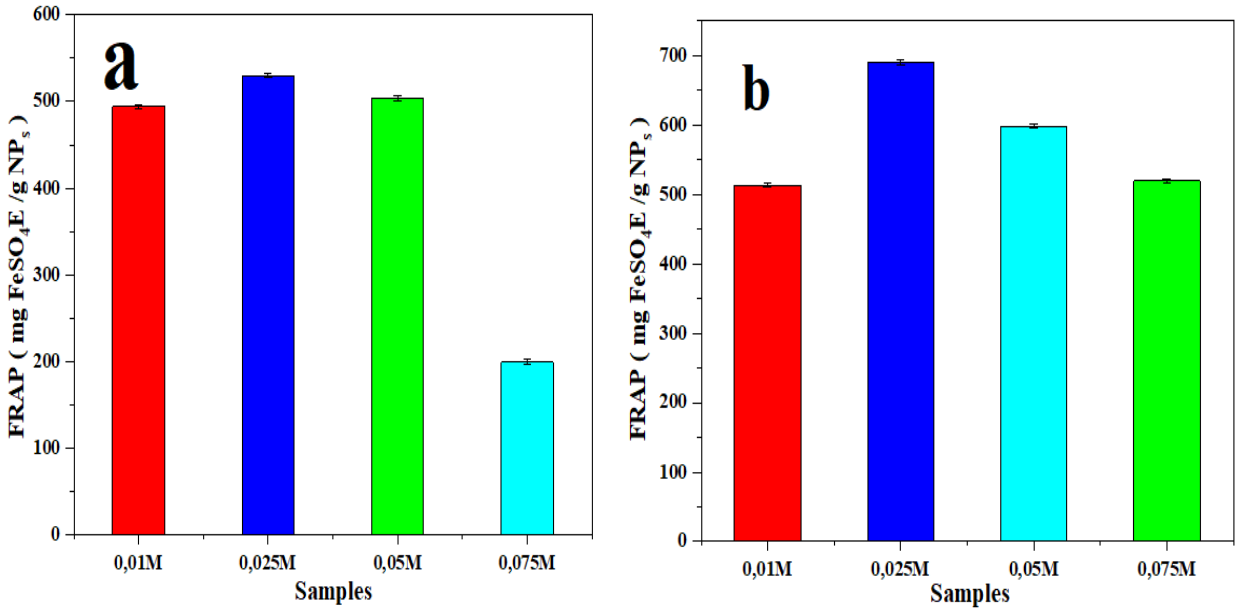

Figure IV.14: Ferric reducing antioxidant power of NONPs samples biosynthesized at different molarities: **(a)** using *Artemisia herba alba* leaves extract, and **(b)** using *Punica granatum L* peel extract.

IV.3.3 DPPH radical scavenging

This method is based on the reduction of an alcoholic DPPH• solution in the presence of a hydrogen donating antioxidant [36]. DPPH• is one of the most widely used substrates for assessing antioxidant activity owing to its stability in radical form and simplicity of analysis [37]. It adapts rapidly to several samples and is sensitive enough to identify active substances at low concentrations, therefore it's used to test synthetic compounds for anti-radical activity [38].

The $IC_{50\%}$ value is a parameter commonly used to measure the antioxidant activity of the tested substance. It is the concentration of antioxidants required to reduce the initial concentration of DPPH• by 50%. Thus, the lower the $IC_{50\%}$ value the higher antioxidant activity of a sample [39].

The $IC_{50\%}$ was measured using the percent inhibition curve for each sample. Another parameter expressing the antiradical power was calculated from the $IC_{50\%}$ (ARP = 1 / IC50%) **[40]**.

Figures (IV.15a), (IV.15b), (IV.15c), (IV.15d), and **(IV.16)** demonstrate the percentage of inhibition and $IC_{50\%}$ for the samples prepared using *Artemisia herba alba* leaves extract at different molarities. The 0.01 M sample exhibited the highest DPPH• radical scavenging activity with an $IC_{50\%}$ value equal to 5.989 ± 0.026 mg/ml and percent inhibition of 78.26 (%), followed by 0.025 and 0.05 M samples with an $IC_{50\%}$ and a percentage of inhibition with values equal to 7.084 ± 0.022, 8.392 ± 0.013 mg/ml, and 67.19, 58.42 (%) respectively. The lowest DPPH• radical scavenging activity was found in 0.075 M sample with an $IC_{50\%}$ and percentage of inhibition with values of 9.382 ± 0.018 mg/ml and 54.83 (%). These results indicate that an increase in nickel nitrate concentration improves DPPH• radical scavenging activity, confirming the effect of crystallite size and precursor concentration on the antioxidant activity of nickel oxide nanoparticles. The antiradical power (ARP) and IC50% values are listed in **table IV.3**.

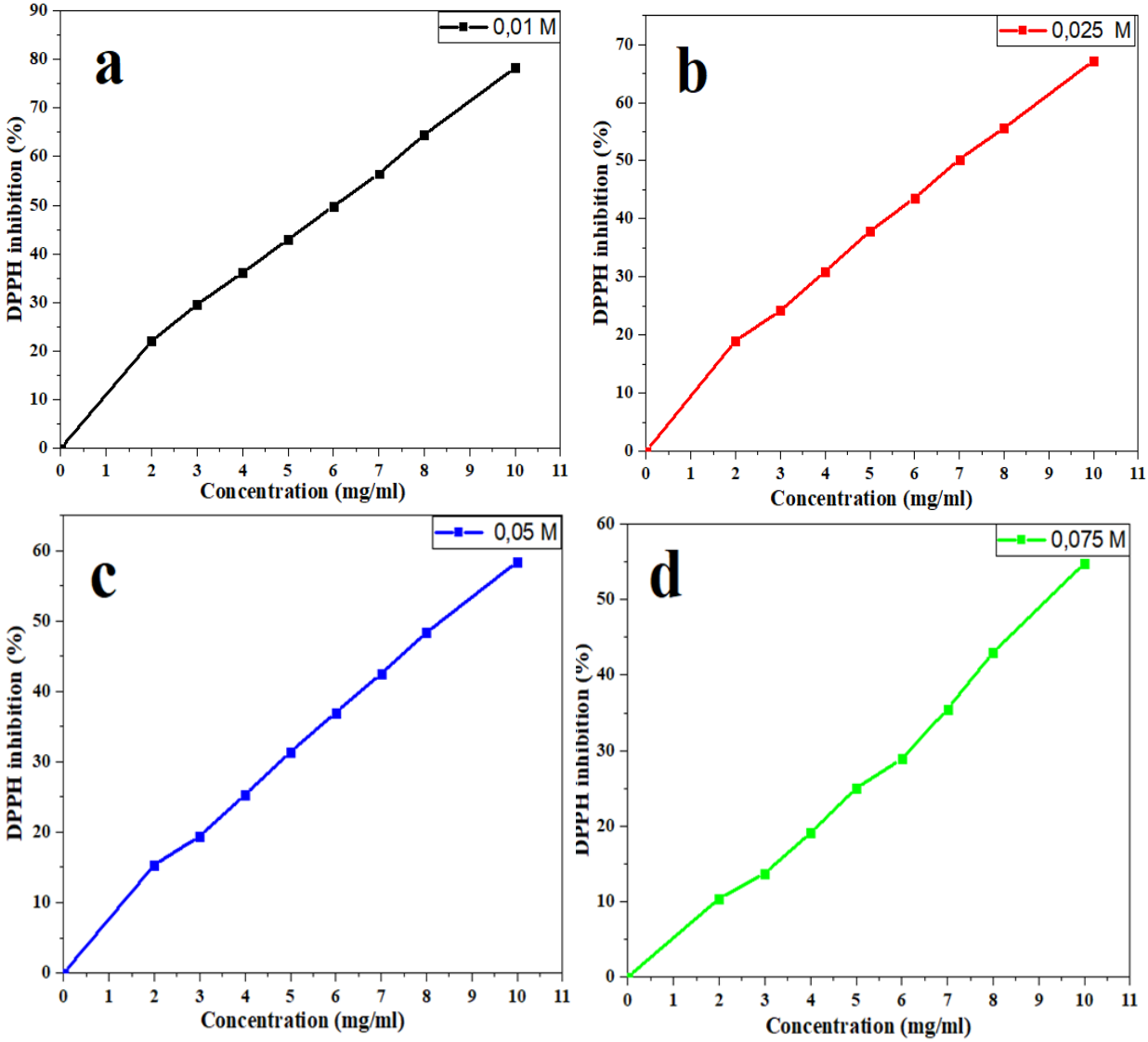

Figure IV.15 Percent inhibition of DPPH• for samples prepared using *Artemisia herba alba* leaves extract at different molarities: (**a)** 0.01M; (**b)** 0.025M; (**c)** 0.05M; and **(d)** 0.075M.

Table IV.3 $IC_{50\%}$ and ARP values of DPPH• for different samples biosynthesized by *Artemisia herba alba* leaves extract.

Samples	IC50% (mg/ml)	ARP
0.01M	5.989 ± 0.026	0.166
0.025M	7.084 ± 0.022	0.141
0.05M	8.392 ± 0.013	0.119
0.075M	9.382 ± 0.018	0.106

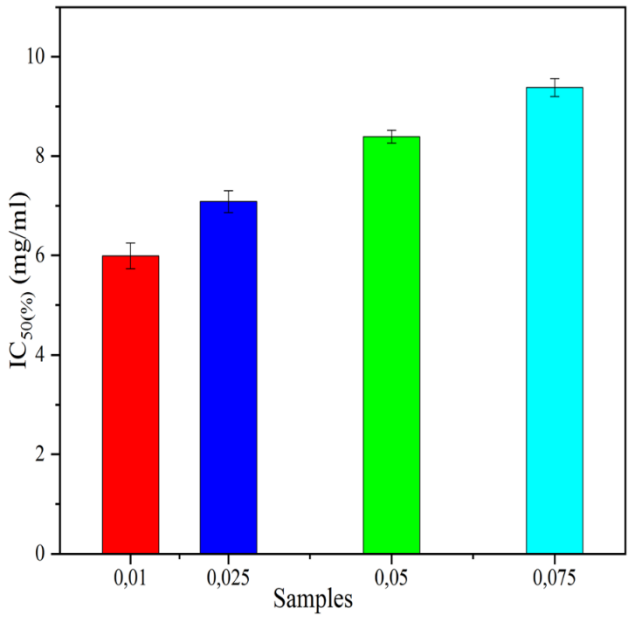

Figure IV.16 $IC_{50\%}$ values of for samples biosynthesized by *Artemisia herba alba* leaves extract.

Figures (IV.17a), (IV.17b), (IV.17c), (IV.17d), and **(IV.18)** demonstrate the percentage of inhibition and $IC_{50\%}$ for the samples prepared using *Punica granatum L* peel extract at different molarities. The 0.01 M sample exhibited the highest DPPH• radical scavenging activity with an $IC_{50\%}$ value equal to 3.97±1.312 mg/ml and percent inhibition of 80.11 (%), followed by 0.025 and 0.05 M samples with an $IC_{50\%}$ and a percentage of inhibition with values equal to 4.83±1.081, 5.5±0.911 mg/ml and 70.23, 70.02 (%) respectively. The lowest DPPH• radical scavenging activity was found in 0.075 M sample with an $IC_{50\%}$ and percentage of inhibition with values of 6.14±0.760 mg/ml and 65.23 (%). These results indicate that an increase in nickel nitrate concentration improves DPPH• radical scavenging activity, confirming the effect of crystallite size and precursor

concentration on the antioxidant activity of nickel oxide nanoparticles. The antiradical power (ARP) and IC50% values are listed in **table IV.4**.

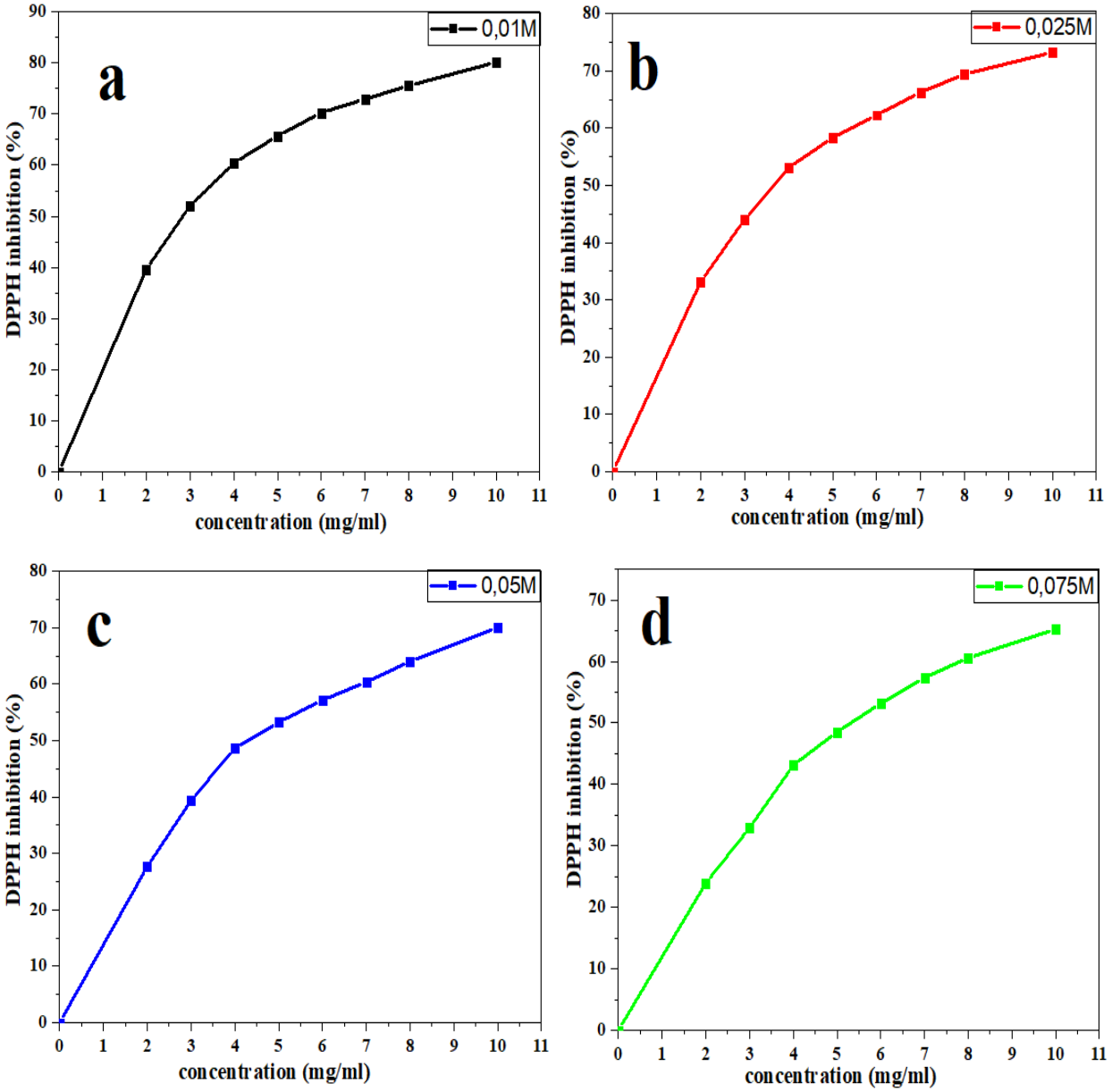

Figure IV.17 Percent inhibition of DPPH• for samples prepared using *Punica granatum L* peel extract at different molarities: **(a)** 0.01M; **(b)** 0.025M; **(c)** 0.05M; and **(d)** 0.075M.

Table IV.4 $IC_{50\%}$ and ARP values of DPPH• for different samples biosynthesized by *Punica granatum L* peel extract.

Samples	IC50% (mg/ml)	ARP
0.01M	3.97±1.312	0.25
0.025M	4.83±1.081	0.21
0.05M	5.5±0.911	0.18
0.075M	6.14±0.760	0.16

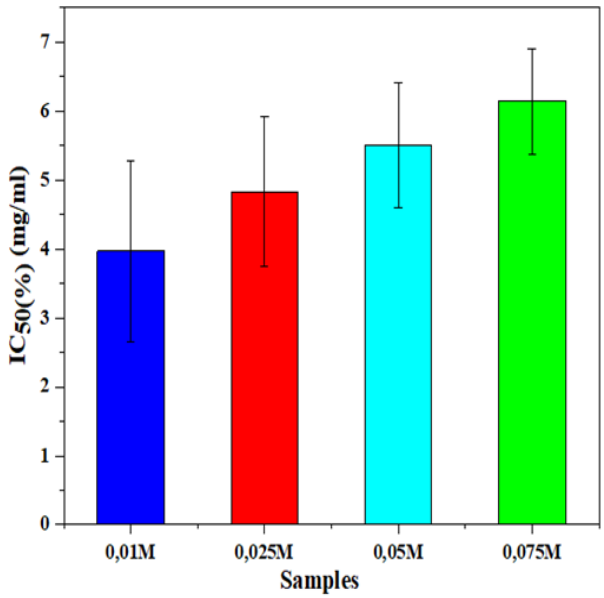

Figure IV.18 $IC_{50\%}$ values of for samples biosynthesized *Punica granatum L* peel extract.

Conclusion

In this thesis, NONPS were successfully biosynthesized by a clear, inexpensive, and environmentally friendly green approach. For the first time, the extract of *Punica granatum L* peel and *Artemisia herba alba* leaves was used to biosynthesize NONPS. The change of the mixture's color from brown to greenish-black indicates the reduction of nickel ions and the creation of nickel oxide nanoparticles. The decrease in polyphenol absorbance bands suggests that polyphenols contribute considerably to the reduction of nickel ions and, therefore, to the stability of nickel oxide nanoparticles. The variation in $NiNO_3$ concentration and the used bio-reducer source has a

considerable effect on the crystallite size and optical band gap of nickel oxide nanoparticles. Compared to other approaches, the use of different plant parts such as the leaves of *Artemisia herba alba* and the peel of *Punica granatum L* is a green and feasible method because it is considered fast, inexpensive, environmentally friendly, and easy to investigate. Moreover, the crystallite size and morphology of NONPs could be controlled by adjusting the concentration of $NiNO_3$.

The in vitro antioxidant activity of nickel oxide nanoparticles biosynthesized using different extracts (*Artemisia herba-alba* leaves and *Punica granatum L* peel) at different molarities (0.01, 0.025, 0.05 and 0.075 M) was evaluated using three different techniques: total antioxidant capacity (TAC), trapping of the free radical DPPH•, and ferric ion reducing antioxidant power assay assays. All of the tested samples showed significant antioxidant activity in the different assays. These results suggest that biosynthesized nickel oxide nanoparticles may be effective antioxidants for the protection against oxidative stresses involved in several disorders.

References

References

[1] J. Iqbal *et al.*, "Phytogenic synthesis of nickel oxide nanoparticles (NiO) using fresh leaves extract of Rhamnus triquetra (Wall.) and investigation of its multiple in vitro biological potentials," *Biomedicines*, vol. 8, no. 5, p. 117, 2020, doi: 10.3390/BIOMEDICINES8050117.

[2] B. A. Abbasi *et al.*, "Green formulation and chemical characterizations of Rhamnella gilgitica aqueous leaves extract conjugated NiONPs and their multiple therapeutic properties," *J. Mol. Struct.*, vol. 1218, no. October, p. 128490, 2020, doi: 10.1016/j.molstruc.2020.128490.

[3] V. Helan *et al.*, "Neem leaves mediated preparation of NiO nanoparticles and its magnetization, coercivity and antibacterial analysis," *Results Phys.*, vol. 6, no. October, pp. 712–718, 2016, doi: 10.1016/j.rinp.2016.10.005.

[4] M. I. Din, M. Tariq, Z. Hussain, and R. Khalid, "Single step green synthesis of nickel and nickel oxide nanoparticles from Hordeum vulgare for photocatalytic degradation of methylene blue dye," *Inorg. Nano-Metal Chem.*, vol. 50, no. 4, pp. 292–297, 2020, doi: 10.1080/24701556.2019.1711401.

[5] M. Imran Din and A. Rani, "Recent advances in the synthesis and stabilization of nickel and nickel oxide nanoparticles: A green adeptness," *Int. J. Anal. Chem.*, vol. 2016, no. 4, pp. 1–14, 2016, doi: 10.1155/2016/3512145.

[6] I. M. Rashid, S. D. Salman, A. K. Mohammed, and Y. S. Mahdi, "Green Synthesis of Nickle Oxide Nanoparticles for Adsorption of Dyes," *Sains Malaysiana*, vol. 51, no. 2, pp. 533–546, 2022, doi: 10.17576/jsm-2022-5102-17.

[7] K. Kannan, D. Radhika, M. P. Nikolova, K. K. Sadasivuni, H. Mahdizadeh, and U. Verma, "Structural studies of bio-mediated NiO nanoparticles for photocatalytic and antibacterial activities," *Inorg. Chem. Commun.*, vol. 113, no. January, p. 107755, 2020, doi: 10.1016/j.inoche.2019.107755.

[8] R. Sathish Kumar, S. Johnson Jeyakumar, M. Jothibas, I. Kartharinal Punithavathy, and J. Prince Richard, "Influence of molar concentration on structural, optical and magnetic properties of NiO nanoparticles," *J. Mater. Sci. Mater. Electron.*, vol. 28, no. 20, pp. 15668–15675, 2017, doi: 10.1007/s10854-017-7456-7.

[9] A. K. H. Bashir *et al.*, "Biosynthesis of NiO nanoparticles for photodegradation of free cyanide solutions under ultraviolet light," *J. Phys. Chem. Solids*, vol. 134, no. June, pp. 133–140, 2019, doi: 10.1016/j.jpcs.2019.05.048.

[10] Z. Sabouri *et al.*, “Plant-based synthesis of NiO nanoparticles using salvia macrosiphon Boiss extract and examination of their water treatment,” *Rare Met.*, vol. 39, no. 10, pp. 1134–1144, 2020, doi: 10.1007/s12598-019-01333-z.

[11] S. Meneceur *et al.*, “Photocatalytic activity of iron oxide nanoparticles synthesized by different plant extracts for the degradation of diazo dyes Evans blue and Congo red,” *Biomass Convers. Biorefinery*, no. May, 2022, doi: 10.1007/s13399-022-02734-4.

[12] T. Nawaz, H. Ali, M. Imran, S. Ahmed, and S. Noreen, “Phytochemical screening and antibacterial activity of green synthesis of nanoparticles of Punica granatum,” vol. 17, no. 1, pp. 160–166, 2020, doi: 10.12692/ijb/17.1.160-166.

[13] A. A. Olajire and A. A. Mohammed, “Green synthesis of nickel oxide nanoparticles and studies of their photocatalytic activity in degradation of polyethylene films,” *Adv. Powder Technol.*, vol. 31, no. 1, pp. 211–218, 2020, doi: 10.1016/j.apt.2019.10.012.

[14] J. A. A. Abdullah, L. Salah Eddine, B. Abderrhmane, M. Alonso-González, A. Guerrero, and A. Romero, “Green synthesis and characterization of iron oxide nanoparticles by pheonix dactylifera leaf extract and evaluation of their antioxidant activity,” *Sustain. Chem. Pharm.*, vol. 17, no. June, p. 100280, Sep. 2020, doi: 10.1016/j.scp.2020.100280.

[15] R. N. Oliveira *et al.*, “Análise por FTIR e quantificação de fenóis e flavonóides de cinco produtos naturais disponíveis comercialmente utilizados no tratamento de feridas,” *Rev. Mater.*, vol. 21, no. 3, pp. 767–779, 2016, doi: 10.1590/S1517-707620160003.0072.

[16] A. A. Ezhilarasi, J. J. Vijaya, K. Kaviyarasu, M. Maaza, A. Ayeshamariam, and L. J. Kennedy, “Green synthesis of NiO nanoparticles using Moringa oleifera extract and their biomedical applications: Cytotoxicity effect of nanoparticles against HT-29 cancer cells,” *J. Photochem. Photobiol. B Biol.*, vol. 164, no. November, pp. 352–360, 2016, doi: 10.1016/j.jphotobiol.2016.10.003.

[17] Z. Sabouri *et al.*, “Plant-based synthesis of NiO nanoparticles using salvia macrosiphon Boiss extract and examination of their water treatment,” *Rare Met.*, vol. 39, no. 10, pp. 1134–1144, 2020, doi: 10.1007/s12598-019-01333-z.

[18] M. S. S. Kumar *et al.*, “Multifunctional applications of Nickel oxide (NiO) nanoparticles synthesized by facile green combustion method using Limonia acidissima natural fruit juice,” *Inorganica Chim. Acta*, vol. 515, p. 120059, Jan. 2021, doi: 10.1016/j.ica.2020.120059.

[19] A. Haider *et al.*, "Green Synthesized Phytochemically (Zingiber officinale and Allium sativum) Reduced Nickel Oxide Nanoparticles Confirmed Bactericidal and Catalytic Potential," *Nanoscale Res. Lett.*, vol. 15, no. 1, p. 50, 2020, doi: 10.1186/s11671-020-3283-5.

[20] S. El-Debaiky, A. El-Badry, and M. El-Shahawy, "Biosynthesis of Nickel Oxide Nanoparticles Using Fusarium verticillioides (Sacc.) and Their Biological Activity against Some Causative Agents of Mycotic Keratitis," *Egypt. J. Bot.*, vol. 57, no. 3, pp. 417–428, 2017, doi: 10.21608/ejbo.2017.899.1066.

[21] R. D. and V. A. Sharanabasava V.Ganachari, Ravishankar Bhat, "Synthesis and characterization of nickel oxide nanoparticles by self-propagating low temperature combustion method," *Recent Res. Sci. Technol.*, vol. 04, no. 04, pp. 50–53, 2012.

[22] S. Uddin *et al.*, "Green Synthesis of Nickel Oxide Nanoparticles from Berberis balochistanica Stem for Investigating Bioactivities," *Molecules*, vol. 26, no. 6, p. 1548, Mar. 2021, doi: 10.3390/molecules26061548.

[23] E. Elias *et al.*, "Enhancement of Tribological Properties of Lubricating Oils Using Cuo and Nio Nanomaterials," *J. Adv. Sci. Res.*, vol. 11, no. 03, pp. 288–295, 2020.

[24] C. R. Rajith Kumar, V. S. Betageri, G. Nagaraju, G. H. Pujar, B. P. Suma, and M. S. Latha, "Photocatalytic, nitrite sensing and antibacterial studies of facile bio-synthesized nickel oxide nanoparticles," *J. Sci. Adv. Mater. Devices*, vol. 5, no. 1, pp. 48–55, 2020, doi: 10.1016/j.jsamd.2020.02.002.

[25] S. Xavier, V. Lakshmi, and R. M. Jenila, "synthesis of NiO nanoparticles using thespesia populnea leaves by green synthesis method," *EPRA Int. J. Res. Dev.*, vol. 7838, no. 9, 2019.

[26] S. Ghazal *et al.*, "Sol-gel biosynthesis of nickel oxide nanoparticles using Cydonia oblonga extract and evaluation of their cytotoxicity and photocatalytic activities," *J. Mol. Struct.*, vol. 1217, no. May, p. 128378, 2020, doi: 10.1016/j.molstruc.2020.128378.

[27] A. B. Habtemariam, "Plant Extract Mediated Synthesis of Nickel Oxide Nanoparticles," *Mater. Int.*, vol. 2, no. 2, pp. 205–209, 2020, doi: 10.33263/materials22.205209.

[28] J. Cao, Y. Wu, Y. Jin, P. Yilihan, and W. Huang, "Response surface methodology approach for optimization of the removal of chromium(VI) by NH2-MCM-41," *J. Taiwan Inst. Chem. Eng.*, vol. 45, no. 3, pp. 860–868, 2014, doi: 10.1016/j.jtice.2013.09.011.

[29] S. U. Din *et al.*, "Investigation of the Biological Applications of Biosynthesized Nickel Oxide Nanoparticles Mediated by Buxus wallichiana Extract," *Crystals*, vol. 12, no. 2, 2022, doi: 10.3390/cryst12020146.

[30] V. Selvanathan *et al.*, "Phytochemical-assisted green synthesis of nickel oxide nanoparticles for application as electrocatalysts in oxygen evolution reaction," *Catalysts*, vol. 11, no. 12, 2021, doi: 10.3390/catal11121523.

[31] B. Ebin, "Simple Preparation of Ni and NiO Nanoparticles Using Raffinate Solution Originated from Spent NiMH Battery Recycling," *J. Inorg. Organomet. Polym. Mater.*, vol. 28, no. 6, pp. 2554–2563, 2018, doi: 10.1007/s10904-018-0926-4.

[32] H. G. Gebretinsae, M. G. Tsegay, and Z. Y. Nuru, "Biosynthesis of nickel oxide (NiO) nanoparticles from cactus plant extract," *Mater. Today Proc.*, vol. 36, no. June, pp. 566–570, 2019, doi: 10.1016/j.matpr.2020.05.331.

[33] M. Nowsath Rifaya, T. Theivasanthi, and M. Alagar, "Chemical Capping Synthesis of Nickel Oxide Nanoparticles and their Characterizations Studies," *Nanosci. Nanotechnol.*, vol. 2, no. 5, pp. 134–138, 2012, doi: 10.5923/j.nn.20120205.01.

[34] S. T. Fardood, A. Ramazani, and S. Moradi, "A novel green synthesis of nickel oxide nanoparticles using arabic gum," *Chem. J. Mold.*, vol. 12, no. 1, pp. 115–118, 2017, doi: 10.19261/cjm.2017.383.

[35] V. Singh, N. Guizani, M. M. Essa, F. L. Hakkim, and M. S. Rahman, "Comparative analysis of total phenolics, flavonoid content and antioxidant profile of different date varieties (Phoenix dactylifera L.) From Sultanate of Oman," *Int. Food Res. J.*, vol. 19, no. 3, pp. 1063–1070, 2012.

[36] M. Fatiha and T. Abdelkader, "Study of antioxidant activity of pyrimidinium betaines by DPPH radical scavenging method," *J. Anal. Pharm. Res.*, vol. 8, no. 2, pp. 33–36, 2019, doi: 10.15406/japlr.2019.08.00308.

[37] S. B. Kedare and R. P. Singh, "Genesis and development of DPPH method of antioxidant assay," *J. Food Sci. Technol.*, vol. 48, no. 4, pp. 412–422, 2011, doi: 10.1007/s13197-011-0251-1.

[38] C. Sánchez-Moreno, "Methods Used to Evaluate the Free Radical Scavenging Activity in Foods and Biological Systems," *Food Sci. Technol. Int.*, vol. 8, no. 3, pp. 121–137, 2002, doi: 10.1106/108201302026770.

[39] J. F. Rivero-Cruz *et al.*, "Phytochemical constituents, antioxidant, cytotoxic, and antimicrobial activities of the ethanolic extract of mexican brown propolis," *Antioxidants*, vol. 9, no. 1, pp. 1–11, 2020, doi: 10.3390/antiox9010070.

[40] A. Mansouri, G. Embarek, E. Kokkalou, and P. Kefalas, “Phenolic profile and antioxidant activity of the Algerian ripe date palm fruit (Phoenix dactylifera),” *Food Chem.*, vol. 89, no. 3, pp. 411–420, 2005, doi: 10.1016/j.foodchem.2004.02.051.

GENERAL CONCLUSION

General conclusion

nanoparticles have piqued the curiosity of researchers in many disciplines due to their distinctive properties applied in the majority of fields. Physicists, chemists, and biologists have a common interest in using the unique properties of these materials to resolve a variety of challenges.

These distinctive properties of nanoparticles are highly affected by their size and shape, which has prompted many researchers to synthesize nanoparticles with desired properties. It was found that synthesis parameters influence the size of nanoparticles, allowing the size to be controlled by modifying these parameters.

Due to the growing demand for nanoparticles and their widespread uses, there are significant concerns over their harmful manufacturing processes. These concerns are faded employing an alternative approach **(**green synthesis approach) in nanoparticles production, which eliminates the use of hazardous products and produces non-toxic and biodegradable nanoparticles, making it a suitable alternative to other synthesis methods in many fields.

This work aims to improve the crystal size and antioxidant activity of nickel nanoparticles by changing plant extract and nickel nitrate concentration. A green synthesis approach was used to biosynthesize NONPs using two plant extracts (*Artemisia herba alba* leaves and *Punica granatum L* peel) with different molarities of nickel nitrate.

Different characterization techniques were employed to validate the formation of NONPs and study their optical, structural, and morphological properties.

UV/ Visible and FTIR absorption spectrums showed characteristic absorption bands which are related to NONPs, confirming their formation. Moreover, FTIR analysis indicated that the polyphenols present in *Artemisia herba alba* and *Punica granatum L* play an important role in reducing and stabilizing NONPs.

XRD findings indicated the formation of a pure NONPs, with an average crystallite size ranging between 7.49 and 14.51 nm. The SEM images indicate that some of the synthesized nanoparticles have a spherical shape, while others have an irregular shape.

$NONP_S$ showed high antioxidant activity in all the performed tests. The results also revealed that the concentration of metallic salt ($Ni(NO_3)_2$) has a substantial effect on the crystallite size of $NONP_S$ as well as DPPH•, TAC, FRAP assays. These findings can be used to control and increase NONPS's anti-oxidant activity.

As part of the continuation of this work, it will be important to control the size and shape of nickel oxide nanoparticles by adjusting the synthesis conditions in order to use them as antioxidants and antimicrobials.

APPENDIXES

Scientific publications

Louafi, O., Khelef, A., Zeroual, S. *et al.* Effect of Nickel Nitrate Concentration on the Size of Nickel Oxide Nanoparticles Bio-synthesized by *Artemisia herba-alba* Aqueous Leaves Extract and Improving Their Antioxidant Activities. *J Inorg Organomet Polym* **32**, 1116–1128 (2022). https://doi.org/10.1007/s10904-021-02152-5

National and international Seminars

Louafi okba, **Khelef Abdelhamid**," Green synthesis of nickel oxide nanoparticles using *Artemisia herba alba leaves* extract". The first National seminar on green chemistry and natural product (GCNP'22) 14-15 March. 2022 El-Oued, Algeria

Louafi okba, **Khelef Abdelhamid**," Green synthesis of nickel oxide nanoparticles using *Artemisia herba alba leaves* extract and improving their antioxidant activities". The first international seminar chemical matter and environment preservation (IC-CMEP'22), 09-10 March. 2022 Ouargla, Algeria

Louafi okba, **Khelef Abdelhamid**," Synthèse verte de nanoparticules d'oxyde de nickel en utilisant l'extrait de feuilles *d'Artemisia herba alba* et améliorant leurs activités antioxydantes ". Journée d'étude sur la science des matériaux et applications (JESMA-21), 08 Décembre. 2021 (Lab. LEVRES) El-Oued, Alger

Louafi okba, **Khelef Abdelhamid**," Green synthesis of nickel oxide nanoparticles and assessment of their DPPH-scavenging activity". The first international conference on applied chemistry and renewable energies (ACREIC), 26-28 Nov. 2022 Tebessa, Algeria

Louafi okba, **Khelef Abdelhamid**," Green synthesis of nickel oxide nanoparticles and study of their ability to reduce MoO2- to MoO+2". 3rd National Conference on Applied Physics & Chemistry (3rdNCAPC23), 12-13 March.2023 Laghouat, Algeria

Louafi okba, **Khelef Abdelhamid**," Green synthesis of nickel oxide nanoparticles using different plant extract and assessment of their DPPH-scavenging activity". National seminar of Physics, Chemistry and their applications (NSPCA'23), 06-07 March.2023 Bordj Bouarreridj, Algeria

Louafi okba, **Khelef Abdelhamid**," Green synthesis of nickel oxide nanoparticles and study their ability to reduce Fe^{3+} into Fe^{2+}". 1st international seminar on valorization of Bio resources in environment and health, 10-11May. 2023 El-Oued, Algeria